Liposomes as Versatile Tools for Signal Enhancement in Surface Plasmon Resonance Spectroscopy

Dissertation zur Erlangung des Doktorgrades der Naturwissenschaften

(Dr. rer. nat.)

der Fakultät Chemie und Pharmazie

der Universität Regensburg

Deutschland

vorgelegt von

Christoph Fenzl

aus Hutthurm (Landkreis Passau)

im Jahr 2015

Die vorgelegte Dissertation entstand in der Zeit von Oktober 2012 bis Oktober 2015 am Institut für Analytische Chemie, Chemo- und Biosensorik der Universität Regensburg.

Die Arbeit wurde angeleitet von Prof. Dr. Antje J. Bäumner.

Promotionsgesuch eingereicht am: 29.10.2015
Kolloquiumstermin: 14.12.2015

Prüfungsausschuss

Vorsitzender: Prof. Dr. Oliver Tepner
Erstgutachterin: Prof. Dr. Antje J. Bäumner
Zweitgutachter: Prof. Dr. Otto S. Wolfbeis
Drittprüfer: Prof. Dr. Reinhard Rachel

“To raise new questions, new possibilities, to regard old problems from a new angle, requires creative imagination and marks real advance in science.”

Albert Einstein

Acknowledgements

First of all, I want to thank **Prof. Dr. Antje J. Bäumner** for providing me with this interesting topic, for the opportunity to work independently, valuable discussions and her continuous support.

Furthermore, I thank my tutor **Dr. Thomas Hirsch** a lot for his great help, good advices and scientific discussions, as well as for his tireless support and encouragement during this thesis.

I also thank **Dr. Katie Edwards, Dr. Stefan Wilhelm, Dr. Alexander Zöpfl, Markus Buchner, Celesztina Domonkos, Carola Figalist, Christa Genslein, Josef Heiland, Cornelia Hermann, Sandy Himmelstoß, Eva Kirchner, Michael Lemberger, Verena Muhr, Joachim Rewitzer, Rosmarie Walter, Lisa Wiesholler** and all my colleagues for the excellent atmosphere and their help.

No less, I want to thank especially **my whole family** and my girlfriend **Tamara Süß** for their invaluable support and their love.

Dedicated to my grandfather Heinz Junge

Declaration of Collaborations

Most of the experimental and theoretical work presented in this thesis was carried out solely by the author. However, some of the results were obtained together with other researchers. In accordance with § 8 Abs. 1 Satz 2 Punkt 7 of the "Ordnung zum Erwerb des akademischen Grades eines Doktors der Naturwissenschaften (Dr. rer. nat.) an der Universität Regensburg vom 18. Juni 2009", this section gives information about these collaborations.

Nanomaterials as versatile tools for signal amplification in (bio)analytical applications (Chapter 1)

The literature search was conducted by the author as well as the writing of the review manuscript. Thomas Hirsch and Antje J. Bäumner revised the manuscript. Antje J. Bäumner is corresponding author.

Investigating non-specific binding to sensor surfaces using liposomes as models (Chapter 2)

Most of the experimental work was carried out by the author solely. Christa Genslein and Celesztina Domonkos repeated some of the SPR measurements for statistical confidence under the author's guidance. Katie A. Edwards discussed liposome stability. The article manuscript was written by the author and revised by Thomas Hirsch, Katie A. Edwards and Antje J. Bäumner. Antje J. Bäumner is corresponding author.

Liposomes with high refractive index encapsulants as tunable signal amplification tools in surface plasmon resonance spectroscopy (Chapter 3)

The author carried out the experimental work solely and wrote the article manuscript. The manuscript was revised by Thomas Hirsch and Antje. J. Bäumner. Antje J. Bäumner is corresponding author.

Contents

Summary

Since their discovery by Bangham *et al.* in 1964, liposomes have proven to be versatile tools ubiquitously used in various fields of research most prominently in (bio)analytical chemistry and pharmaceutical sciences. In both cases their capability of transporting an enormous amount of small marker molecules inside their inner cavity is exploited. This renders them to be high-performing signal amplification tools especially in analytical applications. Highly stable anionic liposomes function as labels for various kinds of sensing formats such as microtiter plates, lateral flow assays or microfluidic devices. However, liposomes do not achieve their true signal amplification potential which theoretically could lead to signal enhancement by a factor of 10^6. This is caused in part by their size and consequently steric hindrance and lower diffusion coefficients. Most importantly though, it is caused by non-specific binding that is a challenge in any analytical assay, as it reduces the signal-to-noise ratio and thus worsens the limit of detection. Therefore, fundamental understanding of the surface interactions is mandatory. This becomes increasingly important for approaches with high surface-to-volume ratios such as point-of-care devices using microfluidic sample handling. The groups of Viitala, Reviakine, Richter and Brisson, and Kasemo intensively studied the behavior of liposomes on surfaces with quartz crystal microbalance, atomic force microscopy as well as surface plasmon resonance (SPR) (as described in detail in Chapter 2). However, they did neither focus on the established liposome formulation used in most of (bio)analytical applications, nor on the typical surface modifications encountered in such approaches. In order to fill this knowledge gap, SPR spectroscopy was applied here for a systematic study of the interactions of anionic liposomes with long-chain alkane thiol modified gold surfaces of varying surface charge and hydrophilicity that are most commonly used in sensing applications. It was found that the recorded binding curves can be well-fitted to the Langmuir models. Also, almost no cooperative binding effects were observable indicating that the liposome – sensor surface interactions are predominant in comparison to the interactions between the liposomes themselves. This was proven for the (bio)analytical relevant temperature range from 25 to 50 °C. Further, the study revealed that the combination of liposomes with highly negative

surface charge and sensor surfaces modified with either hydrophobic terminal $–CH_3$ groups or hydrophilic terminal –COOH groups showed almost no binding, whereas the adhesion to –OH and $–NH_2$ was significant. This knowledge enables clever surface engineering strategies as an attractive alternative to the commonly used bulk-blocking through polymers and proteins and assists significantly improving (bio)analytical applications using liposomes as signal enhancement tools.

Based on these findings, a tunable signal amplification strategy for SPR based on liposomes encapsulating high refractive index solutions was developed. So far liposomes have been utilized seldom for the enhancement of the SPR technique. In general, SPR spectroscopy is a label-free method for online monitoring of binding events, but has certain limitations when it comes to the direct detection of very small refractive index changes, e. g. those caused by small molecules (< 400 Da) or very low analyte concentrations. Therefore, an additional binding event by an enhancement tag is required to amplify the SPR signal. Here, gold and magnetite nanoparticles (NPs) have been described previously, because the localized surface plasmons generated by the Au NPs and the high refractive index and surface mass loading of the magnetite NPs significantly enhance the SPR performance. However, these materials show distinct drawbacks regarding colloidal stability, ease of surface modification or adjustability of the enhancement factor (EF). The results of the present studies showed that liposomes are an ideal choice to overcome these limitations. The binding of streptavidin to a biotinylated SPR surface resulted in very small signal changes that were immensely enhanced and made detectable by liposomes. The enhancement factor strongly depended on the refractive index of the encapsulant solution and therefore can be tuned to the respective need of the analytical task. A maximum EF of 23 was obtained when using 500 mM sucrose solution inside the liposomes leading to an improvement of the limit of detection from 10 nM to 320 pM streptavidin with a much higher sensitivity of 3 mRIU (refractive index units) per logarithmic unit of the concentration between 500 pM and 10 nM. This work demonstrated the great promise of liposome-mediated SPR signal enhancement and showed its applicability and versatility for the development of new SPR-based chemo- and biosensors.

Zusammenfassung

Seit ihrer Entdeckung durch Bangham *et al.* im Jahr 1964, taten sich Liposomen als vielseitige Werkzeuge hervor, die überall in verschiedensten Forschungsbereichen, vor allem in der (bio)analytischen Chemie und der Pharmazie, eingesetzt werden. In beiden Teilbereichen wird ihre Fähigkeit ausgenutzt, riesige Mengen kleiner Markermoleküle in ihrem Inneren zu transportieren. Besonders bei analytischen Anwendungen macht sie das sehr effizient für die Signalverstärkung. Hochstabile anionische Liposomen werden als Label in zahlreichen Plattformen wie z.B. in Mikrotiterplatten, bei Lateral Flow Assays oder in der Mikrofluidik eingesetzt. Sie erreichen jedoch nicht ihr wahres Signalverstärkungspotential, das in der Theorie zu Verstärkungsfaktoren von 10^6 führen könnte. Dies ist zum Teil auf ihre Größe zurückzuführen, mit der sterische Hinderung und niedrigere Diffusionskoeffizenten einhergehen. Hauptsächlich ist aber nicht-spezifische Bindung die Ursache, die eine Herausforderung für alle analytischen Assays darstellt, da sie das Signal-Rausch-Verhältnis und damit die Nachweisgrenze verschlechtert. Deshalb ist ein grundsätzliches Verständnis von den Wechselwirkungen mit Oberflächen obligatorisch. Die Bedeutung nimmt noch weiter bei Anwendungen mit hohem Verhältnis von Oberfläche zu Volumen zu, wie dies in der Point-of-Care-Diagnostik der Fall ist, die oft Mikrofluidik verwendet. Wie detailliert in Kapitel 2 beschrieben, untersuchten die Forschungsgruppen um Viitala, Reviakine, Richter und Brisson, und Kasemo intensiv das Verhalten von Liposomen auf Oberflächen mithilfe der Quarzkristallmikrowaage, der Rasterkraftmikroskopie und auch der Oberflächenplasmonenresonanz (SPR) – Spektroskopie. Sie richteten ihre Aufmerksamkeit jedoch weder auf die bewährte Liposomformulierung, die in den meisten (bio)analytischen Anwendungen genutzt wird, noch auf die typischen Oberflächenmodifizierungen, die man bei diesen verwendet. Um diese Erkenntnislücke zu füllen, wurde hier eine systematische Studie mit SPR – Spektroskopie durchgeführt, die die Wechselwirkung von anionischen Liposomen mit Goldoberflächen untersucht, die mit langkettigen Alkylthiolen mit unterschiedlicher Polarität und Hydrophilie modifiziert wurden, wie sie weit verbreitet in der Analytik eingesetzt werden. Es stellte sich heraus, dass die aufgenommenen Bindungskurven sehr gut mit dem Langmuir-Modell angepasst werden konnten. Zusätzlich konnten kaum

kooperative Bindungseffekte beobachtet werden, was darauf deutet, dass die Wechselwirkung von Liposom und Sensoroberfläche im Vergleich zu den Wechselwirkungen der Liposomen untereinander klar überwiegt. Dies konnte für den (bio)analytisch relevanten Temperaturbereich zwischen 25 und 50 °C gezeigt werden. Des Weiteren offenbarte die Studie, dass die Kombination von Liposomen mit hoher, negativer Oberflächenladung und Sensoroberflächen, die entweder mit einer hydrophoben $–CH_3$ Endgruppe oder einer hydrophilen –COOH Endgruppe modifiziert wurden, so gut wie keine Bindung zuließ, während eine deutliche Adsorption zu –OH und $–NH_2$ beobachtet werden konnte. Diese Erkenntnis ermöglicht clevere Strategien zur Oberflächengestaltung, die als attraktive Alternative zum häufig eingesetzten Blocken mit Polymeren und Proteinen dienen kann und unterstützt die Verbesserung von (bio)analytischen Anwendungen, die Liposomen als Signalverstärker verwenden, bedeutend.

Auf diesen Ergebnissen aufbauend, wurde ein einstellbares Signalverstärkungsprinzip für SPR entwickelt, das auf der Verwendung von Liposomen basiert, welche mit Lösungen mit hohem Brechungsindex gefüllt sind. Bis dato wurden diese nur selten für Verbesserung der SPR – Technik eingesetzt. Grundsätzlich ist die SPR Spektroskopie eine labelfreie Methode, die es erlaubt, Bindungsereignisse in Echtzeit zu verfolgen, erreicht aber ihre Grenzen, wenn sehr kleine Brechungsindexänderungen direkt bestimmt werden sollen, wie es z.B. bei kleinen Molekülen (< 400 Da) oder sehr niedrigen Analytkonzentrationen der Fall ist. Deshalb wird häufig ein zusätzlicher Bindungsschritt mit einem Verstärkungslabel benötigt, das das SPR Signal erhöht. Hierbei bewährten sich bisher Gold und Magnetit Nanopartikel (NPs), da die lokalisierten Oberflächenplasmonen der Au NPs sowie der hohe Brechungsindex und Oberflächenbelegung der Magnetit NPs die Leistungsfähigkeit des SPR deutlich verbessern können. Allerdings zeigen diese Materialien klare Nachteile in Bezug auf kolloidaler Stabilität, der Komplexität der Oberflächenmodifizierung und der Regulierbarkeit des Verstärkungsfaktors (VF). Die Ergebnisse der hierin enthaltenen Studien zeigten, dass Liposomen die ideale Wahl sind, um jene Limitierungen zu überwinden. Streptavidin, das an eine biotinylierte SPR Oberfläche bindet, rief nur sehr geringe Signaländerungen hervor, die durch den Einsatz von Liposomen immens verstärkt und damit detektierbar gemacht wurden. Der Verstärkungsfaktor hing stark vom Brechungsindex der eingekapselten Lösung ab und

kann dadurch an die entsprechenden Anforderungen einer analytischen Fragestellung angepasst werden. Bei der Verwendung von 500 mM Saccharoselösung innerhalb der Liposomen war ein maximaler VF von 23 möglich, der zu einer Verbesserung der Nachweisgrenze von Streptavidin von 10 nM auf 320 pM führte, wobei eine viel höhere Sensitivität von 3 mRIU (RIU = Brechungsindexeinheiten) pro logarithmischer Einheit der Konzentration zwischen 500 pM und 10 nM erreicht werden konnte. Diese Arbeit stellte das große Potential von Liposom-basierter SPR – Signalverstärkung heraus und zeigte seine Anwendbarkeit und Vielseitigkeit für die Entwicklung neuer Chemo- und Biosensoren mit SPR – Detektion.

Structure of the thesis

This thesis describes the preparation, characterization, and (bio)analytical application of highly stable, anionic liposomes as models for mechanistic surface adsorption studies and as versatile signal amplification tools in surface plasmon resonance (SPR) spectroscopy.

Chapter 1 provides an overview of the growing field of nanomaterials for signal enhancement in (bio)sensor and assay development. Two major trends can be identified: (I) Nano-sized particles including liposomes are utilized as amplification labels and improve the sensing performance through their unique physical and chemical properties. (II) The well-established strategy of enzymatic signal enhancement is extended by nanomaterials due to their large surface areas that can carry immense amounts of enzyme molecules. Thus, nanomaterials offer numerous new developments for signal amplification in (bio)analytical systems, which are needed for ultimate sensitivity and specificity to solve challenging analytical tasks such as in single-molecule detection, clinical diagnostics, food safety and environmental protection.

Liposomes are ubiquitously used in drug delivery applications as well as in analytical assays for signal amplification. Here, the understanding and consequent minimization of non-specific binding is a critical task. To address this challenge (**Chapter 2**) two types of highly stable, anionic liposomes with varying negative surface charge are prepared and characterized. The types of liposomes were chosen as they are favorably used in high-performing sensing approaches. Their binding behavior to alkane thiol modified gold surfaces of varying charge and hydrophilicity is investigated via SPR measurements. Langmuir isotherm models were used to interpret the results.

Based on these findings, a viable and highly versatile signal enhancement strategy for SPR using liposomes (**Chapter 3**) was developed, in order to improve one of its major limitations, i.e. the reliable detection of small molecules as well as low analyte concentrations. For this purpose, liposomes that bear biotin on their outer surface and encapsulate solutions providing a high refractive index, including 500 mM sucrose,

300 mM NaCl, and a combination of 130 mM NaCl and 35 mM sucrose, were synthesized and characterized regarding size, surface charge and concentration. The results obtained by SPR measurements were analyzed with respect to the limit of detection, enhancement factor and sensitivity.

In **Chapter 4** the advantages but also drawbacks of a new SPR technique integrated with liposome technology are critically analyzed. The main advantages of liposomes in (bio)analytical applications such as excellent colloidal long-term stability, large enhancement factors and simple surface functionalization are discussed and counterbalanced with perceived disadvantages such as increased assay time and complexity. Future uses of liposomes, surface engineering and the fundamental knowledge gained in this thesis are also presented.

Chapter 1: Nanomaterials as versatile tools for signal amplification in (bio)analytical applications

Abstract

(Bio)analytical applications often require efficient signal enhancement strategies that are directly integrated into the biorecognition process. Nanomaterials are increasingly used for this purpose, as their small size provides numerous unique properties. This review identifies recent trends in (bio)analytical sensing and discusses the use of nanomaterials as signal enhancement tags and as carriers in enzymatic amplification enabling significantly higher performance compared to traditional assays. Gold nanoparticles are one of the most established amplification tools and still play a major role in the development of highly sensitive (bio)assays. These are based on signal enhancement for detection approaches that range from colorimetric over plasmonic and electrochemical to mass spectrometric systems. We also discuss the opportunities of other nanomaterials such as nanocomposites including carbon nanotubes and graphene, magnetite nanoparticles, polymeric nanomaterials, liposomes and quantum dots that are increasingly used in this field. Based on the observed trends, future perspectives in (bio)assay development are presented.

This chapter has been accepted for publication.

Christoph Fenzl, Thomas Hirsch, Antje J. Baeumner, *Trends in Analytical Chemistry,* **2015**, accepted, DOI: 10.1016/j.trac.2015.10.018.

Author contributions

CF wrote the manuscript. TH and AJB revised the manuscript. AJB is corresponding author.

1. Introduction

Nanomaterials have earned increasing attention in recent years in analytical and bioanalytical applications including small species analysis, clinical diagnostics, point-of-care testing, pharmaceutical and therapeutic research as well as environmental and food safety monitoring [1–4]. Due to their small size, they combine various physical and chemical properties such as high surface-to-volume ratios that enable a high loading of receptor or signaling molecules [5,6] as well as special optical [7–9], electrochemical [10,11] or magnetic characteristics [12,13]. Therefore, nanomaterials are extensively used for signal amplification in countless sensing approaches. The great number of recently published reviews accounts for the global interest in this field of research. Ju *et al.* [1] and Chen *et al.* [14] cover the use of nanotailored materials in biosensing and biomarker detection in close detail to the year 2012 and show that such amplification approaches are not limited to special transduction techniques, but can be generally applied to nearly all kinds of detection methods. Nanomaterials have been shown to significantly improve the performance of immunosensors [15] and (bio)sensors based on microfluidics [6,7,16] and are ubiquitously utilized to enhance the signal in optical [1,14,17], electrochemical detection [10–12], or surface plasmon resonance [8] detection. Especially gold nanoparticles (NPs) [3,7], magnetic nanoparticles [12,13] and liposomes [6] have been in the focus of interest and show great promise, because well-established synthesis and surface functionalization protocols allow highly reproducible and versatile application in various assays as signal amplification tools. In addition, nanomaterials provide several current and future challenges for researchers, especially regarding the improvement of colloidal stability [3,9], biocompatibility [1,4], and potential upscaling for (commercial) mass production [14].

In this review, we emphasize the most recent developments in nanomaterials used for signal amplification in (bio)analytical applications. Covering the most promising publications from 2013 to 2015, we show how well-established nanomaterials such as gold NPs are increasingly popular and effective for the improvement of novel analytical assays and how new materials or material combinations are studied for further advancement. Two main trends can be identified and will be discussed in detail (Figure 1): (I) Nanostructured materials are widely used as amplification tags in analytical assays, as

their unique physical and chemical properties (e.g. the plasmonic color of gold nanoparticles) contribute strongly to amplified signal detection. Additionally, their intrinsic high surface area enables the immobilization of a large number of receptors that ensures binding to the target analyte. (II) The well-established protocol of enzymatic signal amplification (e.g. by horseradish peroxidase) is expanded by nanoparticles. They can carry numerous enzyme molecules and therefore upon binding of one particle a significant increase in signal can be generated. For both trends, the discussion is focused on the utilized materials, the chosen amplification and detection strategy as well as the achieved signal enhancement and improved limits of detection (LODs).

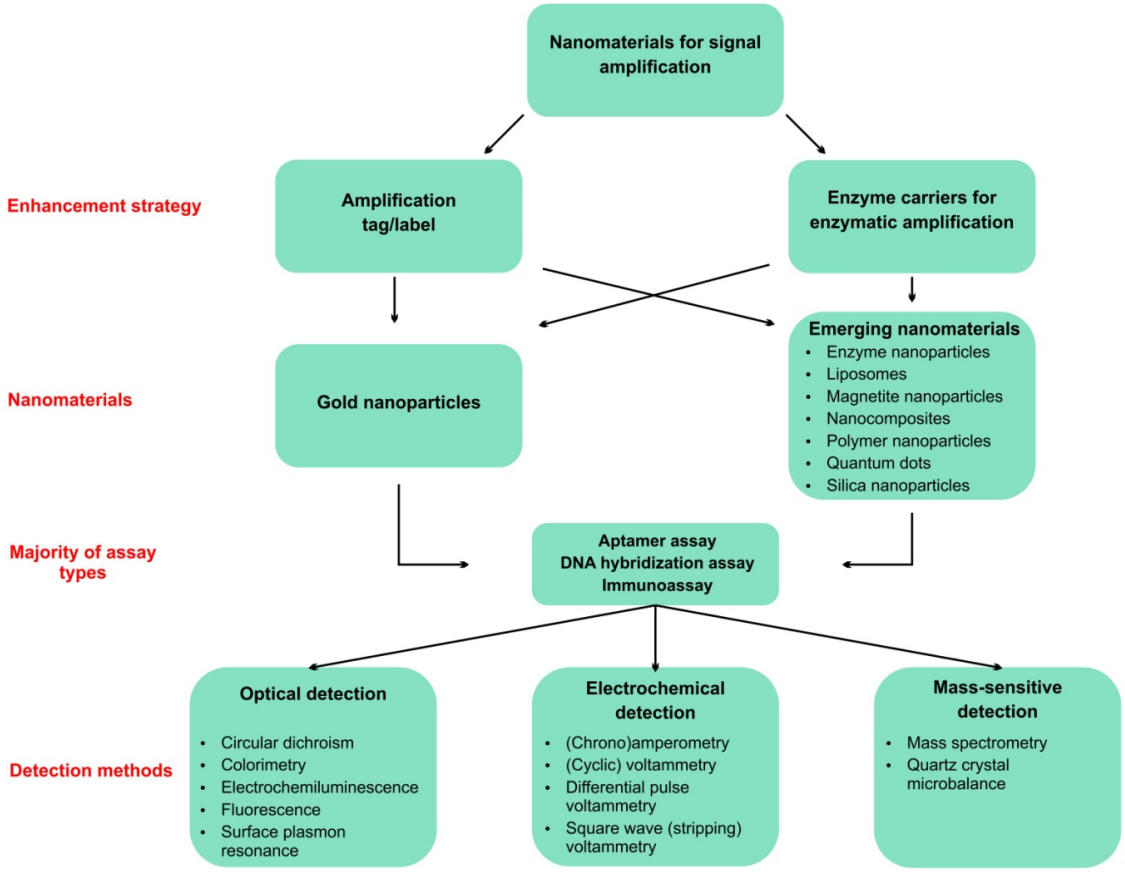

Figure 1. Overview of the recent trends in signal amplification strategies utilizing nanomaterials with respect to the materials used, the chosen assay types and the detection methods.

2. Nanomaterials as amplification tags

Using nanostructured and nano-sized materials – primarily nanoparticles – as signal enhancing labels is a common strategy to improve sensor performance, as it utilizes the intrinsic properties of the nanoparticles such as color [18], plasmonic effect [19], luminescence [20], high mass [21], but also many others. There are numerous materials suitable for generating nanostructures, but gold is still by far the most often described one and will therefore be discussed here first [3].

2.1. Gold nanoparticles-amplified sensing approaches

Gold NPs are commonly used as signal amplification labels for various kinds of sensors and assays. After their first description in immunochemistry by Faulk and Taylor in 1971 they have since long been used also in commercial analytical devices based on e.g. sandwich immunoassays or lateral flow assays [1,3,7]. Recent publications clearly focus primarily on DNA hybridization or aptamers as recognition element, but also standard immunochemistry is still used for the development of highly sensitive assays for biologically relevant targets. Nanospheres in the size ranging from 15 – 150 nm can be easily prepared following the well-established Turkevitch protocol where $HAuCl_4$ is reduced with citrate in boiling water [8]. However, not only spheres but also rods [19], clusters [22] and core-shell [23] particles have been utilized as amplification tags, as anisotropy or the combination of materials can lead to even further improvement. An overview over the recent advances using gold nanostructures as signal enhancing material can be found in Table 1. They have long been and are still very prominently used for colorimetric detection [3], but newer approaches also take advantage of the plasmonic effect in surface plasmon resonance (SPR) spectroscopy [8] or their electrocatalytic properties in electrochemical detection [11].

Table 1. Amplification strategies utilizing gold nanoparticles.

Detection method	Detection principle	Assay approach	Analyte	Limit of detection	Ref.
Optical	Colorimetry	DNA hybridization assay	DNA circuits	14 pM	[18]
		DNA hybridization assay	Cancer related point mutations (two base mismatch)	20 pM	[24]
		Chelation of heavy metal ions with DNA	Mercury (II) ions	1.6 pM	[25]
		Lateral flow assay	Phospholipase A2	1 nM	[26]
			Aflatoxin B1	0.5 nM	[27]
	Surface plasmon resonance	Aptamer sandwich assay	Thrombin	0.1 aM	[19]
		Sandwich immunoassay	Human cardiac myoglobin	10 pM	[28]
		Competitive immunoassay	Testosterone	0.17 nM	[29]
	Surface plasmon resonance / Quartz crystal microbalance	DNA hybridization assay after rolling circle amplification	Thrombin	0.78 aM	[21]
	Fluorescence	Sandwich immunoassay	17β-estradiol	23 fM	[20]
		Competitive immunoassay	Bisphenol A	0.3 fg mL^{-1}	[30]
		Gold nanoparticle-oligonucleotide immunosorbent assay	*Francisella tularensis*	23 CFU mL^{-1}	[31]
	Circular dichroism	Sandwich immunoassay	Microcystin-LR & prostate-specific antigen	0.8 pM & 15 zM	[32]
Electrochemical	Chronoamperometry	DNA hydbridization assay	BRCA1 gene	50 aM	[22]
	Square wave stripping voltammetry	Aptamer sandwich assay	Human epidermal growth factor receptor 2	37 fg mL^{-1}	[33]
Mass spectrometry	Laser desorption / ionization – time of flight	Covalent attachment of gold nanoparticles to the target	Glycoprotein	45 fM	[34]

The great majority of sensor approaches using gold nanoparticles are based on optical detection [18–21,24–32]. The simplest detection principle utilizes the colorimetric readout of the plasmonic band of the Au NPs [18,24–27]. In a DNA hybridization assay, circuits of DNA – as found in the hybridization chain reaction (HCR) or the catalyzed hairpin assembly (CHA) – were detected by intensity changes of the gold NP absorption maximum induced by the periodically ordered linkage of the nanoparticles to the target DNA [18]. In addition to the identification of size-dependent signal amplification, the authors discovered that a 13 nm diameter of NPs worked best for this novel assay format compared to larger sizes and limits of detection as low as 200 pM DNA circuits for HCR and 14 pM for CHA were achieved. A similar approach detected point mutations in the Kirsten rat sarcoma viral oncogene homologue gene, as they are important diagnostics markers for cancer [24]. The nanoparticles bind to magnetic beads in presence of the matching target DNA, but do not bind when the strands contain point mutations (Figure 2). A detection limit of 20 pmol L^{-1} DNA was reached and it was possible to distinguish between the matching strand and one with a single two-base mismatch. Thus, the traditional use of Au NPs described in these two papers demonstrates their immense application potential in genomic research. Expanding on this concept, the size-dependent signals of Au NPs can lead to further decreased LODs [25]. Here, DNA-conjugated gold nanospheres of two different sizes were used simultaneously for the rapid and ultrasensitive sensing of mercury (II) ions in aqueous solution via the specific thymine – mercury (II) – thymine bond with a LOD to 1.6 pmol L^{-1} Hg^{2+} in comparison to 93 pmol L^{-1} when using Au NPs of only one size. A clever approach applying traditional immunochemistry and taking advantage of the intense red color of Au NPs, was shown by the group of Stevens. They were able to develop a lateral flow assay for phospholipase A_2 [26]. The enzyme cleaves lipids in the lipid bilayer of a liposome and releases a polymer linker that leads to a multivalent nanoparticle network on the test strip using the well-known biotin-streptavidin interaction. With this approach a phospholipase A_2 concentration of 1 nM was detectable with bare-eye readout. The well-known concept of a lateral flow assay for aflatoxin B1 with Au NP colorimetric detection was improved by a factor of > 10 by the addition of secondary antibodies to the gold nanospheres [27], as this enabled precise adjustment of the required quantities of specific antibodies and nanoparticles.

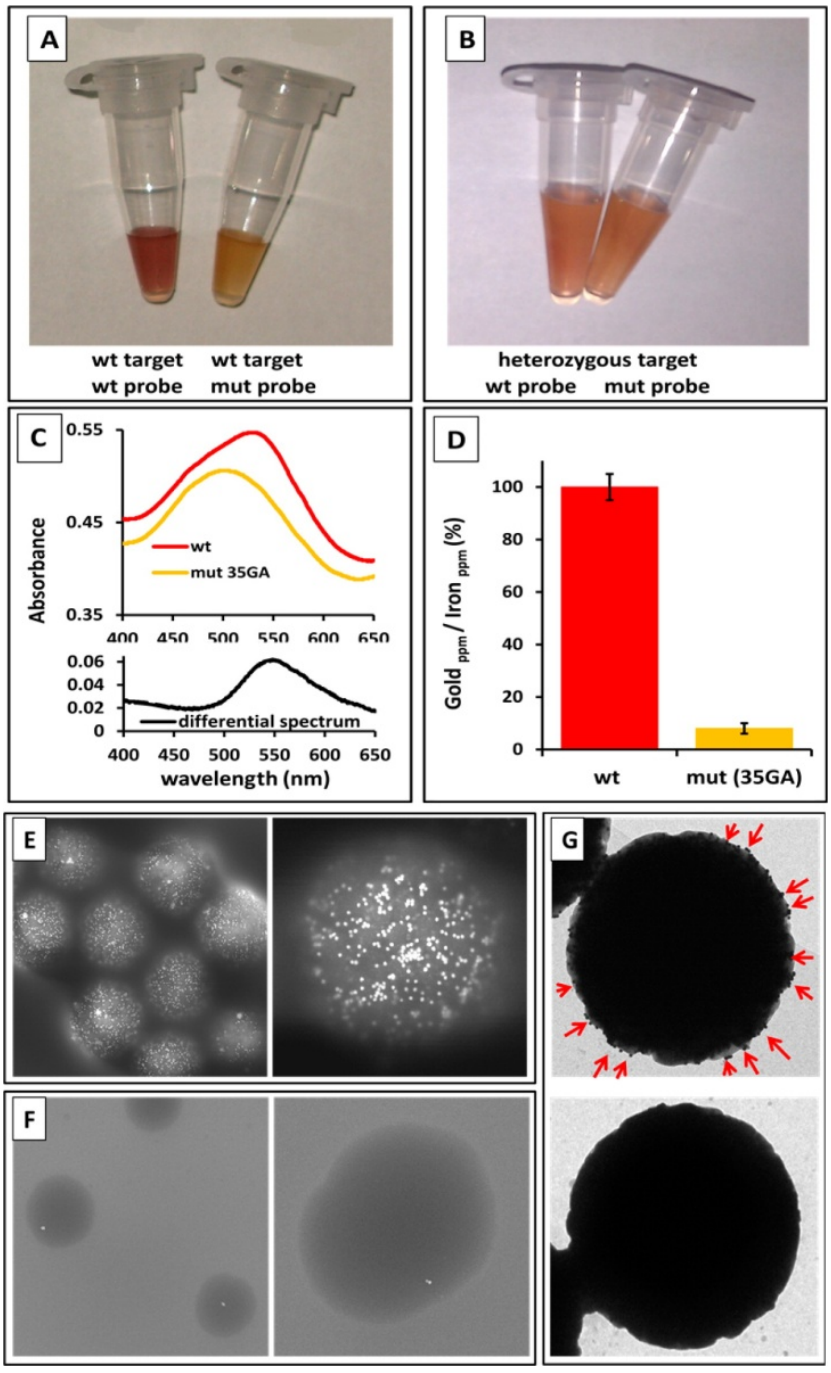

Figure 2. Discrimination of the cancer-related mutation 35G>A in Kirsten rat sarcoma viral oncogene homologue gene. (A) Bare-eye discrimination of point mutation 35G>A. (B) Heterozygous cell line hybridizes partially with both wild-type (wt) and mutant (mut) probes, giving an intermediate color (orange). (C) UV–vis spectra of wt and mut samples, and differential spectrum (wt minus mut spectra). (D) Inductively coupled plasma measurement of gold and iron in samples containing wt or point-mutated target. (E) Scanning electron microscopy images of the magnetic beads after hybridization with target and Au NP probes. In samples containing wt target, the magnetic beads are decorated with several Au NPs (brilliant dots). (F) In samples containing point-mutated targets, only rare Au NPs bind the magnetic beads. (G) Transmission electron microscopy images of samples containing wt target (top picture) and point-mutated target (bottom picture). Arrows highlight Au NP probes hybridized on matched target on the surface of magnetic beads. Reprinted with permission from [24]. Copyright 2013 American Chemical Society.

The phenomena of localized surface plasmons (SPs) generated by gold nanoparticles is extensively discussed in newer publications, as these enhance the performance of sandwich assays with surface plasmon resonance detection. Specifically, the localized SPs can couple to the propagating SPs of the gold sensor surface and thus amplify the signal [19,21,28,29]. Thrombin was detected with this principle at extremely low concentrations facilitating two different novel strategies based on aptamers as recognition elements [19,21]. The consecutive attachment of Au NPs of different shapes – first a nanorod and second a quasi-spherical NP – led to a two-step signal amplification that could measure thrombin at concentrations as low as 0.1 aM [19]. The other strategy relies on the binding of multiple gold nanospheres to a rolling circle amplification product bound to the analyte [21]. The LOD of 0.78 aM is also very low and it was shown that the assay can be transferred to quartz crystal microbalance technique with essentially the same sensitivity. Instead of using aptamers as recognition element, Archakov *et al.* enhanced a traditional sandwich immunoassay for human cardiac myoglobin with Au NPs, which is an early biomarker for the diagnosis of myocardial infarction. They observed a 30-fold improvement with NP enhancement and obtained a LOD of 10 pM that was measured in human blood serum. Finally, as the SPR technique faces a major challenge when trying to directly detect small molecules (molecular weight < 400 Da) competitive approaches are often utilized [8]. Here, the group of Masson showed that even a small molecule such as testosterone can be sensed at concentrations as low as 0.17 nM by facilitating a competitive immunoassay with antibody-conjugated gold nanospheres as competitors [29]. They also controlled the surface chemistry of the NPs in close detailed for optimized colloidal stability of their enhancement labels. These publications are examples of the growing trend of nanolabel-enhanced SPR as a viable strategy for the improvement of the sensing performance in (bio)analytical applications.

In addition to these approaches based on the plasmonic effects of gold NPs, new strategies have evolved utilizing this nanomaterial for the immobilization of a fluorescent dye [20,30,31] on the one hand, or the chirality caused by heterodimers of gold and silver NPs [32] on the other. Very low concentrations of 17β-estradiol (23 fM) – a prominent female sex hormone – were measured by a sandwich immunoassay followed by the release of fluorescein isothiocyanate from the Au NP surface [20]. Based on the same principle, an ultrasensitive competitive immunoassay for the food contaminant bisphenol

A was developed releasing fluorescent Europium (III) that reduced the LOD to 0.3 fg mL^{-1} [30]. In a more complex approach, Hong *et al.* used gold nanoparticles for the detection of the pathogen *Francisella tularensis* [31]. Here, DNA-conjugated gold nanospheres first bound to the lipopolysaccharides of the pathogen via immobilized antibodies. Then, the oligonucleotides were released from the NP surface and a complement RNA strand with conjugated fluorescent dye plus quencher was added. In a third step, RNase H freed the fluorophore from the quencher and thus enabled high sensitivity (LOD = 23 CFU mL^{-1}). A rather unexpected effect of generating chirality was discovered by Kotov *et al.* when building gold and silver nanoparticle pairs via a sandwich assay [32]. This effect led to changes in the circular dichroism spectra and allowed the extremely sensitive detection of proteins at zeptomolar levels.

Finally, beyond these innovative optical approaches, novel amplification strategies with electrochemical detection based on gold nanoparticles have been developed [22,33]. Again, DNA and aptamers are the favored recognition elements for these assays. A breast cancer related gene (BRCA 1) was measured at attomolar concentrations with a DNA hybridization assay followed by the monitoring of the electrochemical oxidation of Au NPs in presence of $HClO_4$ [22]. A sensing scheme for human epidermal growth factor receptor 2 (HER2) – a prognostic marker also for breast cancer – utilizes aptamer-conjugated gold nanospheres that possess additional hydrazine functionalities on the surface [33]. After NP binding, silver ions are reduced by the hydrazine forming an Ag shell around the spheres that is consecutively stripped away by electrochemical means allowing the detection of HER2 with a LOD of 37 fg mL^{-1} as well as the distinction between HER2-positive breast cancer cells and HER2-negative cells. A very different approach that concludes this overview of sensing techniques with Au NPs as amplification tags is based on mass spectrometry [34]. Glycosylated proteins are separated with boronic acid-functionalized magnetic beads followed by covalent attachment of gold nanoparticles to the proteins. Introducing this Au NP-protein conjugates into a laser desorption / ionization – time of flight mass spectrometer, intact glycoproteins at the femtomolar level can be detected due to the distinct mass peak of the nanoparticles.

In general, Au NP-based approaches can reach very high signal enhancement factors that lead to improved LODs. However, the great majority of the described publications rely on the standard surface modification techniques established in this field [1], and did not aim

for optimized surface engineering which is crucial for overcoming certain limitations such as non-specific binding [19] or limited colloidal long-term stability [3]. Additionally, gold nanoparticles are described as highly biocompatible [26,30], but nevertheless nanomaterials can enter the body and cause health risks such as inflammation or foreign body response [4]. Therefore additional efforts to improve biocompatibility would be beneficial.

2.2. Amplification approaches using other nanomaterials

Despite the numerous application possibilities of gold nanoparticles, new strategies using other nanomaterials evolved recently, especially with optical and electrochemical detection utilizing material properties that cannot be found in Au NPs such as fluorescence or electrochemiluminescence. The most promising approaches are summarized (Table 2).

Alternative materials can be a great asset when using fluorescence detection, as elaborate surface modification were necessary for Au NPs to add luminescence [19,30]. Liposomes, for example, are able to encapsulate a large amount of signaling molecules inside their inner cavity that lead to significant signal enhancement upon release [5]. These already very promising features can be even further amplified by additionally introducing magnetic nanoparticles into the liposomes [34]. In a DNA hybridization assay, the application of a magnetic field draws the liposomes to the surface where the target is present avoiding diffusion limited responses. This consequently enhances the performance of the assay by reducing required reaction times and lowering the limit of quantification to 35 pM nucleic acid which is a 15-fold improvement in comparison to a standard microtiter plate assay.

Table 2. Signal enhancement approaches utilizing various nanomaterials.

Detection method	Detection principle	Material	Assay approach	Analyte	Limit of detection	Ref.
Optical	Fluorescence	Dye encapsulating magnetic liposomes	DNA hybridization assay	*Cryptosporidium parvum* DNA	35 pM (limit of quantification)	[35]
		Quantum dots	Sandwich immunoassay	Cancer biomarkers	< 1 aM	[36]
		Quantum dot-containing polymer nanoparticles	Immunochromatographic assay	Aflatoxin B1	1.3 pM	[37]
		Quantum dot-containing polymer nanoparticles	Immunochromatographic assay	Hepatitis B virus surface antigen	3 pM	[38]
		Quantum dot – Au NP – silica nanosphere conjugate	DNA hybridization assay	Oligonucleotides	0.35 nM	[39]
		Dye-conjugated polymer nanoparticles	Fluorescence increase of ultra pH-sensitive nanoprobes on tumor cell encountering	Tumor tissue	-	[40]
	Electrochemiluminescence	Quantum dot-coated silica nanoparticles	Sandwich immunoassay	Prostate-specific antigen	94 fM	[41]
		Ruthenium polypyridyl functionalized ZnO mesocrystals	Sandwich immunoassay	α-fetoprotein	0.5 pM	[42]
	Surface plasmon resonance	Gold-capped Fe_3O_4 nanoparticles	Aptamer sandwich assay	Thrombin	0.1 nM	[23]
		Sucrose encapsulating lipsomes	Sandwich immunoassay	Streptavidin	320 pM	[43]
Electrochemical	Differential pulse voltammetry	Mesoporous Pt nanoparticles	Sandwich immunoassay	Breast cancer tumor markers	1 U L^{-1}	[44]
		Fe_3O_4@Ag-Pd hybrid nanoparticles	Aptamer sandwich assay	MCF-7 and T47D cells	40 cells mL^{-1} and 50 cells mL^{-1}	[45]
	Square wave voltammetry	Quantum dot-coated silica nanoparticles	Sandwich immunoassay	Liver cancer cells	5 cells mL^{-1}	[46]

Quantum dots (QDs) are very small, highly luminescent nanoparticles made of semiconductor materials that are prominently used as signal amplification tags due to their high brightness. However, large amounts of QDs are required for high signal amplification [36–38]. This can be achieved by surface engineering of the QDs followed by a biological self-assembly step [36]. Improved colloidal stability and strengthened resistance against non-specific adsorption was achieved by partially coating the QDs with zwitterionic ligands. With this clever strategy, it is possible to detect subattomolar levels of various cancer biomarkers in a sandwich immunoassay, whereas the assay times are shortened to only half the time required by conventional ELISA. Another approach for high QD amounts is their embedding into polymer particles and has been developed by Wang *et al.* [37,38]. With this point-of-care immunochromatographic assay, they are able to detect aflatoxin B1 in maize [37] and Hepatitis B virus surface antigen in serum [38] at very low concentrations. Again, the assay times were significantly shorter than that of commercial ELISA kits with comparable sensitivity. A very innovative approach to detect oligonucleotides uses QDs immobilized on the surface of silica nanospheres as Förster resonance energy transfer donors and Au NPs as acceptors that even enables multiplexing through different kinds of QDs [39]. However, the relatively high cytotoxicity of QDs remains still an unresolved issue that still strongly limits their *in vivo* use.

Up to now, it is still very challenging to universally monitor tumor tissue regardless of their geno- or phenotypes. For this purpose, highly pH-responsive polymer NPs with covalently attached fluorescent dye (Figure 3) were found to permit the identification of tumors due to the low extracellular pH in this tissue and enable a new sensitive method to the early detection of cancer for rapid treatment [40].

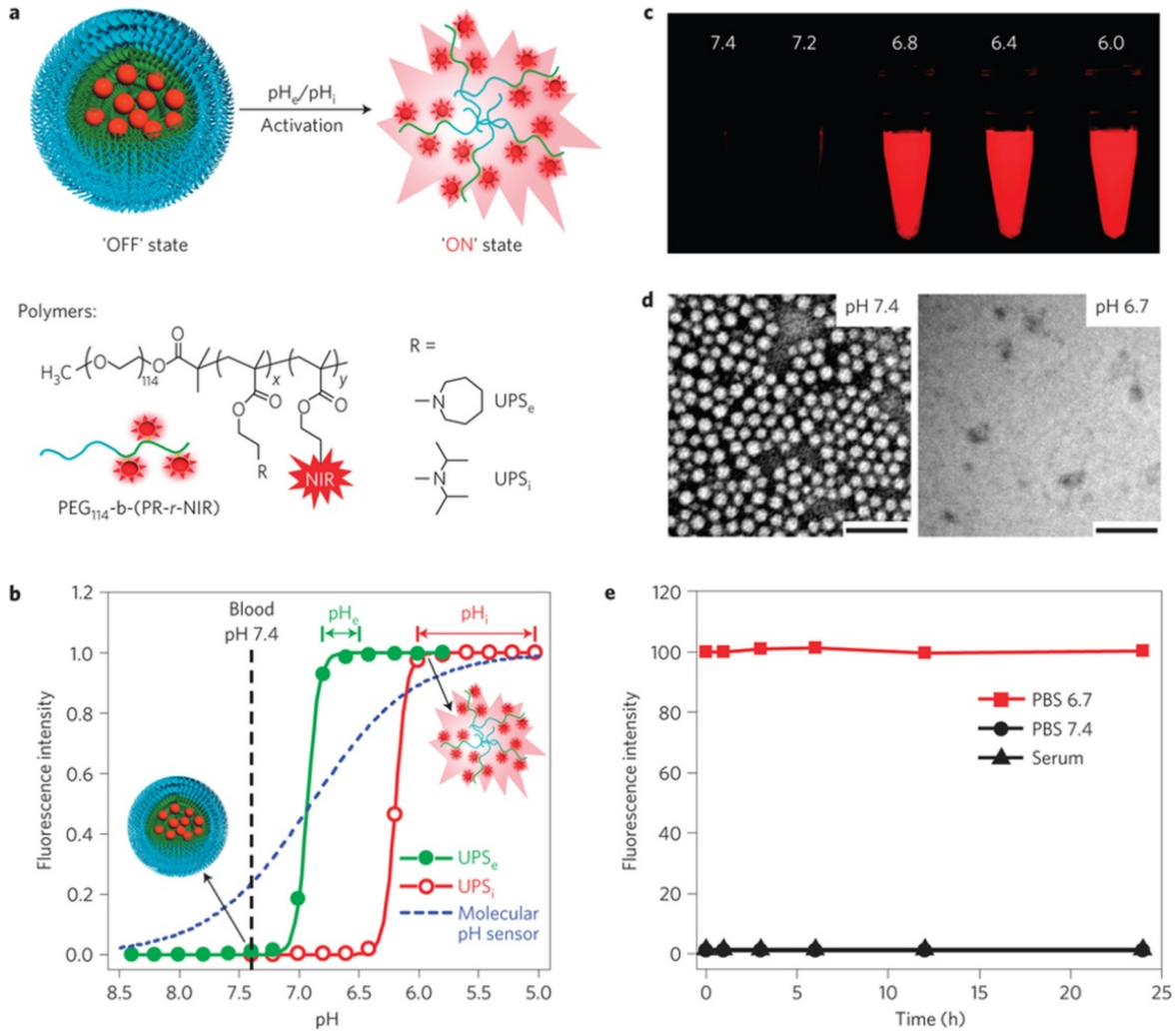

Figure 3. Synthesis and characterization of ultra pH-sensitive (UPS) nanoprobes. (a) Structural composition of two types of nanoprobe, UPS_e and UPS_i, with pH transitions at 6.9 and 6.2, respectively. The UPS_e is specifically designed to activate in acidic tumour extracellular fluid (pH_e = 6.5–6.8). The UPS_i can be activated inside acidic endocytic organelles (for example pH_i = 5.0–6.0). Cy5.5 is used as the near-infrared fluorophore in most of the animal studies. (b) Normalized fluorescence intensity as a function of pH for UPS_e and UPS_i nanoprobes. At high pH (for example, 7.4), both probes stay silent. At pH below their transitions (that is 6.9 and 6.2), the nanoprobes can be activated as a result of micelle dissociation. The blue dashed line simulates the pH response of a small molecular pH sensor with a pK_a of 6.9 based on the Henderson–Hasselbalch equation. For UPS, the pH response (ΔpH 10–90%) is extremely sharp (<0.25 pH unit between ON/OFF states) with >100-fold signal amplification. In contrast, small molecular pH sensors require 3 pH units for a comparable signal change. (c) Fluorescent images of UPS_e–Cy5.5 nanoprobe solution in different pH buffers ($\lambda_{ex}/\lambda_{em}$ = 675/710 nm). (d) Transmission electron micrographs of UPS_e nanoprobes at pH 7.4 and 6.7 (polymer concentration, 1 mg mL^{-1}; scale bars, 100 nm). (e) UPS_e nanoprobes remain stable in fresh mouse serum over 24 h at 37 °C. Reprinted by permission from Macmillan Publishers Ltd: Nature Materials [40], copyright 2013.

One major disadvantage of fluorescence detection is the high background signal often encountered in biological samples. An emerging detection technique that overcomes this limitation is electrochemiluminescence (ECL) [47], as excitation is achieved by electrochemical reaction rather than illumination. Albeit very promising, signal amplification tags are still necessary for highly sensitive immunoassays with ECL readout [41,42]. QD-coated silica nanoparticles [41] and ZnO mesocrystals functionalized with Ruthenium bipyridyl [42] were recently shown to significantly enhance protein detection when used as labels, as they guarantee the presence of an high amount of ECL markers near the electrode. Silica and ZnO was chosen as host material due to their low toxicity and good functionalization possibilities.

New materials are also explored in the field of surface plasmon resonance in order to further improve sensitivity. Whereas signal amplification with Au NPs is based on the coupling of the localized SPs, magnetic nanoparticles enhance the SPR performance due to high refractive index and surface mass loading [8]. As consequence, the combination of both materials by growing a gold shell on Fe_3O_4 nanoparticles generates highly efficient amplification tags for small protein detection [23]. Gold capping also improved the stability and biocompatibility properties of the magnetite particles. Although the absolute limit of detection for the exemplary analyte thrombin is higher than for other approaches using Au NPs, this assay is easier and faster to handle, as it lacks the need of a second labeling step [19] or of a rolling circle amplification step [21]. In order to increase versatility, colloidal stability and biocompatibility, the previously mentioned liposomes were also used in SPR technique [43]. Encapsulating high refractive index sucrose solutions and using these liposomes in a sandwich immunoassay for streptavidin as model analyte it was possible to improve the LOD by a factor of 30 in comparison to non-amplified detection. With electrochemical detection, sandwich-type assays were used to detect tumor markers [44] or whole cells [45,46]. Mesoporous Pt NPs [44] or Fe_3O_4@Ag-Pd hybrid nanospheres [45] show great promise as labels for the improvement of existing electrochemical assays due to their high stability and excellent electrocatalytic activity. Also, silica NPs that are coated with different types of QDs not only enhance the signal, but function also as tracing tags, as different biorecognition events can be identified by the distinct voltammetric peak yielded by each type [46].

In conclusion, it can be observed from publications of the last three years that Au NPs still pave the way for broad application of nanomaterials as signal enhancement tools in a wide variety of detection approaches. Novel investigations though include not only gold as material but also increasingly new nanomaterials with other, unique properties for signal amplification that soon will find equally strong application in (bio)analytical systems, as they try to overcome certain limitations and improve important properties such as colloidal stability and low cytotoxicity.

3. Nanomaterials as carriers for enzymatic signal enhancement

3.1. Enzymatic amplification utilizing gold nanoparticles

A prominently favored assay type in (bio)analytical research and commercial applications is the enzyme-linked immunosorbent assay (ELISA), as it combines the high selectivity of immunoassays with enzyme-mediated signal amplification [15]. However, only one enzyme binds to one analyte molecule in a standard ELISA, which often leads to limitations in sensitivity or to considerably long assay times until enough signal molecules are generated. Here, nanomaterials can elegantly contribute to the improvement of this concept, as they can bind many recognition and enzyme molecules on only one nanoparticle that binds to the analyte [15]. As before, the well-known gold nanoparticles are a standard nanomaterial used for this strategy [3]. The recent advances in this field – again utilizing mainly antibodies, aptamers and DNA as recognition elements – are summarized in Table 3.

Table 3. Enzyme-mediated signal amplification with gold nanoparticles as carriers.

Detection method	Detection principle	Enzyme	Assay approach	Analyte	Limit of detection	Ref.
Optical	Colorimetry	Horseradish peroxidase	Sandwich immunoassay	κ -casein	4.2 ng mL^{-1}	[48]
			Sandwich immunoassay	Respiratory syncytial virus	0.5 pg mL^{-1}	[49]
			Sandwich immunoassay	β -casein	4.8 ng mL^{-1}	[50]
			Antibody-aptamer sandwich assay	*Salmonella enterica* serovar Typhimurium	10^3 CFU mL^{-1}	[51]
			Sandwich immunoassay	*Escherichia coli* O157:H7	100 CFU mL^{-1}	[52]
			Immunoassay	Nogo-66	-	[53]
			Antibody-aptamer sandwich assay	Chloramphenicol	3 pg mL^{-1}	[54]
	Electrochemiluminescence	Glucose oxidase	Sandwich immunoassay	Protein kinase A activity	0.013 U mL^{-1}	[55]
		Xanthine oxidase	Zr^{4+}-mediated chelation sandwich assay	Protein kinase A activity	0.09 U mL^{-1}	[56]
	Fluorescence	Horseradish peroxidase	DNA hybridization assay	Carcinoembryonic antigen gene and colorectal cancer cells	5 fM and 1 cell mL^{-1}	[57]
			Competitive aptamer assay	Adenosine and Cocaine	0.1 pM and 0.5 pM	[58]
Electrochemical	Differential pulse voltammetry	Horseradish peroxidase	Sandwich immunoassay	Procalcitonin	0.5 pg mL^{-1}	[59]
			Aptamer assay	Mucin 1 protein	2.2 nM	[60]
			DNA hybrization assay	Phanerochaetechrysosporium manganese peroxidase gene	8 aM	[61]
	Voltammetry/ Amperometry	Alkaline phosphatase	DNA/RNA hybridization assay	MicroRNA	3 fM	[62]
		Glucoamylase	Aptamer assay	Thrombin	10 pM	[63]
	Cyclic voltammetry	Horseradish peroxidase	Sandwich immunoassay	Diethylstilbestrol	2 pg mL^{-1}	[64]
Surface acoustic wave	Quartz crystal microbalance	Glucoamylase	Sandwich immunoassay	Brevetoxin B	0.6 pg mL^{-1}	[65]

The most direct approach for the improvement of the standard ELISA is to simply exchange the antibody-horseradish peroxide (HRP) label with a Au NP carrying the enzymes and recognition elements, but keeping the colorimetric readout of the enzyme-induced color reaction [48,49]. With this strategy, a 10-fold improvement was achieved for the detection of κ-casein in bovine milk samples [48] and a NP-enhanced ELISA showed an even 50-fold better performance in comparison to a conventional assay for respiratory syncytial virus [49]. In order to further shorten assay times, new dual-particle approaches enabling magnetic separation were developed [50,51]. The protein β-casein was detected at concentrations as low as 4.8 ng mL^{-1} in bovine milk samples which is 700 times lower than the LOD of a comparable micro-sized magnetic bead assay with HRP-antibody labels. Additionally, the probes showed good long-term stability of 6 weeks at 4 °C [50]. The same technique was used for *Salmonella enterica* serovar Typhimurium in an assay binding aptamer-modified magnetic beads and Au NPs with antibodies and HRP to the bacterium [51], which enabled the rapid diagnosis of the food borne pathogen that was not possible with such sensitivity up to this point. Here, the concentration of surface-immobilized biomolecules was optimized that AuNPs were able to withstand solutions with high salt concentrations which usually would lead to aggregation. For all those approaches the Au NPs were modified by simple adsorption of the enzymes to the particles. This has certain limitations in reproducibility. Therefore, Irudayaraj *et al.* used biotinylated Au NPs and streptavidin-conjugated HRP to develop a highly sensitive lateral-flow assay for *E. coli* [52]. Even higher amounts of enzymes and recognition elements per nanoparticle are possible when previously modifying the gold nanospheres with an atom transfer radical polymer. This strategy lowered the LOD for the cancer biomarker Nogo-66 by a factor of 81 compared to a standard ELISA test [53]. This trend of higher amounts of enzymes was continued by Zeng *et al.* who used a polymeric conjugate of horseradish peroxidase and antibody with a high enzyme-to-antibody ratio for the highly sensitive detection of chloramphenicol in fish and duck samples [54].

Enzyme reactions are not only used to generate colored products for a colorimetric readout via HRP, but also to induce an ECL signal in the presence of luminol by generating H_2O_2 *via* oxidases [55,56]. The performance of assays using this detection principle is significantly improved by using Au NPs as enzyme carriers, as much more H_2O_2 is generated in shorter reaction times. This was used for the development of rapid and

low-cost monitoring methods of protein kinase activity on peptides immobilized on gold. As recognition element either anti-phosphoserine antibodies [55] or the chelating effect of Zr^{4+} [56] were chosen to distinguish between phosphorylated and non-phosphorylated peptides. This approach is an emerging alternative to established techniques for the kinase activity monitoring such as mass spectroscopy or SPR.

The recent advances in nanoparticle-enhanced microfluidic point-of-care testing devices display the desire for cost-effective, easy-to-operate and portable diagnostic tools [7]. In order to transfer the immunoassay concept into microfluidics, one faces several challenges such as the elaborate handling of minute volumes of reaction solutions and very short path lengths for optical detection limiting sensitivity [7,57,58]. Therefore, signal amplification with nanomaterials helps improving such devices significantly. Zhang *et al.* developed a DNA hybridization assay for carcinoembryonic antigen gene and colorectal cancer cells [57] as well as an aptamer-based measurement scheme for adenosine and cocaine [58] with fluorescence detection that utilize HRP-conjugated Au NPs and streptavidin-modified quantum dots in a microfluidic channel. They demonstrated that their sensitivity is significantly higher (up to 1000-fold) than in off-chip tests.

For electrochemical detection, the combination of Au NPs with enzymes provides two advantages – the high electrocatalytic activity of the particles themselves plus a second enhancement due to the enzymatic reaction [10]. Employing this strategy for sandwich immunoassays [59,64] as well as assays based on aptamers [60,63] or DNA/RNA hybridization [61,62] resulted in the highly sensitive detection of inflammatory [59] and tumor markers [60], oligonucleotides [61,62], thrombin [63] or the food contaminant diethylstilbestrol [64]. Furthermore, it is also shown that when a single amplification approach is insufficient, further enhancement can be achieved either by modification of the working electrode with nanostructured materials such as carbon nanotubes [59,60] that were additionally modified with chitosan for improved stability and biocompatibility, mesoporous carbon nitride (Figure 4) [61] and Au NPs [64], or by increasing the number of enzyme on the NP label, e.g. by surface modification with enzyme-polymer complexes [64].

The mass-sensitive detection principle of quartz crystal microbalance (QCM) suffers from similar limitations as SPR spectroscopy when trying to monitor small molecules [8,65].

Here, Tang *et al.* presented a novel amplification strategy for the detection of brevetoxin B (molecular weight ~ 900 Da) based on a sandwich-type assay with enzyme-conjugated gold nanospheres [65]. After binding to the analyte, the glucoamylase immobilized on the Au NP hydrolyzes amylopectin to glucose which then displaces dextran by competitively binding to concanavalin A on the QCM surface resulting in a distinct frequency change.

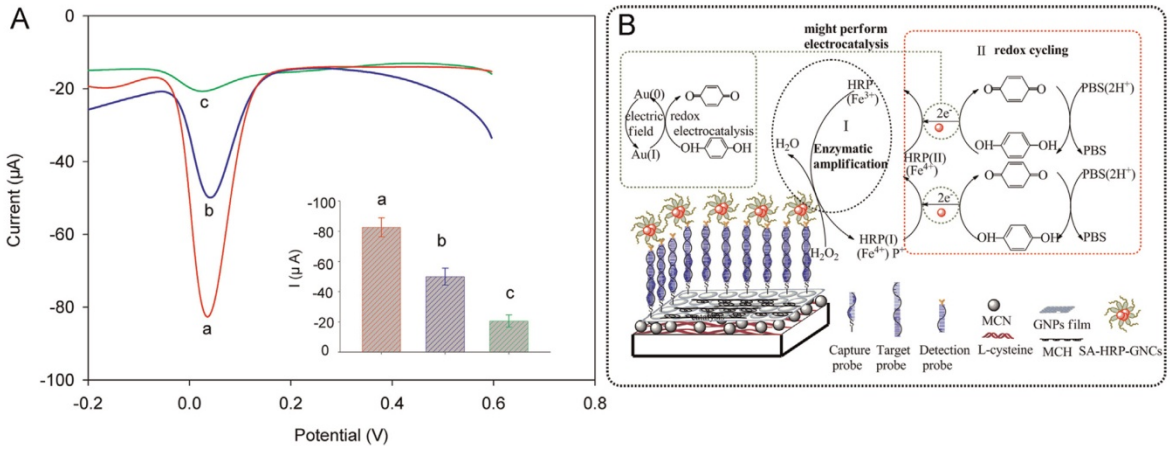

Figure 4. (A) Differential pulse voltammetry curves of (a) 10 pM target with streptavidin – horseradish peroxidase (SA-HRP) – scaffolded – gold nanoclusters (GNCs), (b) 10 pM target with SA-HRP and (c) blank with SA-HRP-scaffolded-GNCs. Inset: the corresponding peak currents. Error bars indicate standard deviations from three replicative tests. (B) Enzymatic amplification and redox cycling mechanism of biosensor. Reprinted from [61], Copyright 2015, with permission from Elsevier.

3.2. Emerging nanomaterials as enzyme carriers for signal enhancement

Although gold nanoparticles build the basis for most NP-based enzymatic amplification strategies, numerous other nanomaterials have been proposed as enzyme carriers in recent years (Table 4), especially for the improvement of ECL [66,67] and electrochemical assays [68–72].

Table 4. Nanomaterials as enzyme carriers for signal amplification.

Detection method	Detection principle	Nanomaterial	Enzyme	Assay approach	Analyte	Limit of detection	Ref.
Optical	Electrochemiluminescence	Carbon nanotube/Au NP/ Pd NP nanocomposite	S-adenosyl-L-homocysteine hydrolase	Sandwich immunoassay	Carcinoembryonic antigen	33 fg mL^{-1}	[66]
Electrochemical	Cyclic voltammetry	Carbon nanotubes functionalized with Pd NPs	Glucose oxidase/ Horseradish peroxidase	Sandwich immunoassay	α-fetoprotein	3.3 fg mL^{-1}	[67]
		Mesoporous silica NPs / Fe_3O_4 nanospheres	Horseradish peroxidase	Sandwich immunoassay	α-fetoprotein	4 pg mL^{-1}	[68]
		Pt nanochains	Glucose oxidase	Sandwich immunoassay	*Escherichia coli* O157:H7	15 CFU mL^{-1}	[69]
		Graphene/ionic liquid/ Au NP nanocomposite	Alkaline phosphatase	Sandwich immunoassay	Human apurinic/apyrimidinic endonuclease 1	0.04 pg mL^{-1}	[70]
		HRP nanospheres / Au NP nanocomposite	Horseradish peroxidase	Sandwich immunoassay	α-fetoprotein	8.3 pg mL^{-1}	[71]
		Silica nanoparticles	Horseradish peroxidase	Competitive immunoassay	Aflatoxin B1	8.7 pM	[72]

Highly sensitive ECL detection requires the presence of both an ECL reactant and coreactant in sufficient amounts [47]. Chai *et al.* used the very large surface area of carbon nanotubes coated with gold and palladium nanoparticles to immobilize a great number of enzyme molecules that *in-situ* generated the ECL coreactant. The immunoassays based on this amplification and detection strategy for the tumor markers carcinoembryonic antigen [66] and α-fetoprotein [67] had extremely low detection limits in the range of a few femtograms per milliliter.

The advantage of large surface-to-volume ratios for the immobilization of enzymes has also been employed with other novel nanomaterials and nanocomposites to amplify the electrochemical signal in sandwich immunoassays [68–71]. For example, mesoporous silica particles were coated with magnetite nanospheres and loaded with HRP resulting in the detection of α-fetoprotein at concentrations as low as 4 pg mL^{-1} [68], which is a higher LOD than with ECL detection (3.3 fg mL^{-1}) [67], but requires a much simpler detection setup. The increase of surface area is also achieved by utilizing platinum nanochains [69] as carriers for glucose oxidase. With this label, *E. coli* was detected with high sensitivity suitable for early clinical detection. This study also improved biocompatibility significantly through their careful choice of materials for the enzyme-conjugated nanolabel as well as for the nanocomposite electrode. Another innovative nanocomposite consisting of graphene, ionic liquid and Au NPs was shown as a highly efficient enzyme carrier for the detection of the cancer marker human apurinic/apyrimidinic endonuclease 1 protein [70]. Crosslinking of the HRP itself in order to form nanospheres and coating those with hollow Au NPs provides an elegant method for the electrochemical detection of α-fetoprotein [71]. Knopp *et al.* further developed the previously mentioned displacement strategy [65] and adopted it for a novel signal-on electrochemical detection of aflatoxin B1 with a LOD of 8.7 pM that can be even suitable for the use in mass production of microfluidic lab-on-chip devices [72].

4. Conclusions and future challenges

Nanomaterials offer versatile opportunities for signal amplification in (bio)analytical systems. Nano-sized gold particles have been used for decades as signaling means in sensors and (bio)assays, yet new discoveries, new assay formats, new detection

approaches and new applications are still going strong in scientific research with more than 1,000 publications found in the Web of Science Database using the keyword “gold nanoparticle assay” in 2013 – 2015 alone. When originally used for absorbance-based detection, transduction principles ranging from surface plasmon resonance to electrochemistry and mass spectrometry demonstrate ever growing possibilities for the integration into analytical systems. The current trend thus also emphasizes their use to answer complex analytical questions such as cancer and pathogen detection at lowest limits of detection, and their integration into lab-on-a-chip devices and point-of-care systems.

New nanomaterials and nanocomposites such as the combination of NPs with carbon nanotubes or graphene are being introduced to hone in on further improvements that are afforded by different material properties. Where gold lacks in fluorescence and luminescence properties, liposomes, quantum dots or upconverting nanoparticles can fill the void. Other materials are used instead of gold and provide even greater enhancement factors. Both trends deserve and require further investigations and material development as (bio)analytical sensors are needed for ultimate sensitivity and specificity to solve the challenging analytical tasks such as in single-molecule detection, clinical diagnostics, food safety and environmental protection. Although there have been remarkable improvements and new discoveries over the last three years, major challenges such as overcoming limited colloidal (long-term) stability or increasing biocompatibility are still very hot topics and require further studying. In addition, the vast majority of the presented approaches do not show sufficient upscaling techniques of their sensing strategy which is however needed for potential commercial production.

The Luminex barcode system and multi-colored fluorescence of quantum dots are prime examples for simultaneous multi-analyte detection. Research on new nanomaterials and nanocomposites can become a leading strategy to move this important effort forward and enable the integration into point-of-care and other simple assay platforms.

5. References

[1] J. Lei, H. Ju, Signal amplification using functional nanomaterials for biosensing, Chem. Soc. Rev. 41 (2012) 2122–2134. doi:10.1039/C1CS15274B.

[2] C. Fenzl, T. Hirsch, O.S. Wolfbeis, Photonic Crystals for Chemical Sensing and Biosensing, Angew. Chem. Int. Ed. 53 (2014) 3318–3335. doi:10.1002/anie.201307828.

[3] L. Dykman, N. Khlebtsov, Gold nanoparticles in biomedical applications: recent advances and perspectives, Chem. Soc. Rev. 41 (2012) 2256–2282. doi:10.1039/C1CS15166E.

[4] V. Scognamiglio, Nanotechnology in glucose monitoring: Advances and challenges in the last 10 years, Biosens. Bioelectron. 47 (2013) 12–25. doi:10.1016/j.bios.2013.02.043.

[5] D. Tang, Y. Cui, G. Chen, Nanoparticle-based immunoassays in the biomedical field, Analyst. 138 (2013) 981–990. doi:10.1039/C2AN36500F.

[6] K.A. Edwards, O.R. Bolduc, A.J. Baeumner, Miniaturized bioanalytical systems: enhanced performance through liposomes, Curr. Opin. Chem. Biol. 16 (2012) 444–452. doi:10.1016/j.cbpa.2012.05.182.

[7] J. Sun, Y. Xianyu, X. Jiang, Point-of-care biochemical assays using gold nanoparticle-implemented microfluidics, Chem. Soc. Rev. 43 (2014) 6239–6253. doi:10.1039/C4CS00125G.

[8] S. Zeng, D. Baillargeat, H.-P. Ho, K.-T. Yong, Nanomaterials enhanced surface plasmon resonance for biological and chemical sensing applications, Chem. Soc. Rev. (2014) 3426–3452. doi:10.1039/c3cs60479a.

[9] V. Muhr, S. Wilhelm, T. Hirsch, O.S. Wolfbeis, Upconversion Nanoparticles: From Hydrophobic to Hydrophilic Surfaces, Acc. Chem. Res. 47 (2014) 3481–3493. doi:10.1021/ar500253g.

[10] C. Zhu, G. Yang, H. Li, D. Du, Y. Lin, Electrochemical Sensors and Biosensors Based on Nanomaterials and Nanostructures, Anal. Chem. 87 (2015) 230–249. doi:10.1021/ac5039863.

[11] L. Ding, A.M. Bond, J. Zhai, J. Zhang, Utilization of nanoparticle labels for signal amplification in ultrasensitive electrochemical affinity biosensors: A review, Anal. Chim. Acta. 797 (2013) 1–12. doi:10.1016/j.aca.2013.07.035.

[12] M. Hasanzadeh, N. Shadjou, M. de la Guardia, Iron and iron-oxide magnetic nanoparticles as signal-amplification elements in electrochemical biosensing, TrAC Trends Anal. Chem. 72 (2015) 1–9. doi:10.1016/j.trac.2015.03.016.

[13] T.A.P. Rocha-Santos, Sensors and biosensors based on magnetic nanoparticles, TrAC Trends Anal. Chem. 62 (2014) 28–36. doi:10.1016/j.trac.2014.06.016.

[14] M. Swierczewska, G. Liu, S. Lee, X. Chen, High-sensitivity nanosensors for biomarker detection, Chem. Soc. Rev. 41 (2012) 2641–2655. doi:10.1039/C1CS15238F.

[15] X. Pei, B. Zhang, J. Tang, B. Liu, W. Lai, D. Tang, Sandwich-type immunosensors and immunoassays exploiting nanostructure labels: A review, Anal. Chim. Acta. 758 (2013) 1–18. doi:10.1016/j.aca.2012.10.060.

[16] C. Hu, W. Yue, M. Yang, Nanoparticle-based signal generation and amplification in microfluidic devices for bioanalysis, Analyst. 138 (2013) 6709–6720. doi:10.1039/C3AN01321A.

[17] P. Holzmeister, G.P. Acuna, D. Grohmann, P. Tinnefeld, Breaking the concentration limit of optical single-molecule detection, Chem. Soc. Rev. 43 (2014) 1014–1028. doi:10.1039/C3CS60207A.

[18] K. Quan, J. Huang, X. Yang, Y. Yang, L. Ying, H. Wang, et al., An enzyme-free and amplified colorimetric detection strategy: assembly of gold nanoparticles through target-catalytic circuits, Analyst. 140 (2015) 1004–1007. doi:10.1039/C4AN02060J.

[19] S.H. Baek, A.W. Wark, H.J. Lee, Dual Nanoparticle Amplified Surface Plasmon Resonance Detection of Thrombin at Subattomolar Concentrations, Anal. Chem. 86 (2014) 9824–9829. doi:10.1021/ac5024183.

[20] L. Du, W. Ji, Y. Zhang, C. Zhang, G. Liu, S. Wang, An ultrasensitive detection of 17β-estradiol using a gold nanoparticle-based fluorescence immunoassay, Analyst. 140 (2015) 2001–2007. doi:10.1039/C4AN01952K.

[21] P. He, L. Liu, W. Qiao, S. Zhang, Ultrasensitive detection of thrombin using surface plasmon resonance and quartz crystal microbalance sensors by aptamer-based rolling circle amplification and nanoparticle signal enhancement, Chem. Commun. 50 (2014) 1481–1484. doi:10.1039/C3CC48223E.

[22] P.A. Rasheed, N. Sandhyarani, A highly sensitive DNA sensor for attomolar detection of the BRCA1 gene: signal amplification with gold nanoparticle clusters, Analyst. 140 (2015) 2713–2718. doi:10.1039/C5AN00004A.

[23] H. Chen, F. Qi, H. Zhou, S. Jia, Y. Gao, K. Koh, et al., Fe_3O_4@Au nanoparticles as a means of signal enhancement in surface plasmon resonance spectroscopy for thrombin detection, Sens. Actuators B Chem. 212 (2015) 505–511. doi:10.1016/j.snb.2015.02.062.

[24] P. Valentini, R. Fiammengo, S. Sabella, M. Gariboldi, G. Maiorano, R. Cingolani, et al., Gold-Nanoparticle-Based Colorimetric Discrimination of Cancer-Related Point Mutations with Picomolar Sensitivity, ACS Nano. 7 (2013) 5530–5538. doi:10.1021/nn401757w.

[25] Y. Deng, X. Wang, F. Xue, L. Zheng, J. Liu, F. Yan, et al., Ultrasensitive and rapid screening of mercury(II) ions by dual labeling colorimetric method in aqueous samples and applications in mercury-poisoned animal tissues, Anal. Chim. Acta. 868 (2015) 45–52. doi:10.1016/j.aca.2015.02.003.

[26] R. Chapman, Y. Lin, M. Burnapp, A. Bentham, D. Hillier, A. Zabron, et al., Multivalent Nanoparticle Networks Enable Point-of-Care Detection of Human Phospholipase-A2 in Serum, ACS Nano. 9 (2015) 2565–2573. doi:10.1021/nn5057595.

[27] A.E. Urusov, A.V. Zherdev, B.B. Dzantiev, Use of gold nanoparticle-labeled secondary antibodies to improve the sensitivity of an immunochromatographic assay for aflatoxin B1, Microchim. Acta. 181 (2014) 1939–1946. doi:10.1007/s00604-014-1288-4.

[28] O.V. Gnedenko, Y.V. Mezentsev, A.A. Molnar, A.V. Lisitsa, A.S. Ivanov, A.I. Archakov, Highly sensitive detection of human cardiac myoglobin using a reverse sandwich immunoassay with a gold nanoparticle-enhanced surface plasmon resonance biosensor, Anal. Chim. Acta. 759 (2013) 105–109. doi:10.1016/j.aca.2012.10.053.

[29] H. Yockell-Lelièvre, N. Bukar, K.S. McKeating, M. Arnaud, P. Cosin, Y. Guo, et al., Plasmonic sensors for the competitive detection of testosterone, Analyst. 140 (2015) 5105–5111. doi:10.1039/C5AN00694E.

[30] L. Du, C. Zhang, L. Wang, G. Liu, Y. Zhang, S. Wang, Ultrasensitive time-resolved microplate fluorescence immunoassay for bisphenol A using a system composed on gold nanoparticles and a europium(III)-labeled streptavidin tracer, Microchim. Acta. 182 (2014) 539–545. doi:10.1007/s00604-014-1356-9.

[31] S.-H. Seo, Y.-R. Lee, J. Ho Jeon, Y.-R. Hwang, P.-G. Park, D.-R. Ahn, et al., Highly sensitive detection of a bio-threat pathogen by gold nanoparticle-based oligonucleotide-linked immunosorbent assay, Biosens. Bioelectron. 64 (2015) 69–73. doi:10.1016/j.bios.2014.08.038.

[32] X. Wu, L. Xu, L. Liu, W. Ma, H. Yin, H. Kuang, et al., Unexpected Chirality of Nanoparticle Dimers and Ultrasensitive Chiroplasmonic Bioanalysis, J. Am. Chem. Soc. 135 (2013) 18629–18636. doi:10.1021/ja4095445.

[33] Y. Zhu, P. Chandra, Y.-B. Shim, Ultrasensitive and Selective Electrochemical Diagnosis of Breast Cancer Based on a Hydrazine–Au Nanoparticle–Aptamer Bioconjugate, Anal. Chem. 85 (2013) 1058–1064. doi:10.1021/ac302923k.

[34] M. Liu, L. Zhang, Y. Xu, P. Yang, H. Lu, Mass spectrometry signal amplification for ultrasensitive glycoprotein detection using gold nanoparticle as mass tag combined with boronic acid based isolation strategy, Anal. Chim. Acta. 788 (2013) 129–134. doi:10.1016/j.aca.2013.05.063.

[35] K.A. Edwards, A.J. Baeumner, Enhancement of Heterogeneous Assays Using Fluorescent Magnetic Liposomes, Anal. Chem. 86 (2014) 6610–6616. doi:10.1021/ac501219u.

[36] J. Park, Y. Park, S. Kim, Signal Amplification via Biological Self-Assembly of Surface-Engineered Quantum Dots for Multiplexed Subattomolar Immunoassays and Apoptosis Imaging, ACS Nano. 7 (2013) 9416–9427. doi:10.1021/nn4042078.

[37] M. Ren, H. Xu, X. Huang, M. Kuang, Y. Xiong, H. Xu, et al., Immunochromatographic Assay for Ultrasensitive Detection of Aflatoxin B1 in Maize by Highly Luminescent Quantum Dot Beads, ACS Appl. Mater. Interfaces. 6 (2014) 14215–14222. doi:10.1021/am503517s.

[38] J. Shen, Y. Zhou, F. Fu, H. Xu, J. Lv, Y. Xiong, et al., Immunochromatographic assay for quantitative and sensitive detection of hepatitis B virus surface antigen using highly luminescent quantum dot-beads, Talanta. 142 (2015) 145–149. doi:10.1016/j.talanta.2015.04.058.

[39] J. Li, H. Qi, H. Wang, Z. Yang, P. Zhu, G. Diao, Fluorescence energy transfer-based multiplexed hybridization assay using gold nanoparticles and quantum dot conjugates on photonic crystal beads, Microchim. Acta. 181 (2014) 1109–1115. doi:10.1007/s00604-014-1217-6.

[40] Y. Wang, K. Zhou, G. Huang, C. Hensley, X. Huang, X. Ma, et al., A nanoparticle-based strategy for the imaging of a broad range of tumours by nonlinear amplification of microenvironment signals, Nat. Mater. 13 (2014) 204–212. doi:10.1038/nmat3819.

[41] Y. Zhang, W. Dai, F. Liu, L. Li, M. Li, S. Ge, et al., Ultrasensitive electrochemiluminescent immunosensor based on dual signal amplification strategy of gold nanoparticles-dotted graphene composites and CdTe quantum dots coated silica nanoparticles, Anal. Bioanal. Chem. 405 (2013) 4921–4929. doi:10.1007/s00216-013-6885-2.

[42] S. Liu, J. Zhang, W. Tu, J. Bao, Z. Dai, Using ruthenium polypyridyl functionalized ZnO mesocrystals and gold nanoparticle dotted graphene composite for biological recognition and electrochemiluminescence biosensing, Nanoscale. 6 (2014) 2419. doi:10.1039/c3nr05944h.

[43] C. Fenzl, T. Hirsch, A.J. Baeumner, Liposomes with High Refractive Index Encapsulants as Tunable Signal Amplification Tools in Surface Plasmon Resonance Spectroscopy, Anal. Chem. (2015). doi:10.1021/acs.analchem.5b03405.

[44] Z. Cui, D. Wu, Y. Zhang, H. Ma, H. Li, B. Du, et al., Ultrasensitive electrochemical immunosensors for multiplexed determination using mesoporous platinum nanoparticles as nonenzymatic labels, Anal. Chim. Acta. 807 (2014) 44–50. doi:10.1016/j.aca.2013.11.025.

[45] T. Zheng, Q. Zhang, S. Feng, J.-J. Zhu, Q. Wang, H. Wang, Robust Nonenzymatic Hybrid Nanoelectrocatalysts for Signal Amplification toward Ultrasensitive Electrochemical Cytosensing, J. Am. Chem. Soc. 136 (2014) 2288–2291. doi:10.1021/ja500169y.

[46] Y. Wu, P. Xue, Y. Kang, K.M. Hui, Highly Specific and Ultrasensitive Graphene-Enhanced Electrochemical Detection of Low-Abundance Tumor Cells Using Silica Nanoparticles Coated with Antibody-Conjugated Quantum Dots, Anal. Chem. 85 (2013) 3166–3173. doi:10.1021/ac303398b.

[47] S.E.K. Kirschbaum, A.J. Baeumner, A review of electrochemiluminescence (ECL) in and for microfluidic analytical devices, Anal. Bioanal. Chem. 407 (2015) 3911–3926. doi:10.1007/s00216-015-8557-x.

[48] Y.S. Li, Y. Zhou, X.Y. Meng, Y.Y. Zhang, J.Q. Liu, Y. Zhang, et al., Enzyme-antibody dual labeled gold nanoparticles probe for ultrasensitive detection of kappa-casein in bovine milk samples, Biosens. Bioelectron. 61 (2014) 241–244. doi:10.1016/j.bios.2014.05.032.

[49] L. Zhan, W.B. Wu, X.X. Yang, C.Z. Huang, Gold nanoparticle-based enhanced ELISA for respiratory syncytial virus, New J. Chem. 38 (2014) 2935–2940. doi:10.1039/C4NJ00253A.

[50] Y.S. Li, X.Y. Meng, Y. Zhou, Y.Y. Zhang, X.M. Meng, L. Yang, et al., Magnetic bead and gold nanoparticle probes based immunoassay for β-casein detection in bovine milk samples, Biosens. Bioelectron. 66 (2015) 559–564. doi:10.1016/j.bios.2014.12.025.

[51] W. Wu, J. Li, D. Pan, J. Li, S. Song, M. Rong, et al., Gold Nanoparticle-Based Enzyme-Linked Antibody-Aptamer Sandwich Assay for Detection of Salmonella Typhimurium, ACS Appl. Mater. Interfaces. 6 (2014) 16974–16981. doi:10.1021/am5045828.

[52] I.-H. Cho, A. Bhunia, J. Irudayaraj, Rapid pathogen detection by lateral-flow immunochromatographic assay with gold nanoparticle-assisted enzyme signal amplification, Int. J. Food Microbiol. 206 (2015) 60–66. doi:10.1016/j.ijfoodmicro.2015.04.032.

[53] F. Chen, S. Hou, Q. Li, H. Fan, R. Fan, Z. Xu, et al., Development of Atom Transfer Radical Polymer-Modified Gold Nanoparticle-Based Enzyme-Linked Immunosorbent Assay (ELISA), Anal. Chem. 86 (2014) 10021–10024. doi:10.1021/ac403872k.

[54] H. Gao, D. Pan, N. Gan, J. Cao, Y. Sun, Z. Wu, et al., An aptamer-based colorimetric assay for chloramphenicol using a polymeric HRP-antibody conjugate for signal amplification, Microchim. Acta. (2015) 1–9. doi:10.1007/s00604-015-1632-3.

[55] R.-P. Liang, C.-Y. Xiang, H.-F. Zhao, J.-D. Qiu, Highly sensitive electrogenerated chemiluminescence biosensor in profiling protein kinase activity and inhibition using a multifunctional nanoprobe, Anal. Chim. Acta. 812 (2014) 33–40. doi:10.1016/j.aca.2013.12.037.

[56] Z. Wang, Z. Yan, N. Sun, Y. Liu, Multiple signal amplification electrogenerated chemiluminescence biosensors for sensitive protein kinase activity analysis and inhibition, Biosens. Bioelectron. 68 (2015) 771–776. doi:10.1016/j.bios.2015.02.006.

[57] H. Zhang, L. Liu, X. Fu, Z. Zhu, Microfluidic beads-based immunosensor for sensitive detection of cancer biomarker proteins using multienzyme-nanoparticle amplification and quantum dots labels, Biosens. Bioelectron. 42 (2013) 23–30. doi:10.1016/j.bios.2012.10.076.

[58] H. Zhang, X. Hu, X. Fu, Aptamer-based microfluidic beads array sensor for simultaneous detection of multiple analytes employing multienzyme-linked nanoparticle amplification and quantum dots labels, Biosens. Bioelectron. 57 (2014) 22–29. doi:10.1016/j.bios.2014.01.054.

[59] Y.-S. Fang, H.-Y. Wang, L.-S. Wang, J.-F. Wang, Electrochemical immunoassay for procalcitonin antigen detection based on signal amplification strategy of multiple nanocomposites, Biosens. Bioelectron. 51 (2014) 310–316. doi:10.1016/j.bios.2013.07.035.

[60] R. Hu, W. Wen, Q. Wang, H. Xiong, X. Zhang, H. Gu, et al., Novel electrochemical aptamer biosensor based on an enzyme-gold nanoparticle dual label for the ultrasensitive detection of epithelial tumour marker MUC1, Biosens. Bioelectron. 53 (2014) 384–389. doi:10.1016/j.bios.2013.10.015.

[61] Y. Zhou, L. Tang, G. Zeng, J. Chen, J. Wang, C. Fan, et al., Amplified and selective detection of manganese peroxidase genes based on enzyme-scaffolded-gold nanoclusters and mesoporous carbon nitride, Biosens. Bioelectron. 65 (2015) 382–389. doi:10.1016/j.bios.2014.10.063.

[62] L. Liu, N. Xia, H. Liu, X. Kang, X. Liu, C. Xue, et al., Highly sensitive and label-free electrochemical detection of microRNAs based on triple signal amplification of multifunctional gold nanoparticles, enzymes and redox-cycling reaction, Biosens. Bioelectron. 53 (2014) 399–405. doi:10.1016/j.bios.2013.10.026.

[63] A.-L. Sun, F.-C. Jia, Y.-F. Zhang, X.-N. Wang, Gold nanocluster-encapsulated glucoamylase as a biolabel for sensitive detection of thrombin with glucometer readout, Microchim. Acta. 182 (2014) 1169–1175. doi:10.1007/s00604-014-1440-1.

[64] P. Xiong, N. Gan, H. Cui, J. Zhou, Y. Cao, F. Hu, et al., Incubation-free electrochemical immunoassay for diethylstilbestrol in milk using gold nanoparticle-antibody conjugates for signal amplification, Microchim. Acta. 181 (2014) 453–462. doi:10.1007/s00604-013-1131-3.

[65] D. Tang, B. Zhang, J. Tang, L. Hou, G. Chen, Displacement-type Quartz Crystal Microbalance Immunosensing Platform for Ultrasensitive Monitoring of Small Molecular Toxins, Anal. Chem. 85 (2013) 6958–6966. doi:10.1021/ac401599t.

[66] H. Wang, Y. Chai, R. Yuan, Y. Cao, L. Bai, Highly enhanced electrochemiluminescent strategy for tumor biomarkers detection with in situ generation of l-homocysteine for signal amplification, Anal. Chim. Acta. 815 (2014) 16–21. doi:10.1016/j.aca.2014.01.040.

[67] H. Niu, R. Yuan, Y. Chai, L. Mao, H. Liu, Y. Cao, Highly amplified electrochemiluminescence of peroxydisulfate using bienzyme functionalized palladium nanoparticles as labels for ultrasensitive immunoassay, Biosens. Bioelectron. 39 (2013) 296–299. doi:10.1016/j.bios.2012.06.004.

[68] H. Wang, X. Li, K. Mao, Y. Li, B. Du, Y. Zhang, et al., Electrochemical immunosensor for alpha-fetoprotein detection using ferroferric oxide and horseradish peroxidase as signal amplification labels, Anal. Biochem. 465 (2014) 121–126. doi:10.1016/j.ab.2014.08.016.

[69] Y. Li, L. Fang, P. Cheng, J. Deng, L. Jiang, H. Huang, et al., An electrochemical immunosensor for sensitive detection of Escherichia coli O157:H7 using C-60 based biocompatible

platform and enzyme functionalized Pt nanochains tracing tag, Biosens. Bioelectron. 49 (2013) 485–491. doi:10.1016/j.bios.2013.06.008.

[70] Z. Zhong, M. Li, Y. Qing, N. Dai, W. Guan, W. Liang, et al., Signal-on electrochemical immunoassay for APE1 using ionic liquid doped Au nanoparticle/graphene as a nanocarrier and alkaline phosphatase as enhancer, Analyst. 139 (2014) 6563–6568. doi:10.1039/C4AN01712A.

[71] Y. Li, R. Yuan, Y. Chai, Y. Zhuo, H. Su, Y. Zhang, Horseradish peroxidase-loaded nanospheres attached to hollow gold nanoparticles as signal enhancers in an ultrasensitive immunoassay for alpha-fetoprotein, Microchim. Acta. 181 (2014) 679–685. doi:10.1007/s00604-014-1179-8.

[72] Y. Lin, Q. Zhou, Y. Lin, D. Tang, R. Niessner, D. Knopp, Enzymatic Hydrolysate-Induced Displacement Reaction with Multifunctional Silica Beads Doped with Horseradish Peroxidase–Thionine Conjugate for Ultrasensitive Electrochemical Immunoassay, Anal. Chem. 87 (2015) 8531–8540. doi:10.1021/acs.analchem.5b02253.

Chapter 2: Investigating non-specific binding to sensor surfaces using liposomes as models

Abstract

Avoiding non-specific binding to receptor surfaces is mandatory for the development of any specific and efficient sensor. Liposomes with varying degree of negative surface charge served here as bioassay component models. Their interaction with four typical chemical surfaces was mechanistically characterized by surface plasmon resonance (SPR) spectroscopy. Through tailoring of surface chemistry as well as liposome surface charge non-specific binding can be significantly minimized. This was achieved for example with carboxyl- or methyl-terminated surfaces, especially when pairing COOH groups on the sensor surface with COOH groups on the liposomes. In contrast, OH-groups on the surface did surprisingly not lead to decreased non-specific binding. Notably, it was shown that the interactions can be described with Langmuir isotherms. These mechanistic studies contribute to the design of improved sensing systems where liposomes as well as other charged nanoparticles are extensively used.

This chapter has been submitted.

Christoph Fenzl, Christa Genslein, Celesztina Domonkos, Katie A. Edwards, Thomas Hirsch, Antje J. Baeumner, **2015**, submitted.

Author contributions

Most of the experimental work was carried out by CF solely. CG and CD repeated some of the SPR measurements for statistical confidence under CF's guidance. KAE discussed liposome stability. The article was written by CF and revised by TH, KAE and AJB. AJB is corresponding author.

1. Introduction

Liposomes – artificial nanoscale vesicles consisting of a hydrophobic lipid bilayer that separates the hydrophilic inner cavity from the outer medium [1,2] – are widely utilized as versatile tools not only in drug delivery [3–5] but also in analytical sciences [6–8], *e.g.* biosensors [1]. Recently, Edwards *et al.* [9] showed magnetic fluorescent liposomes to be very powerful signal amplifiers in heterogeneous binding assay formats where DNA-tagged liposomes were capable of enhancing sensitivity and reducing assay times simultaneously. Further, vesicles encapsulating quantum dots [10] and when paired with high binding biorecognition elements such as ganglioside receptors [11,12] enable attomolar detection of DNA without target amplification. Additionally, liposomes with high refractive index encapsulants have been demonstrated to significantly enhance the signal in surface plasmon resonance (SPR) spectroscopy [13].

In the field of drug delivery, a controllable hydrophilic / hydrophobic system [14] was developed using electrospun vesicles as transporters. Furthermore, magnetic nanoparticles have been shown to support lipid bilayers and to increase the efficacy of unmodified doxorubicin [15]. Maina *et al.* [16] demonstrated that high protein loading and a slow release over 80 days is possible with negatively charged liposomes. Despite the high performance of liposome-based sensors and drug delivery systems, the dynamics of the interactions between the utilized vesicles and their target surfaces have only been marginally studied and are still not well understood. Especially in microfluidic devices – a growing field in (bio)analytical research – high surface areas are encountered that can lead to increasing non-specific adsorption [17] and needs to be avoided by clever surface engineering strategies. Here, mechanistic understanding of the binding processes is crucial for the optimization of sensors as well as therapeutic applications based on liposomes, where high efforts in liposome engineering are made to maximize the uptake of a drug for the desired target [4]. Therefore, it is of high importance to know how much, how fast and how strong the vesicles bind to the target surface specifically and non-specifically.

Liang *et al.* [18] investigated the effect of flow rate and water content on targeted liposome interactions via surface plasmon resonance (SPR) spectroscopy and quartz crystal microbalance (QCM) studies. They found that increasing flow rate decreases the

maximum amount of bound liposomes and the equilibrium constant, as does decreasing water content in the bound vesicle layer. Further, the morphology of the lipid layer on a surface can be controlled by the surface chemistry on the substrate [19]. Granqvist *et al.* [19] showed that low-molecular-weight dextran-based surfaces facilitate the formation of supported lipid bilayers, whereas polyethylene glycol-based thiol-surfaces lead to supported vesicular layers. These findings are of high importance when using liposomes as carriers for drugs [3,20] or signal molecules [9] that should be released in a controlled manner. Recently, Calver *et al.* [21] were able to monitor lipid membrane-surface interactions such as liposome adsorption and deformation using single-particle fluorescence of conjugated poly[5-methoxy-2-(3-sulfopropoxy)-1,4-phenylenevinylene on SiO_2 nanoparticles.

Extensive studies of lipid vesicle adsorption and supported lipid bilayer formation have been performed by the groups of Reviakine [22,23], Richter and Brisson [24,25] and Kasemo [26–28]. They studied the behavior of liposomes on sensor substrates such as SiO_2 [26–28], TiO_2 [22,27], gold [26–28] or mica [24,25] that contributed significantly to the general understanding of liposome binding to standard sensor substrates of SPR, QCM and atomic force microscopy and the conditions for a bilayer formation.

However, studies are missing investigating binding interactions with the predominant surface modifications applied in (bio)analytical assays and sensors, *e.g.* surfaces modified with terminal carboxyl or hydroxyl groups. Yet, this knowledge will lead to optimized surface conditions that contribute to higher selectivity and reusability. In addition, the liposome formulations used in the previous studies differ clearly from those used in high-performing sensing approaches [6,13,29]. As the composition influences sensing performance it must also be used when trying to understand and consequently minimize non-specific binding.

Here, we present the systematic study of non-specific binding interactions between highly stable anionic liposomes and surfaces with varying negative surface charge and hydrophilicity (Figure 1). We focus on this type of liposomes, as it is favorably used in high-performance sensing applications [6,9] that are often combined with microfluidic sample handling [17,30]. Liposomes with negative surface charge have been shown not to rupture as easily as positively charged ones when adsorbing to solid surfaces [31]. Also, with most biological molecules bearing negative charges, non-specific binding of anionic

liposomes favors their use in bioassays. The vesicles were characterized in close detail regarding size and surface charge. The binding studies were performed with SPR spectroscopy that has been shown to be the ideal tool for label-free monitoring of such interactions in real-time resolution [18,19,32]. Further, the influence of varying temperature on the binding behavior was analyzed. With our work, we will broaden the knowledge on liposome – solid surface interactions that we think will benefit a wide range of applications in the field of chemical and biological sensing, pharmaceutics and therapeutics as well as surface modification in (microfluidic) flow systems.

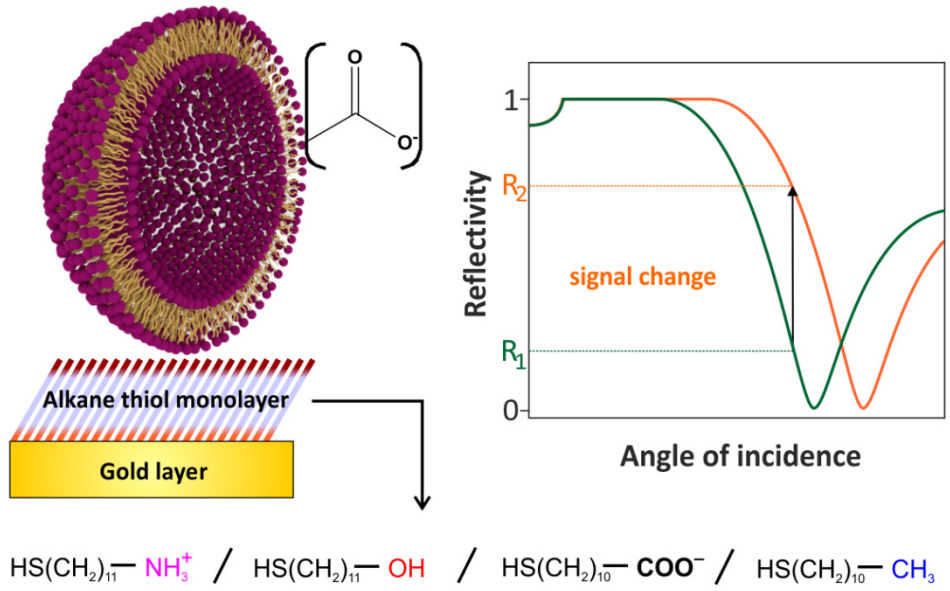

Figure 1. Sensing scheme for the interactions between anionic liposomes and different self-assembled monolayers on gold. High non-specific binding will result in high SPR signal changes.

2. Experimental Section

2.1. Materials

1,2-Dipalmitoyl-*sn*-glycero-3-phosphocholine, 1,2-dipalmitoyl-*sn*-glycero-3-[phospho-rac-(1-glycerol)] sodium salt , N-glutaryl-1,2-dipalmitoyl-*sn*-glycero-3-phosphatidyl-ethanolamine, and the extrusion membranes as well as the extrusion kit were purchased from Avanti Polar Lipids (Alabaster, AL, USA). 4-(2-Hydroxyethyl)piperazine-1-

ethanesulfonic acid (HEPES), sodium azide, cholesterol, phosphotungstic acid (PTA), 11-mercaptoundecanoic acid, 11-mercaptoundecanol, and 1-mercaptoundecane were obtained from Sigma-Aldrich (Taufkirchen, Germany). 11-Mercaptoundecyl amine hydrochloride was purchased from ProChimia Surfaces (Sopot, Poland). All further chemicals in these experiments were ordered from VWR (Darmstadt, Germany).

2.2. Preparation of liposomes

The liposomes were prepared according to a slightly modified protocol developed by Edwards *et al.* [33]. DPPC, DPPG and cholesterol (40.9:20.1:51.7 µmol, respectively) for the untagged liposomes, and DPPC, DPPG, cholesterol and N-glutaryl-DPPE (40.9:20.1:51.7:7.3 µmol, respectively) for the liposomes with additional COOH-tag were dissolved in an organic solvent mixture consisting of 3 mL chloroform and 0.5 mL methanol, and sonicated for 1 min in a sonication bath (Bandelin Sonorex Digitec DT 255 H) at 45 °C for homogeneous mixing. A 45 °C salt solution (2 mL of 300 mmol·L^{-1} NaCl) was added to the lipid mixture and then was again sonicated for 4 min. The organic solvent was removed at 45 °C and 380 mbar for 20 min using a rotary evaporator. The mixture was then vortexed before and after a second addition of 2 mL 45 °C 300 mmol·L^{-1} NaCl. The flask was returned to the rotary evaporator for 20 min at 45 °C and 380 mbar and then for 20 min at 280 mbar. The crude liposome dispersion is further extruded at 50 °C 21 times through 1.0 µm Nucleopore membranes (Whatman, Florham Park, NJ, USA), followed by 21 times through 0.4 µm membranes. The liposomes were purified via size-exclusion chromatography with Sephadex G-50 in a 15 × 1.6 cm column at ~4 mL·min^{-1} using HEPES-saline-sucrose buffer (HSS; 10 mmol·L^{-1} HEPES, 200 mmol·L^{-1} sodium chloride, 200 mmol·L^{-1} sucrose, 1.5 mmol·L^{-1} sodium azide at pH 7.5). The fractions containing liposomes were combined and dialyzed overnight against HSS before storage at 4 °C.

2.3. Liposome characterization

For transmission electron microscopy, the purified liposome dispersions were diluted 1:10 in HEPES-saline buffer (10 mmol·L^{-1} HEPES, 200 mmol·L^{-1} sodium chloride, 1.5 mmol·L^{-1} sodium azide at pH 7.5). A carbon-coated copper grid was covered with a 2 µL drop of the suspension for 90 s. After removing the excess liposomes by washing with 5 µL of 8.7 mmol·L^{-1} PTA aqueous solution, the vesicles left on the TEM-grid were negatively stained [34] with a 5 µL drop of 8.7 mmol·L^{-1} PTA aqueous solution for 30 s in order to enhance the TEM contrast. The excess staining solution was removed with a filter paper. Transmission electron micrographs were acquired with a transmission electron microscope (Philips CM 12). Dynamic light scattering measurements were performed with the same liposome dispersions (1:100 dilution in HEPES-saline buffer). A disposable polystyrene cuvette was filled with 1 mL of the suspension and analyzed with the particle sizer in the backscattering mode at an angle of 173° (Malvern Zetasizer nano series) at 25 °C after an equilibration time of 120 s. The autocorrelation of the intensity recorded over time is related to the geometry of the liposomes under observation. After 30 consecutive measurements, the mean hydrodynamic radius and a polydispersity index were extracted from the autocorrelation data.

The electrophoretic mobility of the liposomes was measured with the 1:100 dilution in HEPES-saline buffer. A Folded Capillary Cell (Malvern DTS1070) was charged with approximately 800 µL of the liposome dispersions and equilibrated to 25 °C for 120 s. The mean electrophoretic mobility was determined by laser Doppler velocimetry with the Zetasizer nano series. The Smoluchowski model was employed to determine the zeta potential of the dispersions [35].

For the determination of the phospholipid concentration of liposomes, inductively coupled plasma – atomic emission spectroscopy (ICP-AES) was used. A volume of 20 µL of liposomes was diluted in HNO_3 (c = 0.5 mol·L^{-1}) to a total volume of 3 mL. The mixture was vortexed and sonicated thoroughly. Phosphorus standard solutions were prepared with concentrations of 1, 5, 10, 25, 50 and 100 µmol·L^{-1} phosphate in 0.5 mol·L^{-1} HNO_3 for calibration. The phosphorus content was measured via ICP-AES (Spectro Flame-EOP, Analytical Instruments GmbH, Kleve, Germany) at the phosphorus specific wavelength of 178.29 nm.

2.4. Characterization of the formation of a self-assembled monolayer on gold

Cyclic voltammograms of gold electrodes (0.37 mm^2) were recorded in HEPES buffer with 5 mM $K_3[Fe(CN)_6]$ from -0.3 V to 0.6 V against a Ag/AgCl reference electrode (scan rate = 100 $mV \cdot s^{-1}$) with an electrochemical analyzer (CH Instruments, CHI660A, Austin, Texas). The electrodes were then immersed in 200 $\mu mol \cdot L^{-1}$ ethanolic solutions of 11-mercaptoundecanoic acid, 11-mercaptoundecanol, 1-mercaptoundecane, or 11-mercaptoundecyl amine hydrochloride for 20 h in order to form a self-assembled monolayer on the gold surface. After rinsing with ethanol, a second CV of each electrode was recorded.

2.5. Surface plasmon resonance spectroscopy (SPR) measurements

The SPR sensor chip consisting of a 50 nm Au layer on a 5 nm Cr adhesive layer on glass with a refractive index of 1.61 (Mivitec, Sinzing, Germany), was immersed in 200 $\mu mol \cdot L^{-1}$ ethanolic solutions of 11-mercaptoundecanoic acid, 11-mercaptoundecanol, 1-mercaptoundecane, or 11-mercaptoundecyl amine hydrochloride for a minimum of 20 h in order to form a SAM on the gold surface. The chips were then rinsed with ethanol and dried under nitrogen flow. The SPR measurements were performed with a two channel SPR device (Mivitec Biosuplar 321, Sinzing, Germany) at ambient temperature with 640 nm laser excitation and equipped with a flow cell of a total volume of approx. 50 µL per channel. Flow rate was adjusted to 200 $\mu L \cdot min^{-1}$. The measurements were performed at a fixed angle by read-out of the change of the intensity of the reflected light. After calibration of the measured signal intensity with sodium chloride solutions of known refractive index, liposome dispersions were diluted to phospholipid concentrations of 1, 5, 10, 25, 50, and 100 $\mu mo \cdot L^{-1}$ with degassed HEPES-saline buffer. The dispersions were consecutively injected with increasing phospholipid concentration, each for 20 min followed by a washing step with HEPES-saline buffer for 10 min. The average signal changes and errors for the four different thiol surfaces were calculated from three independent measurements. For the measurement of blank gold, the error bars were obtained by taking 3x signal noise. For the temperature dependence studies

the SPR device was placed in a thermally controlled room at 25 °C or a flow cell with temperature control was adjusted to 37 or 50 °C respectively. The calibration with the NaCl solutions was corrected with the adequate refractive index at these temperatures.

3. Results and Discussion

In this study, the binding interactions between highly stable anionic liposomes with varying negative surface charge and differently modified gold surfaces are investigated via SPR spectroscopy (Figure 1). Strong binding will result in high SPR signal changes due to the high refractive index of the lipid bilayer and liposome encapsulant (300 mM NaCl), whereas weak binding leads to only small changes.

Liposomes were characterized with respect to their size and surface charge. Dynamic light scattering was used to determine their hydrodynamic diameters. The non-tagged liposomes had a diameter of 170 nm, with a polydispersity index (PDI) of 0.16. Liposomes with N-glutaryl-1,2-dipalmitoyl-*sn*-glycero-3-phosphatidylethanolamine (N-glutaryl-DPPE) are 240 nm in diameter (PDI of 0.22). The carboxylic groups provide additional negative surface charges, causing such an increase. Glutaryl-tags on the liposome surface lead to higher electrostatic repulsion between the liposomes. As a consequence, the incorporation of charged tags in the bilayer membrane enables to improve the colloidal stability. However, the higher surface charge enhances the colloidal stability in solution due to better repulsion, but on the other hand it can increase binding to the surfaces of opposite surface charge.

Electrophoretic mobility measurements confirm the higher colloidal stability. The zeta potential of COOH-tagged liposomes (-47 ± 3 mV) is more negative than for the untagged ones (-34 ± 3 mV). Both types of liposomes show extreme long term stability and keep their physical and hydrodynamic diameters as well as the high negative zeta potential for at least 400 days [36]. This exceeds by far the colloidal stability of numerous other nanomaterials such as polystyrene nanospheres [37,38] or magnetite nanoparticles [39].

Transmission electron microscopy (TEM) images show the successful formation of the liposomes that display good regularity of size and shape (Figure 2). Deviations from the perfectly spherical shape of liposomes on the images are likely due to the drying and staining process on the TEM grid.

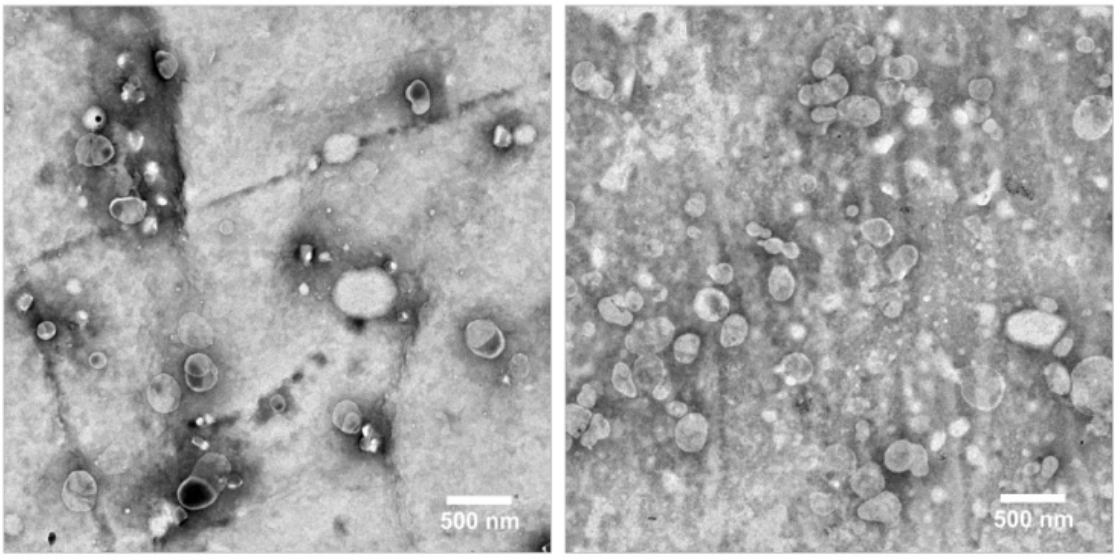

Figure 2. Figure Caption. TEM images of a 1:10 diluted dispersions of untagged liposomes (left) and liposomes with N-glutaryl-DPPE tag (right). Scale bars are 500 nm.

The phospholipid concentration was determined via ICP-AES resulting in 6.14 ± 0.12 mmol·L^{-1} for the untagged batch and 11.17 ± 0.13 mmol·L^{-1} for the liposomes with N-glutaryl-DPPE tag. The total lipid concentration can be calculated using the molar ratios of the lipid composition (see Experimental Section) to 11.3 ± 0.2 and 19.7 ± 0.2 mmol·L^{-1}, respectively. The total number of lipids per liposome is given by the following equation (1) [40]:

$$N_{tot} = (\pi / a_L)[d^2 + (d - 2t)^2] \quad (1)$$

where d is the hydrodynamic diameter of the liposomes, t is bilayer thickness of supposing 40 Å, and a_L is the average headgroup surface area per lipid that is calculated to be 42.5 Å^2 by using for 1,2-Dipalmitoyl-*sn*-glycero-3-phosphocholine (DPPC), 1,2-dipalmitoyl-*sn*-glycero-3-[phospho-rac-(1-glycerol)] (DPPG), and cholesterol the values of 71, 45, and 19 Å^2 [41,42] weighted with the respective mole fraction neglecting the N-glutaryl-DPPE. The concentration of liposomes was then obtained by dividing the total lipid concentration of dispersion by N_{tot} resulting in 27.7 ± 0.5 nmol·L^{-1} for the untagged liposomes and 23.9 ± 0.3 nmol·L^{-1} for the liposomes with COOH-tag. The obtained liposome characteristics are summarized in Table 1.

Table 1. Properties of liposomes.

Surface tag	Diameter / nm	PDI[a)]	Zeta potential / mV	c (phospholipid) / mmol·L^{-1}	c (liposomes) / nmol·L^{-1}
none	170	0.16	-34 ± 3	6.14 ± 0.12	27.7 ± 0.5
N-glutaryl-DPPE	240	0.22	-47 ± 3	11.17 ± 0.13	23.9 ± 0.3

[a)]polydispersity index

The successful formation of closely packed alkanethiol monolayers on gold provide an insulation barrier [43] for the hexacyanoferrate and can be seen in a drastic change of the redox peaks in the cyclic voltammograms (CV) (Figure 3). All four different thiols show successful formation of a self-assembled monolayer (SAM) on the gold electrodes, as the surface is blocked for the redox reaction and the redox peak currents are significantly decreased. Best blocking is exhibited by the CH_3-terminated thiol monolayer, followed by the COOH- and OH-modified surface. For electrode modified with 11-mercaptoundecyl amine hydrochloride a hindered charge-transfer can be seen by the large separation of the peak potentials, indicating a formation of a monolayer.

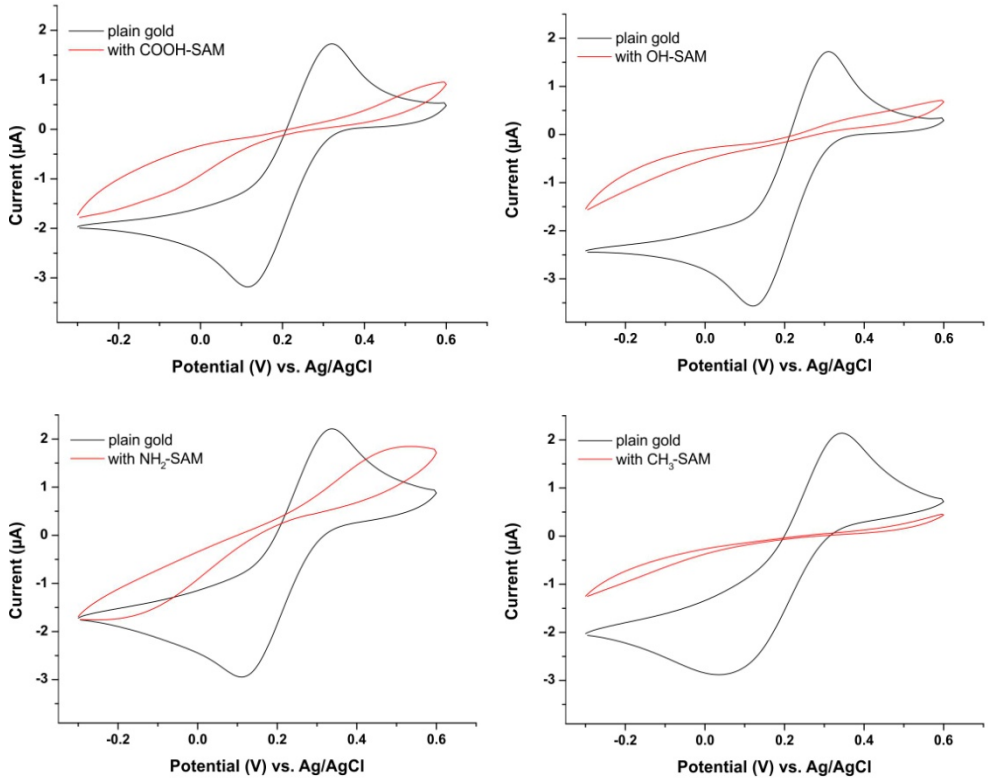

Figure 3. Cyclic voltammograms before and after the formation of self-assembled monolayers on gold electrodes. The solutions are 5 mM $Fe(CN)_6^{3-}$ in HEPES buffer. Scan rate 100 mV·s^{-1}.

3.1. Binding characteristics of anionic liposomes without COOH-tag

After device calibration with sodium chloride solutions of known refractive index, the liposome dispersions in a concentration range from 0 to 100 µmol·L^{-1} phospholipid content (corresponding to 0 to 453 pmol·L^{-1} total liposome concentration and covering the concentration range usually used in analytical applications [13,44]) were allowed an interaction time of 20 min with the modified sensor surface in a continuous flow system, followed by a 10 min washing step to remove all loosely bound liposomes. The concentration dependent signal change in refractive index units (RIU) was compared for the blank gold surface and four self-assembled monolayers of long-chained alkanethiols with varying terminal groups of -CH_3, -OH, -COOH, and -NH_2 (Figure 4).

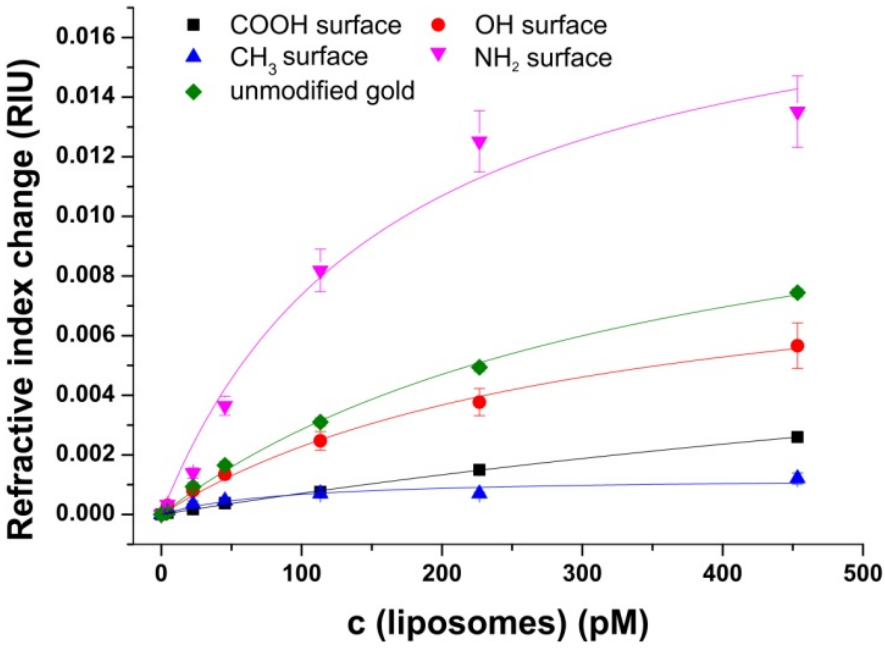

Figure 4. Refractive index changes in SPR measurements induced by the interaction of anionic liposomes (300 mM NaCl encapsulant) with an unmodified and with -COOH, -OH, -CH_3, and -NH_2 SAM modified gold surfaces at varying liposome concentrations at room temperature and at pH 7.5. Fit according to Langmuir model. n=3

The binding curves were fitted to the extended Langmuir model following equation (2):

$$\Delta n_D = \Delta n_{D,\max} \frac{K_L c^h}{1 + K_L c^h} \qquad (2)$$

where Δn_D is the observed refractive index change, $\Delta n_{D,\,max}$ is the refractive index change at maximum surface loading, K_L is the Langmuir equilibrium constant and c is the liposome concentration and h represents a coefficient describing the cooperativity.

Positively cooperative binding is given by $h > 1$, negatively cooperative binding by $h < 1$. For non-cooperative binding h is equal to 1. The fitting parameters are displayed in Tables 2 and 3 for both the simple Langmuir model (h fixed to 1), which neglects cooperative binding effects, and for the extended fit, which takes such effects into account. The Langmuir model was chosen over the Freundlich isotherm, as the experimental data display saturation behavior.

Table 2. Parameters for the interaction of untagged liposomes with self-assembled monolayers on gold obtained by binding isotherms.

Fit model	Surface	$\Delta n_{D,\,max}$ [a] / RIU	K_L [b] / L·pmol^{-1}	K_D [c] / pmol·L^{-1}	h	R^2
simple	-COOH	0.0104±0.0013	0.00074±0.00012	1400±200		0.9991
	-OH	0.0094±0.0009	0.0032±0.0005	310±60		0.9924
	-CH_3	0.0013±0.0002	0.012±0.006	80±40		0.8501
	-NH_2	0.019±0.002	0.0061±0.0018	160±50		0.9730
	gold	0.0134±0.0010	0.00271±0.0003	370±40		0.9968
Fit model	**Surface**	$\Delta n_{D,\,max}$ [a] / RIU	K_L [b] / (L·pmol^{-1})^h	K_D [c] / (pmol·L^{-1})^h	h	R^2
extended	-COOH	0.014±0.010	0.0007±0.0003	1400±600	0.95±0.08	0.9989
	-OH	0.026±0.006	0.0036±0.0006	280±50	0.71±0.02	0.9998
	-CH_3	-	-	-	-	-
	-NH_2	0.0148±0.0008	0.0006±0.0005	2000±1400	1.62±0.19	0.9941
	gold	0.020±0.006	0.0035±0.0004	290±30	0.84±0.07	0.9985

[a] refractive index change at maximum surface loading, [b] Langmuir equilibrium constant, [c] Dissociation constant $K_D = 1/K_L$

Table 3. Parameters for the interaction of liposomes with N-glutaryl-DPPE tag with self-assembled monolayers on gold obtained by simple and extended Langmuir fits.

Fit model	Surface	$\Delta n_{D,max}$ [a] / RIU	K_L [b] / L·pmol^{-1}	K_D [c] / pmol·L^{-1}	*h*	R^2
simple	-COOH	0.0052±0.0019	0.0024±0.0012	400±200		0.9830
	-OH	0.0143±0.0009	0.0030±0.0003	330±30		0.9992
	-CH_3	0.0018±0.0005	0.02±0.013	50±30		0.7174
	-NH_2	0.018±0.002	0.014±0.004	70±20		0.9791
	gold	0.022±0.012	0.0010±0.0006	1000±600		0.9930
Fit model	**Surface**	$\Delta n_{D,max}$ [a] / RIU	K_L [b] / (L·pmol^{-1})^h	K_D [c] / (pmol·L^{-1})^h	*h*	R^2
extended	-COOH	0.01±0.03	0.002±0.004	500±1000	0.9±0.3	0.9780
	-OH	0.020±0.005	0.0029±0.0004	340±50	0.91±0.04	0.9995
	-CH_3	-	-	-	-	-
	-NH_2	0.0142±0.0004	0.0028±0.0009	360±110	1.57±0.10	0.9983
	gold	0.011±0.009	0.0012±0.0005	800±300	1.1±0.3	0.9915

[a] refractive index change at maximum surface loading, [b] Langmuir equilibrium constant, [c] Dissociation constant $K_D=1/K_L$

The non-specific binding of anionic liposomes on varying surfaces can be mainly classified by two parameters: the total refractive index change at a certain liposome concentration and the binding affinity. Liposomes strongly bind to an unmodified gold surface resulting in a refractive index change of 0.007 RIU at 453 pM under physiological pH, as shown in Figure 4. By modifying the gold surface with an amino-terminated monolayer, the binding interaction is even stronger and a signal change of 0.014 RIU can be observed. In the case of 11-mercaptoundecanol monolayers, signals (0.006 RIU) comparable to the unmodified gold were obtained. However, the 11-mercaptoundecanoic acid induces electrostatic repulsion leading to a clear blocking effect (0.003 RIU) which is even stronger for the

hydrophobic surface (1-mercaptoundecane) which prevents the hydrophilic liposomes from binding (0.001 RIU).

Regarding the binding affinity, the standard Langmuir isotherms (*h* = 1) display decreasing dissociation constants with increasing positively charged sensor surface charge starting at K_D = 1400 pM for HS-$(CH_2)_{10}$-COO^- due to the repulsive interactions. The uncharged hydrophilic surface self-assembled by HS-$(CH_2)_{11}$-OH results in lower K_D value of 310 pM, whereas for the highly attractive interactions caused by the positively charged surface consisting of a SAM of HS-$(CH_2)_{11}$-NH_3^+ a dissociation constant of 160 pM is obtained. For all hydrophilic surfaces, the refractive index change at maximum surface loading $\Delta n_{D,\,max}$ lies consistently in the same range between 0.01 and 0.02 RIU, indicating similar surface loading for the three surfaces at infinite liposome concentration. The SAM of the hydrophobic HS-$(CH_2)_{10}$-CH_3 on the other hand results in a very low $\Delta n_{D,\,max}$ of 0.0013 RIU. This can be explained by the fact that the Langmuir fit is not very accurate for this hydrophobic surface (R^2 = 0.85) due to the high differences in polarity of the liposome dispersions and the sensor surface. All other Langmuir fits show R^2 values of higher than 0.97 assuring the applicability of the model without the need to use more elaborate adsorption isotherms.

The standard Langmuir isotherms do not consider cooperative binding effects, especially for interaction of positively charged amino groups to negatively charged phospholipids at pH 7.5. In accordance to this, the binding isotherms fitted by an extended Langmuir equation indicate positively cooperative binding for $–NH_2$ SAM, non-cooperative binding in case of –COOH SAM, negatively cooperative binding for blank gold and –OH SAM (Table 2). The fitting of $–CH_3$ SAM did not converge for this model, indicating that there is almost no interactions of the liposomes with this surface. In general, the coefficient referring to the cooperative effects is in all cases close to 1, and the accuracy of the binding constants are significantly lower than of those obtained by the simple Langmuir isotherms.

3.2. Comparison of liposomes with and without N-glutaryl-DPPE tag

Liposomes offer a great variability in surface modification possibilities. As starting point for conjugation to biomolecules N-glutaryl-DPPE is commonly used to add COOH-groups [45], with an even higher negative surface charge (zeta potential = -47 ± 3 mV) compared to liposomes without this tag (-34 ± 3 mV). The liposome dispersions in a concentration range from 0 to 100 µmol·L^{-1} phospholipid content (corresponding to 0 to 206 pmol·L^{-1} total liposome concentration) were allowed an interaction time of 20 min with the modified sensor surface in a continuous flow stream followed by a 10 min washing step to remove non-bound liposomes. The concentration dependent non-specific binding displayed by signal change in refractive index units (RIU) was again compared for the four model surfaces of $–CH_3$, –OH, –COOH, and $–NH_2$ and unmodified gold (Figure 5). All binding curves are fitted to the simple and extended Langmuir model as before following the equation (2). The parameters resulting from the fit are listed in Table 3.

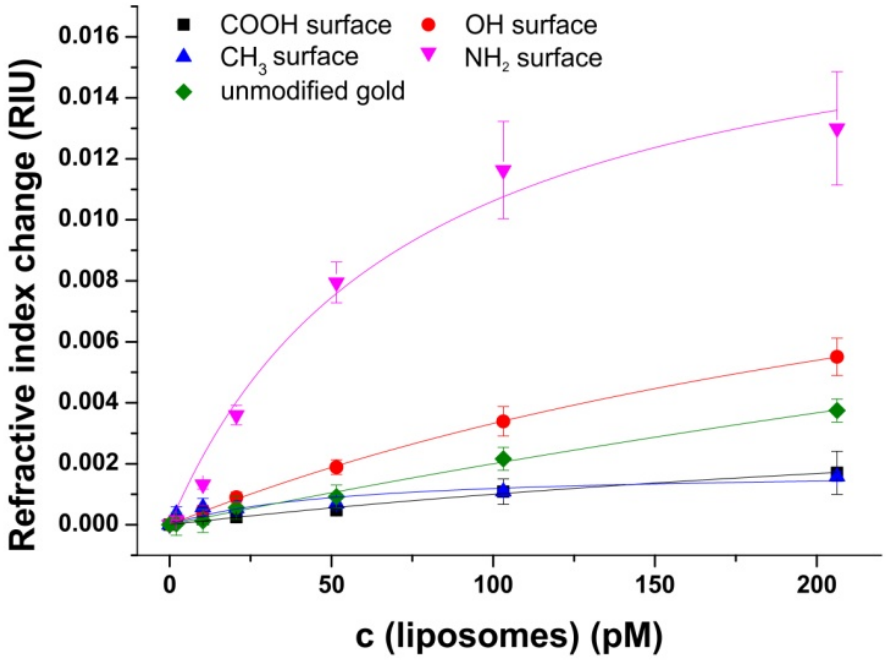

Figure 5. Refractive index changes in SPR measurements induced by the interaction of anionic liposomes (300 mM NaCl encapsulant, with N-glutaryl-DPPE tag) with an unmodified and with -COOH, -OH, $-CH_3$, and $-NH_2$ SAM modified gold surfaces at varying liposome concentrations. Fit according to Langmuir model. n=3

The very strong attractive interactions between the highly negatively charged liposomes with the cationic SAM consisting of $HS-(CH_2)_{11}-NH_3^+$ lead to a high signal change of

0.012 RIU at a liposome concentration of 200 pmol·L^{-1}, whereas the uncharged hydroxyl surface results in 0.004 RIU (Figure 5). Only very small changes can be observed for the interactions to the carboxyl- and the hydrophobic CH_3- moiety (0.001 RIU). This is caused by the strong electrostatic repulsion of the first and the significant differences in polarity of the second surface.

As already observed for the untagged liposomes, the dissociation constants obtained from the Langmuir fits of the hydrophilic surfaces with the liposomes with N-glutaryl-DPPE tag decrease from 400 pM for repulsive interaction of the carboxyl surface, over 330 pM for the 11-mercaptoundecanol to only 70 pM for the strong attractive interactions of the positively charged amino surface. The refractive index change at maximum surface loading lies in the range between 0.01 and 0.02 RIU for the hydroxyl- and amino-teminated surface and is significantly reduced to 0.0052 RIU for $HS\text{-}(CH_2)_{10}\text{-}COO^-$ due to the strong electrostatic repulsion. The differences in polarity between the liposomes and $HS\text{-}(CH_2)_{10}\text{-}CH_3$ is the reason for the very low signal change at maximum surface loading of 0.0018 RIU and the rather low R^2 value of 0.72 for the fit. All other Langmuir fits show R^2 values of higher than 0.97 assuring the applicability of the model and showing no need of more elaborate fitting curves.

The additional negative surface charges introduced by the N-glutaryl-DPPE phospholipid influence the interactions between the charged liposomes themselves and as consequence the number of binding sites on all surfaces is reduced. When comparing the same phospholipid concentrations, for all surface modifications, except the $–CH_3$ terminated surface, the signal change for the N-glutaryl-DPPE tagged liposomes is lower (Figure 6). In case of the 11-mercaptoundecane all findings suggest that there is nearly no binding and therefore the signal changes are almost equal.

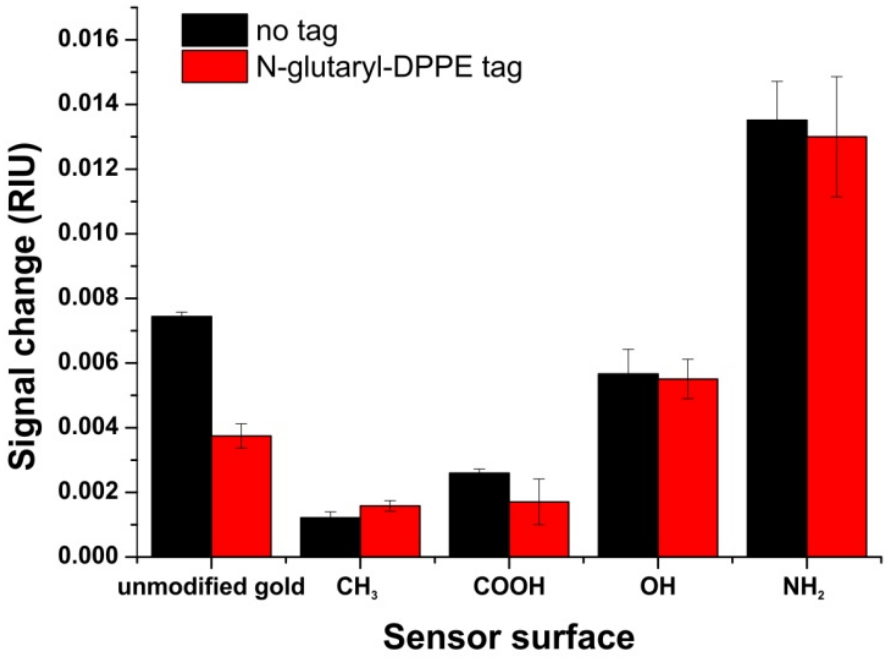

Figure 6. Comparison of the refractive index changes in SPR measurements induced by the interaction of anionic liposomes (300 mM NaCl encapsulant, with and without N-glutaryl-DPPE tag) with an unmodified and with -COOH, -OH, $-CH_3$, and $-NH_2$ SAM modified gold surfaces at the same phospholipid concentration (100 µM). n=3

Additional –COOH-tags provide the possibility for further functionalization and due to slightly more negative zeta potential better colloidal stability is achieved. In general the lipid composition of the liposomes is already optimized for long term stability [36]. The detailed study of the non-specific binding towards model surfaces, reflecting different chemical functionalities typically present in most biomolecules and sensor substrates, shows that the adhesion of this type of liposomes is only weak. Even for the positively charged amino surfaces the electrostatic repulsion between the liposomes themselves only leads to low total surface coverage. Simulation of the binding of such liposomes neglecting their own electrostatic repulsion results in an expected shift in the SPR angle of at least 1.8° (640 nm light source, triangular prism (50°)). This value is significantly higher than the shift found in the experiment for saturation (0.8°) (Figure 7).

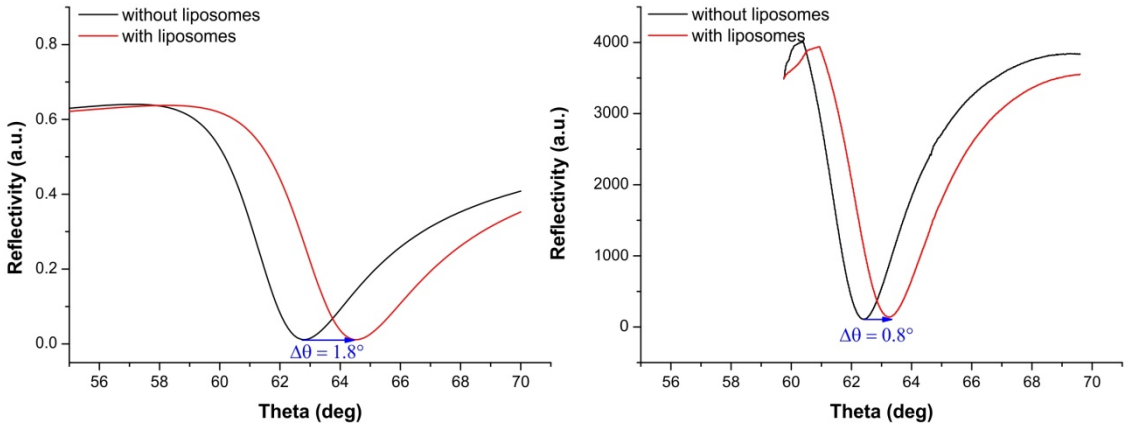

Figure 7. Change of the minimum of the SPR angle induced by anionic liposomes (300 mM NaCl encapsulant, without N-glutaryl-DPPE tag) on a $–NH_2$ SAM modified gold surface simulated for maximum surface loading (left) and obtained from experiment at 100 µM phospholipid concentration (right).

The simulations were performed with the software Winspall (Freeware from MPIP Mainz, Germany). The layer setup and respective parameters that was used for approximation of a closest packed liposome monolayer are summarized in Table 4.

Table 4. Layer setup for the Winspall SPR simulation.

Layer	Thickness / nm	*εX - real*	*εX - imaginary*
Glass	Infinite (starting layer)	2.59	0
Chromium [46]	3	-6.901	28.818
Gold [47]	50	-12.555	1.1464
Thiol	1.5	1.847	0
Lipid bilayer	4.8	2.25	0
300 mM NaCl	200	1.786	0
Lipid bilayer	4.8	2.25	0
Water	Infinite (ending layer)	1.778	0

Liposomes consisting of only zwitterionic phospholipids, as primarily used in the studies of Kasemo *et al.,* show significantly higher non-specific surface adsorption and tend to

rupture to form a supported lipid bilayer [26,28]. The low non-specific binding is therefore afforded by overall lower binding ability and has to be taken into consideration in the design of analytical assays, *i.e.* the highly charged liposomes may ultimately be ideally suited for low analyte concentrations [45] and microfluidic testing devices [17,30].

3.3. Temperature dependency of liposome binding

Binding events as well as the refractive index are strongly dependent on the temperature [48]. Therefore, the interactions between the model surface consisting of HS-$(CH_2)_{11}$-OH and liposomes without the N-glutaryl-DPPE tag were recorded at 25, 37 and 50 °C (Figure 8), as these cover the temperature range at which most (bio)assays and (microfluidic) analytical applications with liposomes are carried out.

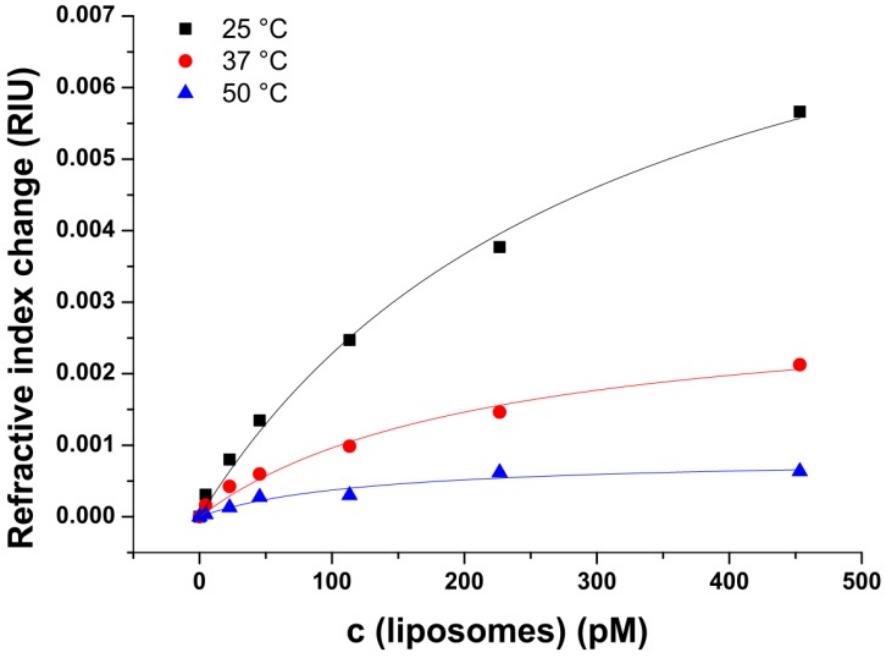

Figure 8. Refractive index changes caused by the interaction of anionic liposomes (300 mM NaCl encapsulant, no tag) with -OH SAM modified gold surfaces at varying phospholipid concentrations at different temperatures.

The decrease in the overall signal change of liposomes binding to the sensor surface is in accordance with the decreasing refractive index of aqueous solutions with increasing temperature [48]. The K_D of the liposome binding determined by simple Langmuir fit decreases between 25 and 50 °C from 310 ± 60 pM to 130 ± 50 pM indicating stronger

interactions between the liposomes and the model sensor surface with increasing membrane fluidity (Figure 9). Additionally, this displays the applicability of the Langmuir model over the whole examined temperature range.

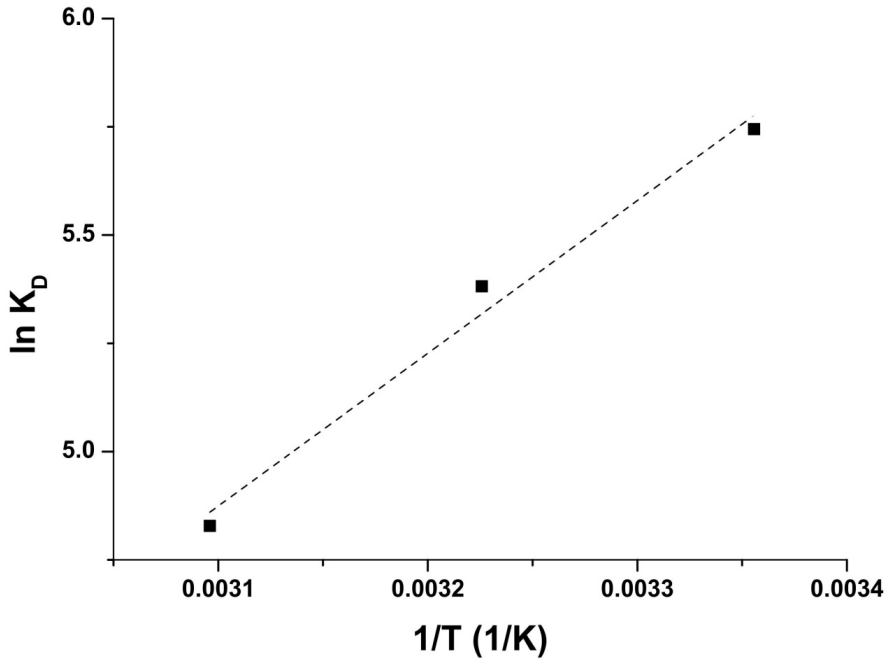

Figure 9. Van 't Hoff plot of the K_D values obtained from the Langmuir fits of the temperature dependent interactions of anionic liposomes (300 mM NaCl encapsulant, no tag) with -OH SAM modified gold surfaces at varying phospholipid concentrations at different temperatures.

4. Conclusions

The binding studies of anionic liposomes consisting of DPPC, DPPG and cholesterol with and without N-glutaryl-DPPE presented herein enable a better mechanistic understanding of the non-specific binding behavior of these liposomes to model surfaces as used in numerous (bio)analytical sensors or assays as well as point-of-care testing devices. We showed that the binding events can be fitted to Langmuir isotherms with high R^2 values (> 0.97) for hydrophilic sensor surfaces. Thus, we were able to determine the K_D values and the refractive index changes at maximum surface loading for these surface/liposome combinations. This is crucial when using liposomes as signal amplification tools [13,17,36,44], as non-specific binding can almost be prevented by introducing N-glutaryl-DPPE into the liposomes and modifying the sensor surface with COOH groups. Hydroxyl groups are known to minimize non-specific bindings, but we demonstrated that

liposomes significantly adhere to –OH surfaces. This finding is important especially for miniaturized bioanalytical detection systems, such as microfluidic biosensors based on liposomes [17,30] with large surface areas compared to the total volume, where non-specific adsorption can cause significant problems and leads to high background signals and low sensing performance. Here, clever surface engineering providing electrostatic repulsion or opposite polarity enables minimization of non-specific interactions and hopefully will lead in the future to intelligently blocked sensor surfaces and not bulk-blocking as customarily done through polymers and proteins. We will further study these conditions by investigations of the specific binding of receptor modified liposomes to optimized surfaces. We propose these findings herein will have a big impact on the general understanding of liposome interactions and thus strongly contribute in the development of new and the improvement of existing applications using liposomes as drug carriers as well as for signal enhancement in sensing devices ranging from standard microtiter plate assays to microfluidic point-of-care diagnostic tools.

5. References

[1] Q. Liu, B.J. Boyd, Liposomes in biosensors, Analyst. 138 (2013) 391–409. doi:10.1039/c2an36140j.

[2] B. Gruber, B. König, Self-Assembled Vesicles with Functionalized Membranes, Chem. Eur. J. 19 (2013) 438–448. doi:10.1002/chem.201202982.

[3] L. Zhang, F. Gu, J. Chan, A. Wang, R. Langer, O. Farokhzad, Nanoparticles in Medicine: Therapeutic Applications and Developments, Clin. Pharmacol. Ther. 83 (2008) 761–769. doi:10.1038/sj.clpt.6100400.

[4] R. Tarallo, A. Accardo, A. Falanga, D. Guarnieri, G. Vitiello, P. Netti, et al., Clickable Functionalization of Liposomes with the gH625 Peptide from Herpes simplex Virus Type I for Intracellular Drug Delivery, Chem. Eur. J. 17 (2011) 12659–12668. doi:10.1002/chem.201101425.

[5] P. Pierrat, G. Laverny, G. Creusat, P. Wehrung, J.-M. Strub, A. VanDorsselaer, et al., Phospholipid–Detergent Conjugates as Novel Tools for siRNA Delivery, Chem. Eur. J. 19 (2013) 2344–2355. doi:10.1002/chem.201203071.

[6] K.A. Edwards, A.J. Baeumner, Liposomes in analyses, Talanta. 68 (2006) 1421–1431. doi:10.1016/j.talanta.2005.08.044.

[7] F. Patolsky, A. Lichtenstein, I. Willner, Amplified Microgravimetric Quartz-Crystal-Microbalance Assay of DNA Using Oligonucleotide-Functionalized Liposomes or Biotinylated Liposomes, J. Am. Chem. Soc. 122 (2000) 418–419. doi:10.1021/ja992834r.

[8] M. Mukai, K. Maruo, Y. Sasaki, J. Kikuchi, Intermolecular Communication on a Liposomal Membrane: Enzymatic Amplification of a Photonic Signal with a Gemini Peptide Lipid as a Membrane-Bound Artificial Receptor, Chem. Eur. J. 18 (2012) 3258–3263. doi:10.1002/chem.201103552.

[9] K.A. Edwards, A.J. Baeumner, Enhancement of Heterogeneous Assays Using Fluorescent Magnetic Liposomes, Anal. Chem. 86 (2014) 6610–6616. doi:10.1021/ac501219u.

[10] J. Zhou, Q. Wang, C. Zhang, Liposome–Quantum Dot Complexes Enable Multiplexed Detection of Attomolar DNAs without Target Amplification, J. Am. Chem. Soc. 135 (2013) 2056–2059. doi:10.1021/ja3110329.

[11] S. Ahn, R.A. Durst, Detection of cholera toxin in seafood using a ganglioside-liposome immunoassay, Anal. Bioanal. Chem. 391 (2008) 473–478. doi:10.1007/s00216-007-1551-1.

[12] S. Ahn-Yoon, T.R. DeCory, R.A. Durst, Ganglioside–liposome immunoassay for the detection of botulinum toxin, Anal. Bioanal. Chem. 378 (2004) 68–75. doi:10.1007/s00216-003-2365-4.

[13] C. Fenzl, T. Hirsch, A.J. Baeumner, Liposomes with High Refractive Index Encapsulants as Tunable Signal Amplification Tools in Surface Plasmon Resonance Spectroscopy, Anal. Chem. (2015). doi:10.1021/acs.analchem.5b03405.

[14] W. Li, T. Luo, Y. Yang, X. Tan, L. Liu, Formation of Controllable Hydrophilic/Hydrophobic Drug Delivery Systems by Electrospinning of Vesicles, Langmuir. 31 (2015) 5141–5146. doi:10.1021/la504796v.

[15] S.J. Mattingly, M.G. O'Toole, K.T. James, G.J. Clark, M.H. Nantz, Magnetic Nanoparticle-Supported Lipid Bilayers for Drug Delivery, Langmuir. 31 (2015) 3326–3332. doi:10.1021/la504830z.

[16] J.W. Maina, J.J. Richardson, R. Chandrawati, K. Kempe, M.P. van Koeverden, F. Caruso, Capsosomes as Long-Term Delivery Vehicles for Protein Therapeutics, Langmuir. (2015) 7776-7781. doi:10.1021/acs.langmuir.5b01667.

[17] L.E. Locascio, J.S. Hong, M. Gaitan, Liposomes as signal amplification reagents for bioassays in microfluidic channels, Electrophoresis. 23 (2002) 799–804. doi:10.1002/1522-2683(200203)23:5<799::AID-ELPS799>3.0.CO;2-P.

[18] H. Liang, J.-P. Tuppurainen, J. Lehtinen, T. Viitala, M. Yliperttula, Non-labeled monitoring of targeted liposome interactions with a model receptor surface: Effect of flow rate and water content, Eur. J. Pharm. Sci.. 50 (2013) 492–501. doi:10.1016/j.ejps.2013.08.011.

[19] N. Granqvist, M. Yliperttula, S. Välimäki, P. Pulkkinen, H. Tenhu, T. Viitala, Control of the Morphology of Lipid Layers by Substrate Surface Chemistry, Langmuir. 30 (2014) 2799–2809. doi:10.1021/la4046622.

[20] D. Peer, J.M. Karp, S. Hong, O.C. Farokhzad, R. Margalit, R. Langer, Nanocarriers as an emerging platform for cancer therapy, Nat Nano. 2 (2007) 751–760. doi:10.1038/nnano.2007.387.

[21] C.F. Calver, H.-W. Liu, G. Cosa, Exploiting Conjugated Polyelectrolyte Photophysics toward Monitoring Real-Time Lipid Membrane-Surface Interaction Dynamics at the Single-Particle Level, Langmuir. (2015). doi:10.1021/acs.langmuir.5b00979.

[22] E. Tellechea, D. Johannsmann, N.F. Steinmetz, R.P. Richter, I. Reviakine, Model-Independent Analysis of QCM Data on Colloidal Particle Adsorption, Langmuir. 25 (2009) 5177–5184. doi:10.1021/la803912p.

[23] I. Reviakine, M. Gallego, D. Johannsmann, E. Tellechea, Adsorbed liposome deformation studied with quartz crystal microbalance, J. Chem. Phys. 136 (2012) 084702. doi:10.1063/1.3687351.

[24] R. Richter, A. Mukhopadhyay, A. Brisson, Pathways of Lipid Vesicle Deposition on Solid Surfaces: A Combined QCM-D and AFM Study, Biophys. J. 85 (2003) 3035–3047. doi:10.1016/S0006-3495(03)74722-5.

[25] R.P. Richter, A.R. Brisson, Following the Formation of Supported Lipid Bilayers on Mica: A Study Combining AFM, QCM-D, and Ellipsometry, Biophys. J. 88 (2005) 3422–3433. doi:10.1529/biophysj.104.053728.

[26] C.A. Keller, B. Kasemo, Surface Specific Kinetics of Lipid Vesicle Adsorption Measured with a Quartz Crystal Microbalance, Biophys. J. 75 (1998) 1397–1402. doi:10.1016/S0006-3495(98)74057-3.

[27] E. Reimhult, F. Höök, B. Kasemo, Intact Vesicle Adsorption and Supported Biomembrane Formation from Vesicles in Solution: Influence of Surface Chemistry, Vesicle Size, Temperature, and Osmotic Pressure, Langmuir. 19 (2003) 1681–1691. doi:10.1021/la0263920.

[28] E. Reimhult, M. Zäch, F. Höök, B. Kasemo, A Multitechnique Study of Liposome Adsorption on Au and Lipid Bilayer Formation on SiO_2, Langmuir. 22 (2006) 3313–3319. doi:10.1021/la0519554.

[29] C.-H. Yoon, J.-H. Cho, H.-I. Oh, M.-J. Kim, C.-W. Lee, J.-W. Choi, et al., Development of a membrane strip immunosensor utilizing ruthenium as an electro-chemiluminescent signal generator, Biosens. Bioelectron. 19 (2003) 289–296. doi:10.1016/S0956-5663(03)00207-0.

[30] N. Wongkaew, P. He, V. Kurth, W. Surareungchai, A.J. Baeumner, Multi-channel PMMA microfluidic biosensor with integrated IDUAs for electrochemical detection, Anal Bioanal Chem. 405 (2013) 5965–5974. doi:10.1007/s00216-013-7020-0.

[31] K. Dimitrievski, B. Kasemo, Influence of Lipid Vesicle Composition and Surface Charge Density on Vesicle Adsorption Events: A Kinetic Phase Diagram, Langmuir. 25 (2009) 8865–8869. doi:10.1021/la9025409.

[32] V. Shpacovitch, V. Temchura, M. Matrosovich, J. Hamacher, J. Skolnik, P. Libuschewski, et al., Application of Surface Plasmon Resonance Imaging Technique for the Detection of Single Spherical Biological Submicron-particles, Anal. Biochem. (2015). doi:10.1016/j.ab.2015.06.022.

[33] K.A. Edwards, A.J. Baeumner, Optimization of DNA-tagged dye-encapsulating liposomes for lateral-flow assays based on sandwich hybridization, Anal. Bioanal. Chem. 386 (2006) 1335–1343. doi:10.1007/s00216-006-0705-x.

[34] V. Bello, G. Mattei, P. Mazzoldi, N. Vivenza, P. Gasco, J.M. Idee, et al., Transmission Electron Microscopy of Lipid Vesicles for Drug Delivery: Comparison between Positive and Negative Staining, Microsc. Microanal. 16 (2010) 456–461. doi:10.1017/S1431927610093645.

[35] R.J. Hunter, Zeta Potential in Colloid Science: Principles and Applications, Academic Press, London, 1981; pp. 69-74.

[36] K.A. Edwards, K.J. Meyers, B. Leonard, A.J. Baeumner, Superior performance of liposomes over enzymatic amplification in a high-throughput assay for myoglobin in human serum, Anal. Bioanal. Chem. 405 (2013) 4017–4026. doi:10.1007/s00216-013-6807-3.

[37] C. Fenzl, S. Wilhelm, T. Hirsch, O.S. Wolfbeis, Optical Sensing of the Ionic Strength Using Photonic Crystals in a Hydrogel Matrix, ACS Appl. Mater. Interfaces. (2012). doi:10.1021/am302355g.

[38] C. Fenzl, C. Genslein, A. Zöpfl, A.J. Baeumner, T. Hirsch, A photonic crystal based sensing scheme for acetylcholine and acetylcholinesterase inhibitors, J. Mater. Chem. B. 3 (2015) 2089–2095. doi:10.1039/C4TB01970A.

[39] P. Fraga García, M. Freiherr von Roman, S. Reinlein, M. Wolf, S. Berensmeier, Impact of Nanoparticle Aggregation on Protein Recovery through a Pentadentate Chelate Ligand on Magnetic Carriers, ACS Appl. Mater. Interfaces. 6 (2014) 13607–13616. doi:10.1021/am503082s.

[40] A.K. Singh, P.K. Kilpatrick, R.G. Carbonell, Application of Antibody and Fluorophore-Derivatized Liposomes to Heterogeneous Immunoassays for D-dimer, Biotechnol. Prog. 12 (1996) 272–280. doi:10.1021/bp9500674.

[41] C. Ege, K.Y.C. Lee, Insertion of Alzheimer's Aβ40 Peptide into Lipid Monolayers, Biophys. J. 87 (2004) 1732–1740. doi:10.1529/biophysj.104.043265.

[42] J.N. Israelachvili, D.J. Mitchell, A model for the packing of lipids in bilayer membranes, Biochim. Biophys. Acta, Biomembr. 389 (1975) 13–19. doi:10.1016/0005-2736(75)90381-8.

[43] P. Diao, D. Jiang, X. Cui, D. Gu, R. Tong, B. Zhong, Studies of structural disorder of self-assembled thiol monolayers on gold by cyclic voltammetry and ac impedance, J. Electroanal. Chem. 464 (1999) 61–67. doi:10.1016/S0022-0728(98)00470-7.

[44] K.A. Edwards, A.J. Baeumner, Periplasmic Binding Protein-Based Detection of Maltose Using Liposomes: A New Class of Biorecognition Elements in Competitive Assays, Anal. Chem. 85 (2013) 2770–2778. doi:10.1021/ac303258n.

[45] K.A. Edwards, K.J. Meyers, B. Leonard, J.T. Connelly, Y. Wang, T. Holter, et al., Engineering liposomes as detection reagents for CD4+ T-cells, Anal. Methods. 4 (2012) 3948–3955. doi:10.1039/C2AY25480H.

[46] A.D. Rakic, A.B. Djurišic, J.M. Elazar, M.L. Majewski, Optical Properties of Metallic Films for Vertical-Cavity Optoelectronic Devices, Appl. Opt. 37 (1998) 5271–5283. doi:10.1364/AO.37.005271.

[47] R.L. Olmon, B. Slovick, T.W. Johnson, D. Shelton, S.-H. Oh, G.D. Boreman, et al., Optical dielectric function of gold, Phys. Rev. B. 86 (2012) 235147. doi:10.1103/PhysRevB.86.235147.

[48] P.N. Yi, R.C. MacDonald, Temperature dependence of optical properties of aqueous dispersions of phosphatidylcholine, Chem. Phys. Lipids. 11 (1973) 114–134. doi:10.1016/0009-3084(73)90029-7.

Chapter 3: Liposomes with high refractive index encapsulants as tunable signal amplification tools in surface plasmon resonance spectroscopy

Abstract

One major goal in the surface plasmon resonance (SPR) technique is the reliable detection of small molecules as well as low analyte concentrations. This can be achieved by a viable signal amplification strategy. We therefore investigated optimal liposome characteristics for use as signal enhancement system for SPR sensors, as liposomes excel not only at versatility, but also at colloidal stability and ease of functionalization. These characteristics include the encapsulation of high refractive index markers, lipid composition, liposome size and surface modifications to best match the requirements of the SPR system. Our studies of the binding of biotinylated liposomes to surface-immobilized streptavidin show that the refractive index of the encapsulant has a major influence on the SPR signal and outweighs the influence of the thin lipid bilayer. Thus, the signal amplification properties of liposomes can be adjusted to the respective needs of any analytical task by simply exchanging the encapsulant solution. In this work, a maximum enhancement factor of 23 was achieved by encapsulating a 500 mM sucrose solution. Dose-response studies with and without liposome enhancement revealed an improvement of the limit of detection from 10 $nmol \cdot L^{-1}$ to 320 $pmol \cdot L^{-1}$ streptavidin concentration with a much higher sensitivity of 3 mRIU per logarithmic unit of the concentration between 500 $pmol \cdot L^{-1}$ and 10 $nmol \cdot L^{-1}$.

This chapter has been published.

Christoph Fenzl, Thomas Hirsch, Antje J. Baeumner, *Analytical Chemistry*, **2015**, 87 (21), 11157 – 11163, DOI: 10.1021/acs.analchem.5b03405.

Author contributions

CF carried out the experimental work solely and wrote the article. The manuscript was revised by TH and AJB. AJB is corresponding author.

1. Introduction

Surface plasmon resonance (SPR) technique is a powerful sensing tool for real-time monitoring interactions of numerous analytes and therefore extensively used in analytical and pharmaceutical research. However, it faces a major challenge when trying to directly detect very small refractive index changes, e. g. caused by small molecules (< 400 Da) or very low analyte concentrations [1–3]. For example, significant efforts are required to distinguish between biomolecules of very similar mass such as a protein with and without its glycoprofile [4]. Therefore, various approaches to improve the performance have been investigated. One possibility for signal enhancement is the modification of the sensor substrate [5–8]. Zhai *et al.* [5] used bimetallic silver/gold films and obtained up to 2.7 times higher SPR signals than with ordinary gold surfaces, but the inferior chemical stability of silver makes these substrates harder to handle. Nanohole arrays [7] on the other hand are an emerging technique to improve the figures of merit for SPR sensing. Here, periodic arrangements of holes in a gold sensor surface are prepared by nanoimprinting and sputtering methods. However, the more complicated and time-consuming fabrication methods as well as the fact that small variations in hole diameter, depth or periodicity have a significant influence on the sensor properties [7] are identified as drawbacks of nanohole arrays. Another successful surface modification is the addition of a graphene monolayer on the gold substrate. It changes the propagation constant of surface plasmon polaritons leading to higher sensitivity for changes of the refractive index (RI) [8]. However, immobilization of recognition elements on the graphene-modified surface becomes more difficult, i.e. the well-established gold – thiol chemistry cannot be used and instead elaborate surface chemistry using non-covalent π-stacking interactions of functionalized pyrene derivates is required [8].

To keep the gold surface as standard, generate an easy-to-functionalize sensing substrate, and achieve signal amplification, numerous approaches using nanoparticles as amplification tags have been developed [1,9–14]. Gold nanoparticles are the most commonly used material in this field of research, as their inherent plasmonic effect adds to the sensitivity [9–12]. Their synthesis protocol is well known and the particle surface can be modified following similar workflows as in the formation of a self-assembled monolayer on the SPR sensor. Willner's group demonstrated that molecularly imprinted

boronic acid-functionalized gold nanoparticle composites enable the detection of various antibiotics in milk samples with limits of detection (LODs) down to 200 fmol L^{-1} [9]. With ion-imprinted nanocomposites the group showed the detection possibilities for small alkaline-earth metal ions in the femtomolar concentration regime [10]. Baek *et al.* demonstrated an enhancement strategy with two different Au nanoparticles that allowed thrombin detection at the subattomolar level [11]. In a competitive assay, gold nanospheres can also be used to detect the small molecule testosterone with a LOD of 170 pmol L^{-1} in a sensing strategy that combines traditional SPR with readout of the localized surface plasmons [12]. Most of these enhancement approaches use Au nanospheres with diameters ranging between 10 and 20 nm, even though these sizes are not ideal for the highest signal amplification, but the synthesis of larger particles is not straightforward [1]. In addition, elaborate efforts are required for their surface modification in order to optimize colloidal stability [12]. Magnetic nanoparticles, e.g. Fe_3O_4 are also widely used in SPR sensing, as they are convenient to separate and posses a high refractive index [1]. By utilizing clustered magnetic microparticles, cancer biomarkers in serum can be monitored at attomolar concentrations [13]. In general, those approaches using colloidal metal or metal oxide nanoparticles as signal amplification tools need very careful experimental design regarding colloidal stability and surface modification.

Here, we present an alternative, highly versatile approach to signal enhancement with liposomes as amplification tags in SPR. Liposomes – nanoscopic vesicles consisting of a lipid bilayer membrane – are widely used in drug delivery [15,16] and (bio)analytical sensing [17,18]. Although liposomes have been shown to be ideal amplification mediators in fluorescent [19] and electrochemical [20] sensing as well as in quartz crystal microbalance technique [21], the potential of liposomes as signal enhancers in SPR has been mainly neglected. Wink *et al.* [14] developed a sandwich immunoassay for interferon-γ using liposomes as tags, but did not investigate the influence of varying refractive index inside the hydrophilic cavity on the signal amplification properties. In this work, we systematically studied the signal amplification afforded by liposomes in a well-established SPR set-up. We characterized the liposomes regarding their size and surface charge and investigated the influence of encapsulants with varying RI on the capability of

enhancing the SPR performance using streptavidin-biotin as a model biorecognition approach.

2. Experimental Section

2.1. Materials

1,2-Dipalmitoyl-sn-glycero-3-phosphocholine (DPPC), 1,2-dipalmitoyl-sn-glycero-3 [phospho-rac-(1-glycerol)], sodium salt (DPPG), N-biotinyl-1,2-dipalmitoyl-sn-glycero-3-phosphatidylethanolamine (N-biotinyl-DPPE), and the extrusion kit and membranes were obtained from Avanti Polar Lipids (Alabaster, AL, USA). 4-(2-Hydroxyethyl)piperazine-1-ethanesulfonic acid (HEPES), sodium azide, cholesterol, Phosphotungstic acid (PTA), and 11-mercaptoundecanoic acid were purchased from Sigma-Aldrich (Taufkirchen, Germany). N-(1-mercapto-11-undecyl)-biotinamide was ordered from ProChimia Surfaces (Sopot, Poland) and Streptavidin from Life Technologies (Carlsbad, CA, USA). All further chemicals were purchased from VWR (Darmstadt, Germany).

2.2. Preparation of liposomes

The liposomes were prepared following a modified protocol previously described by Edwards et al. [22]. Briefly, DPPC, DPPG, cholesterol and N-biotinyl DPPE (40.9:20.1:51.7:2.1 µmol, respectively) were dissolved in a organic solvent mixture consisting of 3 mL chloroform and 0.5 mL methanol, and sonicated for 1 min in a sonication bath (Bandelin Sonorex Digitec DT 255 H) at 45 °C for homogeneous mixing. A 2 mL volume of aqueous solutions of varying refractive index (300 mmol L^{-1} NaCl, 500 mmol L^{-1} sucrose or 130 mmol L^{-1} NaCl/35 mmol L^{-1} sucrose, respectively) at 45 °C was added to the lipid mixture and then was again sonicated for 4 min. The organic solvent was removed at 45 °C and 380 mbar for 20 min using a rotary evaporator. The mixture was then vortexed before and after a second addition of 2 mL 45 °C aqueous solution. The flask was returned to the rotary evaporator for 20 min at 45 °C and

380 mbar and then for 20 min at 280 mbar. The crude liposome dispersion is then extruded at 50 °C 21 times through 1.0 µm Nucleopore membranes (Whatman, Florham Park, NJ, USA), followed by 21 times through 0.4 µm membranes. The liposomes were purified via size-exclusion chromatography with Sephadex G-50 in a 15 × 1.6 cm column at ~4 mL min^{-1} using HEPES-saline-sucrose buffer (HSS; 10 mmol·L^{-1} HEPES, 200 mmol·L^{-1} sodium chloride, 200 mmol·L^{-1} sucrose, 1.5 mmol·L^{-1} sodium azide at pH 7.5) for the liposomes with 300 mmol·L^{-1} NaCl and 500 mmol·L^{-1} sucrose as encapsulant, and using HEPES-saline buffer (10 mmol·L^{-1} HEPES, 200 mmol·L^{-1} sodium chloride, 1.5 mmol·L^{-1} sodium azide at pH 7.5) for the liposomes with 130 mmol·L^{-1} NaCl/35 mmol·L^{-1} sucrose as encapsulant. The fractions containing liposomes were combined and dialyzed overnight against HSS or HEPES-saline buffer, respectively, before storage at 4 °C.

2.3 Liposome characterization

Dynamic light scattering (DLS) measurements were performed with a 1:100 dilution of liposomes in HEPES-saline buffer resulting in an approximate phospholipid concentration of 100 µmol·L^{-1}. A disposable polystyrene cuvette was filled with 1 mL of the suspension and analyzed with the particle sizer in the backscattering mode at an angle of 173° (Malvern Zetasizer nano series) at 25 °C after an equilibration time of 120 s. The autocorrelation of the intensity recorded over time is related to the geometry of the liposomes under observation. After 30 consecutive measurements, the mean hydrodynamic radius and a polydispersity index (PDI) were extracted from the autocorrelation data. The electrophoretic mobility of the purified liposomes was measured with the same 1:100 dilution of liposomes in HEPES-saline buffer. A Folded Capillary Cell (Malvern DTS1070) was filled with approx. 800 µL of the liposome dispersions and equilibrated to 25 °C for 120 s. The mean electrophoretic mobility was determined by laser Doppler velocimetry with the Zetasizer nano series. The Smoluchowski model was employed to determine the zeta potential of the dispersions [23].

For transmission electron microscopy (TEM), a 1:10 dilution of liposomes in HEPES-saline buffer was used. A carbon-coated copper grid was covered with a 2 µL drop of the

suspension for 90 s. After removing the excess of liposomes by washing with 5 µL of 8.7 mmol·L^{-1} PTA aqueous solution, the vesicles left on the TEM-grid were negatively stained [24] with a 5 µL drop of 8.7 mmol·L^{-1} PTA aqueous solution for 30 s. The excess staining solution was removed with a filter paper. Transmission electron micrographs were recorded with a transmission electron microscope (Philips CM 12).

The phospholipid concentration of liposomes was measured by inductively coupled plasma – atomic emission spectroscopy (ICP-AES). A volume of 20 µL of liposomes was diluted in nitric acid (c = 0.5 mol·L^{-1}) to a total volume of 3 mL. The mixture was vortexed and sonicated thoroughly. Phosphorus standard solutions were prepared with concentrations of 1, 5, 10, 25, 50 and 100 µmol L^{-1} phosphate in 0.5 mol·L^{-1} HNO_3 for calibration. The phosphorus content was measured via ICP-AES (Spectro Flame-EOP, Analytical Instruments GmbH, Kleve, Germany) at the phosphorus specific wavelength of 178.29 nm.

2.4. Surface plasmon resonance spectroscopy (SPR) measurements

Following a modified protocol of Knoll *et al.* [25], the SPR sensor chip consisting of a 50 nm Au layer on a 5 nm Cr adhesive layer on glass with a refractive index of 1.61 (Mivitec, Sinzing, Germany), was immersed in an ethanolic solution containing 160 µmol·L^{-1} 11-mercaptoundecanoic acid and 40 µmol·L^{-1} N-(1-mercapto-11-undecyl)-biotinamide for a minimum of 20 h in order to form a dense SAM on the gold surface. The chips were then rinsed with ethanol and dried under nitrogen flow. The complete coverage of the gold surface was proven using cyclic voltammetry as previously established in our laboratory (data not shown). The SPR measurements were conducted with a two channel SPR device (Mivitec Biosuplar 321, Sinzing, Germany) at ambient temperature with 640 nm laser excitation and equipped with a flow cell of a total volume of approx. 50 µL per channel. Flow rate was adjusted to 200 µL·min^{-1}. The measurements were performed at a fixed angle by read-out of the change of the intensity of the reflected light. Fluctuations in temperature or laser intensity were compensated by using one channel as reference channel with a continuous flow of ultrapure water. After calibration of the measured signal intensity with sodium chloride solutions of known

refractive index, streptavidin (1 µmol·L^{-1}) was immobilized on the sensor chip for 90 min at a flow rate of 50 µL·min^{-1} followed by a washing step with degassed HEPES-saline buffer for 20 min at a flow rate of 200 µL min^{-1}. Then, liposome dispersions were diluted to phospholipid concentrations of 1, 5, 10, 25, 50, and 100 µmol·L^{-1} with degassed HEPES-saline buffer. The dispersions were consecutively injected with increasing phospholipid concentration, each for 20 min followed by a washing step with HEPES-saline buffer for 10 min. In a following experiment in order to record the dose – response curves of streptavidin with and without liposome enhancement, the immobilization time of the streptavidin (at concentrations ranging from 10 pmol·L^{-1} to 1 µmol·L^{-1}) was shortened to 20 min at a flow rate of 200 µL·min^{-1} followed by a 10 min washing step with HEPES-saline buffer. Then, liposomes encapsulating 500 mmol·L^{-1} sucrose were added at a phospholipid concentration of 25 µmol·L^{-1} for 20 min before washing with HEPES-saline buffer for 10 min. All errors were calculated using three times the signal noise. The limit of detection of the enhancement method was determined by the refractive index change induced by liposome binding which must exceed three times the signal noise.

3. Results and Discussion

In this study, the signal enhancement properties of highly stable anionic liposomes are investigated via SPR spectroscopy using the strong biotin-streptavidin binding affinity as model system. The binding of small molecules to a monolayer leads to weak signal changes and needs signal amplification strategies for reliable detection [1]. Liposomes encapsulating high refractive index solutions amplify this signal upon binding and thus improve the sensitivity (Figure 1).

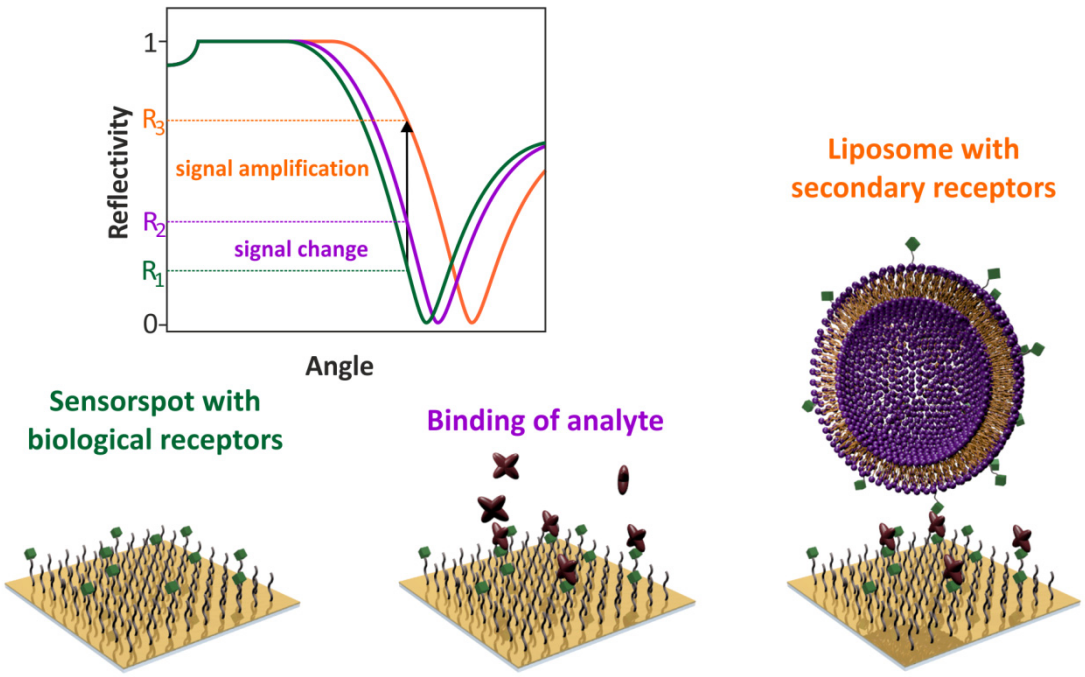

Figure 1. Sensing scheme for the SPR signal amplification with liposomes. Liposomes are used as label subsequent to the analyte binding to the SPR surface. While this renders the traditionally label-free SPR method to a label-based detection system, this approach will enable the detection of bound analytes present at low concentration, and those providing only minimal changes in RI.

Previous studies of non-specific binding of liposomes to SPR surfaces had shown that negatively-charged SPR surfaces bearing COOH groups combined with negatively-charged liposomes lead to limited non-specific binding without the need for additional blocking of the SPR surface. For the goal of developing liposomes for specific analyte detection, size and surface charge of the liposomes were investigated here for detailed characterization. Dynamic light scattering measurements determined the hydrodynamic diameters. The biotin-tagged liposomes with 500 mM sucrose encapsulant had a diameter of 180 nm, with a polydispersity index (PDI) of 0.11. The liposomes encapsulating 300 mM NaCl are 240 nm (PDI of 0.23) and those with 130 mM NaCl/35 mM sucrose encapsulant are 230 nm (PDI of 0.19) in diameter. The sizes are all in the 200-nm-regime and as a consequence the evanescent field of the SPR can penetrate the whole liposome, as the diameters are smaller than half of the wavelength of the SPR device [26].

Liposomes are synthesized with about 40 mol% of DPPG which leads to electrostatic repulsion between the liposomes and hence leads to high colloidal stability.

The zeta potentials measured by electrophoretic mobility gave values of -24.7 ± 1.7 mV for liposomes encapsulating 500 mM sucrose, -24.5 ± 1.2 mV for 300 mM NaCl and -27.1 ± 1.7 mV for 130 mM NaCl/35 mM sucrose containing ones. As expected, all three types exhibit outstanding long term stability (> 1 year) and retain their diameters as well as the negative zeta potentials. This high colloidal stability is better than that of various other nanomaterials such as silica nanoparticles [27] or polystyrene nanospheres [28].

Transmission electron microscopy (TEM) proves the formation of the nanovesicles. The diameters of the liposomes are consistent with the results of dynamic light scattering. In addition, the TEM images show good regularity of size and shape of the formed liposomes (Figure 2) consisting of a mixture of unilamellar and multilamellar vesicles. Deviations from the perfectly spherical shape of liposomes on the images are likely caused by the drying and staining process on the TEM grid.

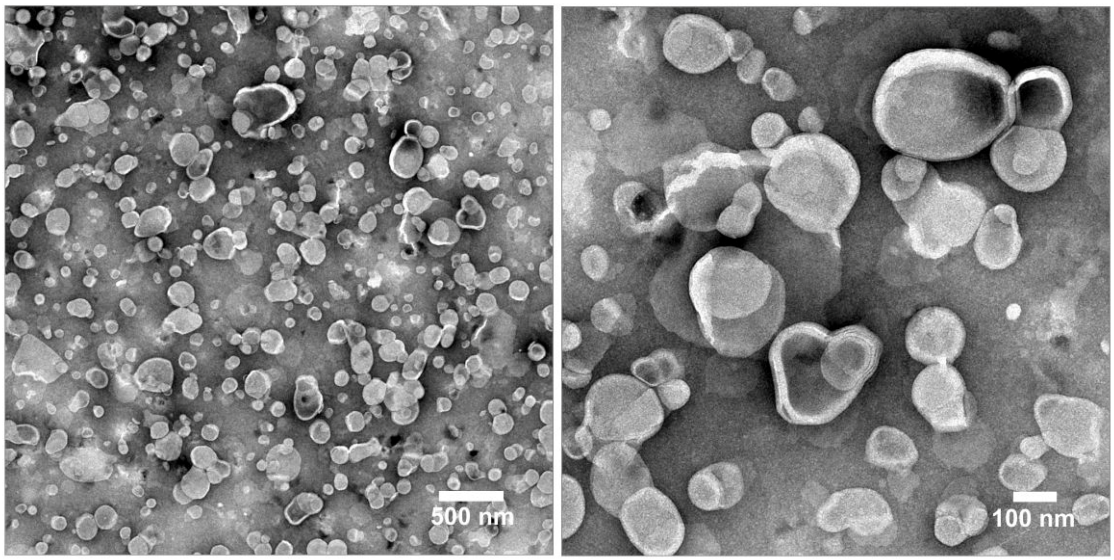

Figure 2. TEM images of a 1:10 diluted dispersion of liposomes. Scale bars are 500 nm (left) and 100 nm (right).

The phospholipid concentration was determined via ICP-AES resulting in 9.3 mmol L^{-1} for the batch with 500 mM sucrose encapsulant, 12.6 mmol·L^{-1} for 300 mM sodium chloride and 8.6 mmol·L^{-1} for 130 mM NaCl/35 mM sucrose encapsulant. The total lipid concentration can be calculated using the molar ratios to 16.9, 22.9 and 15.6 mmol·L^{-1}, respectively. All liposome characteristics are summarized in Table 1.

Table 1. Properties of liposomes synthesized with different encapsulants.

Encapsulant	Diameter / nm	PDI[a)]	Zeta potential / mV	c (phospholipid) / mM	c (total lipid) /mM	RI[b)] of encapsulant
500 mM sucrose	180	0.11	-24.7 ± 1.7	9.3	16.9	1.3575
300 mM NaCl	240	0.23	-24.5 ± 1.2	12.6	22.9	1.3360
130 mM NaCl + 35 mM sucrose	230	0.19	-27.1 ± 1.7	8.6	15.6	1.3360

[a)]polydispersity index [b)]refractive index

3.1. SPR signal enhancement through liposome binding

SPR sensor surfaces were prepared with a densely packed self-assembled monolayer consisting of 11-mercaptoundecanoic acid and N-(1-mercapto-11-undecyl)-biotinamide with a reaction time of > 20 h in order to allow for specific streptavidin binding to the surface. Based on prior studies of Knoll *et al.* [25], we found a ratio of 80% COOH-terminated thiols and 20% biotin-terminated thiols (translating into a ratio 4:1) to be the optimum in respect to maximized specific and minimized non-specific binding. After device calibration with sodium chloride solutions of known refractive index, the sensor surface was then saturated with streptavidin (1 µM) resulting in an expected small signal change (Figure 3). Afterwards, liposome dispersions containing biotin functionality (1.8% of the liposome surface) were continuously injected for a 20 min interaction time with the streptavidin sensor surface, followed by a 10 min washing step to remove non-bound liposomes. Liposome concentrations in a range of 0 to 100 µmol·L^{-1} phospholipid were studied.

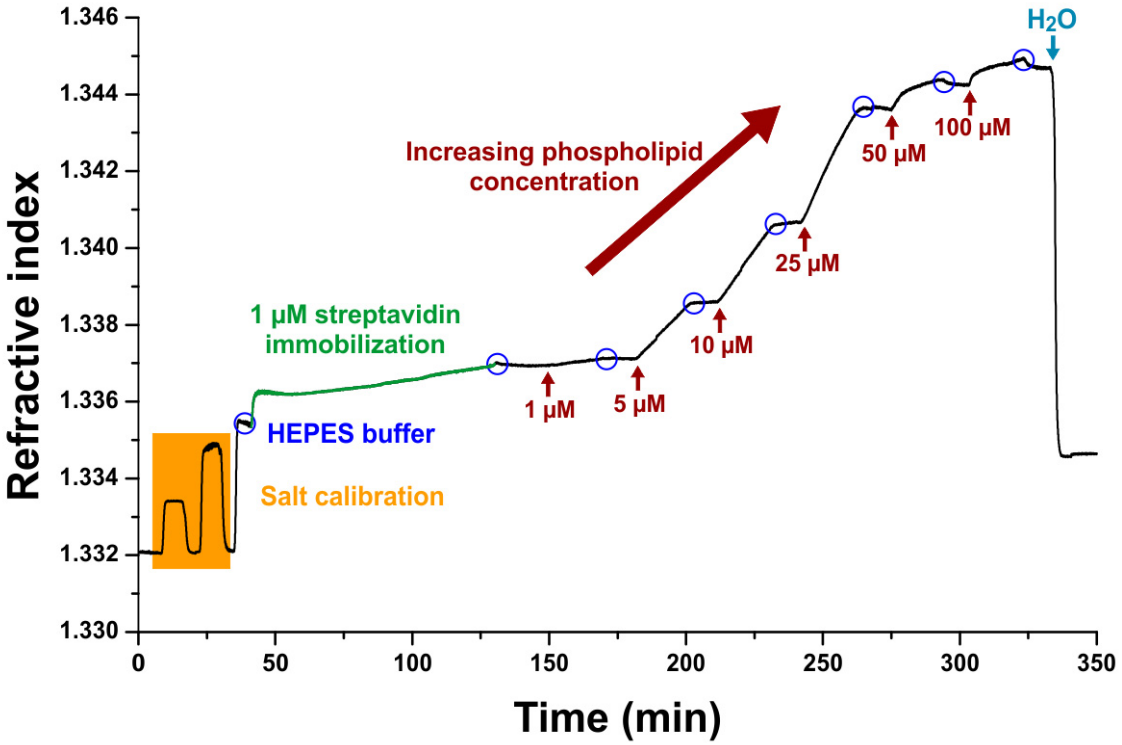

Figure 3. Exemplary sensorgram of the refractive index changes in SPR measurements induced by the interactions of biotinylated liposomes (300 mM NaCl encapsulant) at varying phospholipid concentrations with streptavidin (1 µM) immobilized on a biotinylated gold sensor surface.

As Figure 3 shows, the small signal change of streptavidin binding to the biotinylated gold sensor surface is significantly enhanced by liposome addition. Increasing liposome concentration resulted in increasing refractive index changes due to binding of the biotinylated vesicles to the sensor surface. At higher concentrations, a slow desorption process during the washing step with HEPES buffer is observed. In the end, ultrapure water was injected over the sensor surface indirectly prove the successful binding of intact liposomes to the sensor surface. The water will cause lysis of the bound intact liposomes due to the high difference of the osmotic pressure. As expected, a significant drop of the SPR signal is observed.

Penetration length of the evanescent wave is a function of the effective surface refractive index [29] and is thus also influenced by the size of the liposomes and its distribution. Ong *et al.* determined the penetration length to be in the range of 175 nm for SPR measurements of glucose solutions on a 44 nm gold layer with a 633 nm light source [30]. As these conditions match our experimental setup in good accordance, liposomes with diameters of approx. 200 nm are presumed to be penetrated almost completely by the

evanescent wave. Therefore, the RI of the encapsulant has an important influence on the signal amplification properties of the liposomes. Encapsulants of the same RI should result in similar SPR signal changes, when the liposomes bind to the sensor surface covered with streptavidin (1 µM). On the other hand, increasing the RI will result in higher signal amplification. As a consequence, we compare liposomes encapsulating 300 mM sodium chloride with those encapsulating 130 mM sodium chloride and 35 mM sucrose, as the RI of both solutions is comparable. For higher amplification, 500 mM sucrose is encapsulated. The SPR signal change in refractive index units (RIU) was recorded in dependence of the phospholipid concentration of the liposome dispersions. The absolute changes corrected by the signal changes induced by non-specific binding are presented in Figure 4.

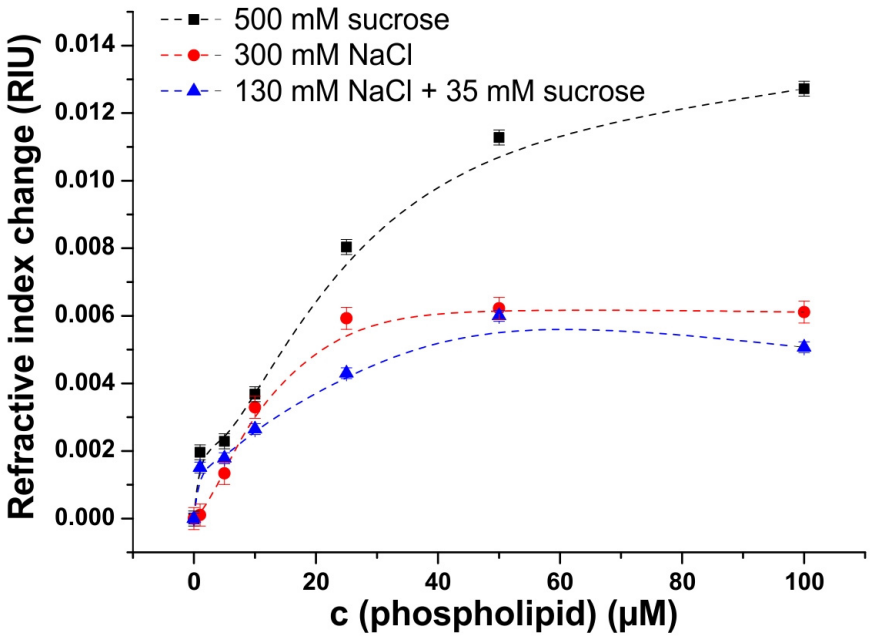

Figure 4. Comparison of liposomes encapsulating different solutions for signal amplification with SPR sensors. Liposomes entrapping 500 mM sucrose, 300 mM NaCl or 130 mM NaCl + 35 mM sucrose were able to specifically bind to the sensor surface via biotin on the liposome membrane and streptavidin on the sensor surface.

The binding curves of all three liposome batches exhibit saturation characteristics starting at phospholipid concentrations between 25 and 50 µmol·L^{-1}. The liposomes encapsulating solutions of the same refractive index of 1.3360 (300 mM NaCl and 130 mM NaCl + 35 mM sucrose) show similar binding characteristics over the whole concentration range,

resulting in a maximum signal change of 0.005 RIU at the highest concentration of 100 µmol·L^{-1} phospholipid content. Using 500 mM sucrose solution as encapsulant, the higher RI of 1.3575 inside the liposomes causes the signal change to nearly double to 0.013 RIU at 100 µmol·L^{-1} phospholipid concentration. These findings lead to two interesting conclusions: (1) the refractive index of the encapsulant has a major influence on the SPR signal upon liposome binding and outweighs the influence of the thin lipid bilayer. (2) The signal amplification properties of liposomes can be adjusted to the personal need of any analytical task by simply exchanging the encapsulant solution. This tuning is very difficult for other SPR enhancement techniques using nanoparticles [11,31], as the RI of the particles itself is usually a fixed parameter.

In order to compare liposome-afforded signal enhancement to other approaches, the resulting signal should be correlated to the change caused by the analyte – in our case streptavidin – itself. Therefore, we calculate the signal amplification percentage after the following equation (1):

$$Enhancement\ factor = \frac{\Delta n_{D,spec}(liposomes)}{\Delta n_{D,spec}(analyte)} \quad (1)$$

where $\Delta n_{D,\ spec}$ *(liposomes)* is the specific refractive index change induced by liposome binding to the sensor surface and $\Delta n_{D,\ spec}$ *(analyte)* is the specific change in RI caused by analyte binding without liposome amplification. In Figure 5, the signal amplification of liposomes with three different encapsulants are shown at one phospholipid concentration in the dynamic range of liposome binding (25 µM) and at one concentration in the saturation regime of the binding curve (100 µM).

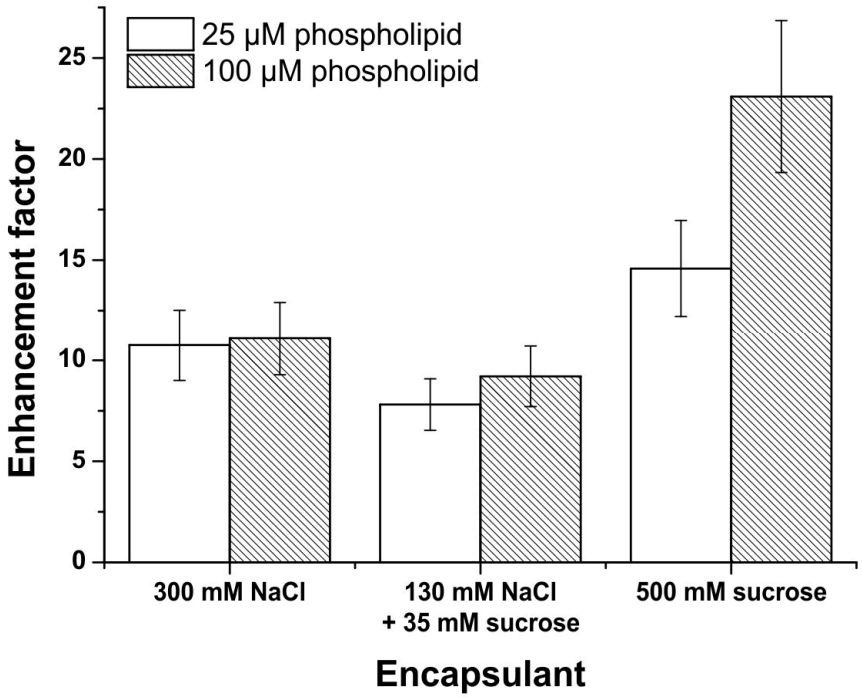

Figure 5. Comparison of the enhancement factors of liposomes with varying encapsulants (500 mM sucrose, 300 mM NaCl or 130 mM NaCl + 35 mM sucrose) at two different phospholipid concentrations. Specific liposome binding was achieved by biotinylated phospholipids in the bilayer and streptavidin on the sensor surface.

Enhancement factors of 9 to 10 are possible with liposomes encapsulating solutions with a RI of 1.3360 (e.g. 300 mM NaCl or 130 mM NaCl + 35 mM sucrose) at 25 µM phospholipid content which only slightly increases at the higher concentration of 100 µM indicating that the RI in the liposomes is too low to overcome the increased non-specific binding at increasing concentrations. In contrast, the much higher RI of 500 mM sucrose (1.3575) inside the liposomes more than doubles the signal amplification to 23-fold at 100 µM phospholipid content. In addition, a distinct increase of approx. 8.5-fold amplification is observed when increasing the liposome concentration from 25 to 100 µM. These results show the great versatility that can be achieved with liposomes. By tailoring the RI inside and choosing an adequate phospholipid concentration for the desired sensing application, liposomes can provide nearly infinite variable enhancement factors from 0 to 23 in SPR, and thus enabling the adjustment of the dynamic range in such a way that it is best suited for the specific analytical question at hand.

In order to determine the improved performance of liposome-amplified SPR sensing, dose-response curves for streptavidin were recorded with and without liposome enhancement (500 mM sucrose encapsulant, 25 µM phospholipid concentration) with streptavidin concentrations ranging from 10 pmol·L^{-1} to 1 µmol·L^{-1} (Figure 6).

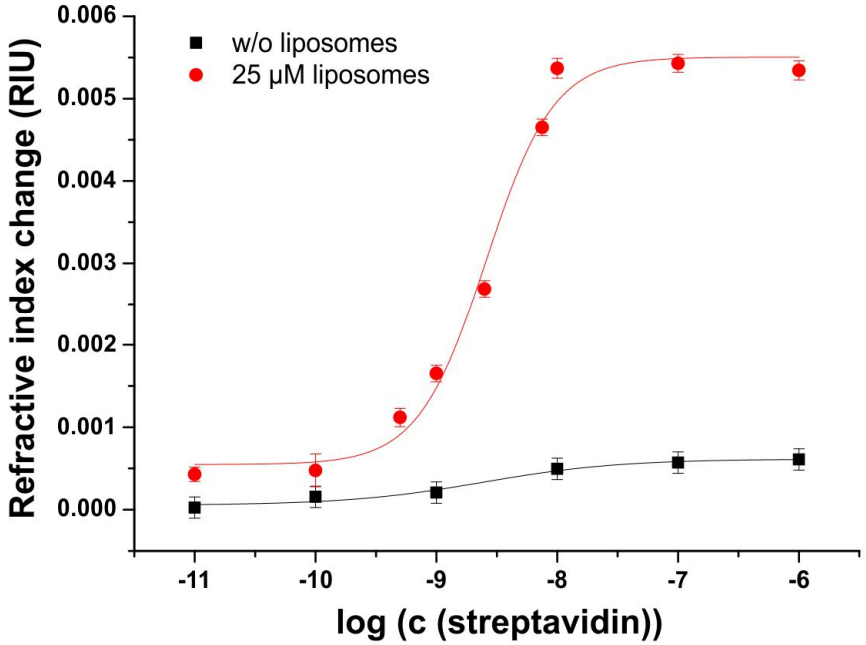

Figure 6. Dose-response curves for the interaction of streptavidin with COOH/biotin(4:1)-SAM modified gold surfaces with and without liposome enhancement (500 mM sucrose encapsulant, biotin-tag, 25 µM phospholipid) measured by SPR.

The data for this binding of streptavidin to a gold sensor surface modified with a self-assembled monolayer with and without liposomes are fitted both to the dose-response model following the Hill equation (2) [32]:

$$\Delta n_D = S + \frac{E - S}{1 + \left(\frac{EC_{50}}{c}\right)^h} \qquad (2)$$

where Δn_D is the refractive index change in RIU, S is the minimum asymptote, E is the maximum asymptote, c is the concentration of streptavidin, h is the Hill slope and EC_{50} is the half maximal effective concentration. The fitting parameters are summarized in Table 2.

Table 2. Fitting parameters for the dose-response model.

	S / RIU	E / RIU	EC_{50} / mol·L^{-1}	h	R^2
Without liposomes	$(5 \pm 6) \cdot 10^{-5}$	$(6.1 \pm 0.6) \cdot 10^{-4}$	$(2.5 \pm 1.6) \cdot 10^{-9}$	0.8 ± 0.4	0.946
With liposomes	$(5.5 \pm 1.9) \cdot 10^{-4}$	$(5.50 \pm 0.19) \cdot 10^{-3}$	$(2.6 \pm 0.4) \cdot 10^{-9}$	1.5 ± 0.3	0.984

The signal change for the streptavidin binding without liposome enhancement is very low over the whole concentration range resulting in high errors for the fitting parameters and only a R^2 of 0.946. The first detectable RI change is measured at a streptavidin concentration of 10 nmol·L^{-1}. This performance is significantly improved through liposomes. Whereas the EC_{50} values of approx. 2.5 nmol·L^{-1} are in good accordance for both fits, the liposome amplification approach results in a higher Hill slope (1.5 vs. 0.8) indicating a weak cooperative effect of the binding, and in a higher R^2 of 0.984.

In general, SPR signals are very sensitive to the distance between substrate surfaces and bound species which may lead to broadened SPR dips and thus deteriorated sensitivities. However, this was not observed in the described study. In contrast, the RI changes are much higher than without enhancement. The limit of detection is improved to a low streptavidin concentration of 320 pmol·L^{-1} and streptavidin can be measured with a sensitivity of 3 mRIU per logarithmic unit of the concentration between 500 pmol·L^{-1} and 10 nmol·L^{-1}. While this is afforded by a small increase in measurement time by 20 min, it is justified by the significantly improved sensor performance. Optimization of flow-through and assay times will be the focus of future studies. This sensing approach generally shows a higher performance than those based on local surface plasmons which yielded detection limits of 16.6 nM [33], 3 nM [34] or 420 pM [35], respectively. Furthermore, no real-time monitoring of binding events is possible with this colorimetric sensing scheme in contrast to the here described principle.

Bruck *et al.* [36] monitored streptavidin binding with a Mach-Zehnder interferometer down to only 1.66 nM which is 5 times higher than our reported LOD, but without any amplification strategy. Also, high-performing silicon ring resonators [37] demonstrated a LOD of only 0.06 nM. However both of these approaches require time-consuming clean room preparation of the sensor chip and high temporal and instrumental effort. Instead,

the usage of liposomes to enhance the well established technique of SPR excels at versatility and ease of applicability combined with high sensitivity.

4. Conclusions

In these studies, we demonstrated that liposomes containing solutions with high refractive index are versatile tools for signal amplification in SPR. They can be synthesized with a great variety of encapsulants, are highly colloidally stable preventing non-specific binding, and are easy to modify with biological receptors. In our proof-of-principle investigation, we used biotinylated liposomes in order to enhance the signal change of streptavidin binding to a biotinylated gold sensor surface. The signal amplification properties can be adjusted by tuning the refractive index of the encapsulant solution. This versatile signal amplification tool may improve numerous applications in (bio)analytical sensing. Liposomes can be used in competitive binding assays and thus overcome the limitations of SPR detecting small molecules due to their high refractive index. Studies of phospholipase activity are recently in the focus of interest, as these enzymes play an important role in physiological processes as well as clinical diagnostics [38]. Surface-immobilized liposomes could be used for monitoring phospholipase activity via SPR, as the high refractive index encapsulant will be released upon hydrolysis of the lipid membrane accompanied by a decrease in the SPR signal. In addition, the possibility to encapsulate solutions of varying RI enables the adjustment of the enhancement factor when using liposomes as signal amplification tags and thus increasing the versatility in the dynamic range of a sensor application. This is a unique property hardly found with other amplification tags. Already frequently used in fluorescence [19] or electrochemical [39] detection as well as with quartz-crystal microbalance [21], liposomes as versatile, easy-to-handle amplification tools could also be a great benefit for other mass-sensitive techniques such as the previously mentioned Mach-Zehnder interferometer [36] or reflectometric interference spectroscopy [40]. In addition, the countless possibilities for encapsulants make liposomes ideal for combined approaches. For example, the introduction of fluorescent dye enables studies of surface plasmon fluorescence spectroscopy [41] with liposome enhancement. The findings of this study will offer new

possibilities for the development of novel sensor applications and will help with the improvement of existing techniques using liposomes for signal enhancement.

5. References

[1] S. Zeng, D. Baillargeat, H.-P. Ho, K.-T. Yong, Nanomaterials enhanced surface plasmon resonance for biological and chemical sensing applications, Chem. Soc. Rev. (2014) 3426–3452. doi:10.1039/c3cs60479a.

[2] J. Homola, Surface Plasmon Resonance Sensors for Detection of Chemical and Biological Species, Chem. Rev. 108 (2008) 462–493. doi:10.1021/cr068107d.

[3] D. Zhang, Y. Yan, W. Cheng, W. Zhang, Y. Li, H. Ju, et al., Streptavidin-enhanced surface plasmon resonance biosensor for highly sensitive and specific detection of microRNA, Microchim. Acta. 180 (2013) 397–403. doi:10.1007/s00604-013-0945-3.

[4] K.P.M. Geuijen, L.A. Halim, H. Schellekens, R.B. Schasfoort, R.H. Wijffels, M.H. Eppink, Label-Free Glycoprofiling with Multiplex Surface Plasmon Resonance: A Tool To Quantify Sialylation of Erythropoietin, Anal. Chem. 87 (2015) 8115–8122. doi:10.1021/acs.analchem.5b00870.

[5] P. Zhai, J. Guo, J. Xiang, F. Zhou, Electrochemical Surface Plasmon Resonance Spectroscopy at Bilayered Silver/Gold Films, J. Phys. Chem. C. 111 (2007) 981–986. doi:10.1021/jp065525d.

[6] T. Lang, T. Hirsch, C. Fenzl, F. Brandl, O.S. Wolfbeis, Surface Plasmon Resonance Sensor for Dissolved and Gaseous Carbon Dioxide, Anal. Chem. 84 (2012) 9085–9088. doi:10.1021/ac301673n.

[7] K. Yokoyama, M. Oishi, M. Oshima, Development of an enhanced surface plasmon resonance sensor substrate by investigating a periodic nanohole array configuration, J. Appl. Phys. 118 (2015) 023101. doi:10.1063/1.4926502.

[8] M. Singh, M. Holzinger, M. Tabrizian, S. Winters, N.C. Berner, S. Cosnier, et al., Noncovalently Functionalized Monolayer Graphene for Sensitivity Enhancement of Surface Plasmon Resonance Immunosensors, J. Am. Chem. Soc. 137 (2015) 2800–2803. doi:10.1021/ja511512m.

[9] M. Frasconi, R. Tel-Vered, M. Riskin, I. Willner, Surface Plasmon Resonance Analysis of Antibiotics Using Imprinted Boronic Acid-Functionalized Au Nanoparticle Composites, Anal. Chem. 82 (2010) 2512–2519. doi:10.1021/ac902944k.

[10] Y. Ben-Amram, R. Tel-Vered, M. Riskin, Z.-G. Wang, I. Willner, Ultrasensitive and selective detection of alkaline-earth metal ions using ion-imprinted Au NPs composites and surface plasmon resonance spectroscopy, Chem Sci. 3 (2012) 162–167. doi:10.1039/C1SC00403D.

[11] S.H. Baek, A.W. Wark, H.J. Lee, Dual Nanoparticle Amplified Surface Plasmon Resonance Detection of Thrombin at Subattomolar Concentrations, Anal. Chem. 86 (2014) 9824–9829. doi:10.1021/ac5024183.

[12] H. Yockell-Lelièvre, N. Bukar, K.S. McKeating, M. Arnaud, P. Cosin, Y. Guo, et al., Plasmonic sensors for the competitive detection of testosterone, Analyst. 140 (2015) 5105–5111. doi:10.1039/C5AN00694E.

[13] S. Krishnan, V. Mani, D. Wasalathanthri, C.V. Kumar, J.F. Rusling, Attomolar Detection of a Cancer Biomarker Protein in Serum by Surface Plasmon Resonance Using Superparamagnetic Particle Labels, Angew. Chem. Int. Ed. 50 (2011) 1175–1178. doi:10.1002/anie.201005607.

[14] T. Wink, S.J. van Zuilen, A. Bult, W.P. van Bennekom, Liposome-Mediated Enhancement of the Sensitivity in Immunoassays of Proteins and Peptides in Surface Plasmon Resonance Spectrometry, Anal. Chem. 70 (1998) 827–832. doi:10.1021/ac971049z.

[15] D. Peer, J.M. Karp, S. Hong, O.C. Farokhzad, R. Margalit, R. Langer, Nanocarriers as an emerging platform for cancer therapy, Nat. Nanotechnol. 2 (2007) 751–760. doi:10.1038/nnano.2007.387.

[16] L. Zhang, F. Gu, J. Chan, A. Wang, R. Langer, O. Farokhzad, Nanoparticles in Medicine: Therapeutic Applications and Developments, Clin. Pharmacol. Ther. 83 (2008) 761–769. doi:10.1038/sj.clpt.6100400.

[17] Q. Liu, B.J. Boyd, Liposomes in biosensors, Analyst. 138 (2013) 391–409. doi:10.1039/c2an36140j.

[18] K.A. Edwards, A.J. Baeumner, Liposomes in analyses, Talanta. 68 (2006) 1421–1431. doi:10.1016/j.talanta.2005.08.044.

[19] K.A. Edwards, A.J. Baeumner, Enhancement of Heterogeneous Assays Using Fluorescent Magnetic Liposomes, Anal. Chem. 86 (2014) 6610–6616. doi:10.1021/ac501219u.

[20] N. Wongkaew, P. He, V. Kurth, W. Surareungchai, A.J. Baeumner, Multi-channel PMMA microfluidic biosensor with integrated IDUAs for electrochemical detection, Anal. Bioanal. Chem. 405 (2013) 5965–5974. doi:10.1007/s00216-013-7020-0.

[21] L. Alfonta, I. Willner, D.J. Throckmorton, A.K. Singh, Electrochemical and Quartz Crystal Microbalance Detection of the Cholera Toxin Employing Horseradish Peroxidase And GM1-Functionalized Liposomes, Anal. Chem. 73 (2001) 5287–5295. doi:10.1021/ac010542e.

[22] K.A. Edwards, A.J. Baeumner, Optimization of DNA-tagged dye-encapsulating liposomes for lateral-flow assays based on sandwich hybridization, Anal. Bioanal. Chem. 386 (2006) 1335–1343. doi:10.1007/s00216-006-0705-x.

[23] R.J. Hunter, Zeta Potential in Colloid Science: Principles and Applications, Academic Press, London, 1981; pp. 69-74.

[24] V. Bello, G. Mattei, P. Mazzoldi, N. Vivenza, P. Gasco, J.M. Idee, et al., Transmission Electron Microscopy of Lipid Vesicles for Drug Delivery: Comparison between Positive and Negative Staining, Microsc. Microanal. 16 (2010) 456–461. doi:10.1017/S1431927610093645.

[25] J. Spinke, M. Liley, H.J. Guder, L. Angermaier, W. Knoll, Molecular recognition at self-assembled monolayers: the construction of multicomponent multilayers, Langmuir. 9 (1993) 1821–1825. doi:10.1021/la00031a033.

[26] R.P.H. Kooyman, R.M. Corn, A. Wark, H.J. Lee, E. Gedig, G. Engbers, et al., Handbook of Surface Plasmon Resonance, The Royal Society of Chemistry, Cambridge, 2008; p. 17. http://dx.doi.org/10.1039/9781847558220.

[27] H. Matsushita, S. Mizukami, F. Sugihara, Y. Nakanishi, Y. Yoshioka, K. Kikuchi, Multifunctional Core–Shell Silica Nanoparticles for Highly Sensitive ^{19}F Magnetic Resonance Imaging, Angew. Chem. 126 (2014) 1026–1029. doi:10.1002/ange.201308500.

[28] C. Fenzl, C. Genslein, A. Zöpfl, A.J. Baeumner, T. Hirsch, A photonic crystal based sensing scheme for acetylcholine and acetylcholinesterase inhibitors, J Mater Chem B. 3 (2015) 2089–2095. doi:10.1039/C4TB01970A.

[29] T. Itoh, T. Asahi, H. Masuhara, Direct Demonstration of Environment-Sensitive Surface Plasmon Resonance Band in Single Gold Nanoparticles, Jpn. J. Appl. Phys. 41 (2002) L76–L78. doi:10.1143/JJAP.41.L76.

[30] B.H. Ong, X. Yuan, S.C. Tjin, J. Zhang, H.M. Ng, Optimised film thickness for maximum evanescent field enhancement of a bimetallic film surface plasmon resonance biosensor, Sens. Actuators B Chem. 114 (2006) 1028–1034. doi:10.1016/j.snb.2005.07.064.

[31] H. Chen, F. Qi, H. Zhou, S. Jia, Y. Gao, K. Koh, et al., Fe_3O_4@Au nanoparticles as a means of signal enhancement in surface plasmon resonance spectroscopy for thrombin detection, Sens. Actuators, B. 212 (2015) 505–511. doi:10.1016/j.snb.2015.02.062.

[32] S.R. Gadagkar, G.B. Call, Computational tools for fitting the Hill equation to dose–response curves, J. Pharmacol. Toxicol. Methods. 71 (2015) 68–76. doi:10.1016/j.vascn.2014.08.006.

[33] N. Nath, A. Chilkoti, A Colorimetric Gold Nanoparticle Sensor To Interrogate Biomolecular Interactions in Real Time on a Surface, Anal. Chem. 74 (2002) 504–509. doi:10.1021/ac015657x.

[34] X. Li, L. Jiang, Q. Zhan, J. Qian, S. He, Localized surface plasmon resonance (LSPR) of polyelectrolyte-functionalized gold-nanoparticles for bio-sensing, Colloids Surf. Physicochem. Eng. Asp. 332 (2009) 172–179. doi:10.1016/j.colsurfa.2008.09.009.

[35] C.-D. Chen, S.-F. Cheng, L.-K. Chau, C.R.C. Wang, Sensing capability of the localized surface plasmon resonance of gold nanorods, Biosens. Bioelectron. 22 (2007) 926–932. doi:10.1016/j.bios.2006.03.021.

[36] R. Bruck, E. Melnik, P. Muellner, R. Hainberger, M. Lämmerhofer, Integrated polymer-based Mach-Zehnder interferometer label-free streptavidin biosensor compatible with injection molding, Biosens. Bioelectron. 26 (2011) 3832–3837. doi:10.1016/j.bios.2011.02.042.

[37] M. Iqbal, M.A. Gleeson, B. Spaugh, F. Tybor, W.G. Gunn, M. Hochberg, et al., Label-Free Biosensor Arrays Based on Silicon Ring Resonators and High-Speed Optical Scanning Instrumentation, IEEE J. Sel. Top. Quantum Electron. 16 (2010) 654–661. doi:10.1109/JSTQE.2009.2032510.

[38] D. Aili, M. Mager, D. Roche, M.M. Stevens, Hybrid Nanoparticle−Liposome Detection of Phospholipase Activity, Nano Lett. 11 (2011) 1401–1405. doi:10.1021/nl1024062.

[39] W.-C. Liao, J.A. Ho, Attomole DNA Electrochemical Sensor for the Detection of Escherichia coli O157, Anal. Chem. 81 (2009) 2470–2476. doi:10.1021/ac8020517.

[40] A.K. Krieg, G. Gauglitz, Ultrasensitive label-free immunoassay for optical determination of amitriptyline and related tricyclic antidepressants in human serum, Anal. Chem. (2015). doi:10.1021/acs.analchem.5b01895.

[41] F. Yu, B. Persson, S. Löfås, W. Knoll, Attomolar Sensitivity in Bioassays Based on Surface Plasmon Fluorescence Spectroscopy, J. Am. Chem. Soc. 126 (2004) 8902–8903. doi:10.1021/ja048583q.

Chapter 4: Conclusions and future perspectives

The results in this thesis demonstrate the successful combination of liposome technology with the online monitoring capability afforded by SPR, and hence provides answers to several important questions regarding liposome interactions with solid surfaces. Additionally, the findings build the basis for further mechanistic studies for an even better understanding of these interactions that is necessary for intelligent surface engineering. The results revealed that even with the highest non-specific binding of negatively charged liposomes with positively charged amino-terminated surfaces only 40% of the simulated maximum signal change was obtained. It is thus concluded that the surface coverage of the SPR chip is surprisingly low. It is assumed to be caused by steric and charge-related repelling effects that have to be taken into account. Thus, systematic studies with liposomes of different sizes will provide further insight into the role of the optimum liposome size for SPR signal enhancement in the future. Here, a certain tradeoff exists between (i) an optimal liposome size large enough to enable the evanescent wave penetrating the encapsulant solution as long as possible and (ii) with making them small enough to minimize steric hindrances and maximize surface coverage. Although negatively charged liposomes are used in the vast majority of sensing applications and positively charged ones excel in their drug delivery capabilities, some assay approaches – especially for the detection of negatively charged species such as nucleic acids [1] – are based on electrostatic interactions to positively charged phospholipid head groups. Furthermore, positive liposomes can be used for additional signal amplification when binding as a second layer to negative liposomes. For both strategies, binding studies with SPR spectroscopy will contribute to better understand liposome interactions and therefore improve assay quality and limits of detection.

Liposomes have been used for the encapsulation of a variety of molecules including those used for fluorescence, absorbance and electrochemical detection. A more recent trend is the encapsulation of nanoparticles (NPs) such as magnetite NPs [2] or quantum dots (QDs) [3]. They are employed to further improve the performance of the assays. For example, magnetite NPs are used to overcome diffusion-based limitations by applying a magnetic field that draws the liposomes to the microtiter plate surface [2], whereas

encapsulated QDs enable the measurement of attomolar concentrations of DNA by single-particle detection without the need of DNA amplification techniques [3]. The combination of the high colloidal stability and analytical versatility of liposomes with signal-amplifying nanoparticles can also be a great asset for SPR spectroscopy. Gold NPs with their localized surface plasmons or magnetite NPs with their high refractive index in combination with a high refractive index aqueous solution as dispersing medium will lead to even higher enhancement factors for (bio)analytical applications using SPR. However, the above mentioned approaches utilize hydrophobic NPs localized in the lipid bilayer, which limits the number of NPs per liposome [2,3]. High particle density inside the vesicles is crucial for signal enhancement in SPR, thus encapsulation of the particles in the inner hydrophilic cavity would be advantageous. In order to achieve this, a detailed investigation of the optimum lipid composition is necessary, as the liposomes ought to retain their high colloidal stability; yet electrostatic repulsion must be low enough not to prevent particle encapsulation and successful liposome formation. One possible strategy is the reduction of the cholesterol content which will result in a more fluid and flexible lipid membrane, albeit this will also cause a decrease of the liposomes' long-term stability.

In general, using a label in a standard label-free detection method such as SPR does not come without drawbacks as well. First, it must be assured that the analyte molecules provide at least a second binding moiety for the sandwich assay approach to work. Second, the additional species in the measurement system means a potential source for more non-specific adhesion and demands very careful surface engineering for the analytical task as discussed in close detail in this study. Furthermore, binding kinetics of the analyte to the sensor surface cannot be monitored anymore, when measuring species that are only detectable with a label. Finally, the binding step of liposomes requires additional measurement time (20 min in the studied case). This obvious drawback requires a more detailed analysis though. Label-free SPR detection time always depends on analyte concentration and at the same time its binding affinity to the surface-immobilized receptor. This means that the detection time can be a few minutes for high concentrations and low K_D values, whereas it can take hours for low affinity analytes at low concentrations. Here, long incubation times typically result in increased non-specific binding and background signals. Consequently, as labels are proposed to be useful for

low-concentration and low-refractive index analytes, employing an additional label-based step does in fact reduce the overall assay time, as long binding incubations are not required.

As discussed in this thesis, liposome-enhanced SPR provides significant quantitative improvements of the ability to detect low analyte concentrations. The question to be asked is how this new approach compares to other label-free detection methods on the one hand and to SPR technique with other nanomaterials as amplification tags on the other hand. There are numerous label-free methods that compete directly with SPR. Recently, very sensitive bioassay approaches with quartz crystal microbalance [4], reflectometric interference spectroscopy [5], Mach-Zehnder interferometer [6] or silicon ring resonators [7,8] have been demonstrated. These techniques outperform SPR on some occasions with respect to sensitivity, many of these approaches – especially Mach-Zehnder interferometers and silicon ring resonators – yet they require time-consuming clean room fabrication and very elaborate instrumental set-ups. Using liposome-enhanced SPR provides thus a viable analytical alternative. At the same time liposome amplification can also be transferred to these techniques for improved sensitivity, as they also face the typical limitations of label-free sensing when concerning very small analytes or very low concentrations. As discussed in detail in Chapter 1, high quality enhancement labels are of great importance in (bio)analytical applications and several approaches have been developed for SPR [9]. Gold nanoparticles are most commonly used for this task, as their inherent plasmonic effect can couple to the propagating surface plasmons and thus increase the sensitivity [10,11]. Magnetite nanoparticles possess a high refractive index and are easy to separate which makes them also a good choice for enhancement tags in SPR [12]. Both materials provide excellent enhancement factors (EF) and can achieve very low limits of detection, but are hampered by distinct limitations with respect to colloidal stability, ease of surface modification and versatility. Here, liposomes can fill the void and act as viable alternatives that are highly colloidally stable, easy to functionalize and provide individually adjustable amplification factors due to varying refractive indices in the liposomes' inner cavities. Currently, reported EFs for gold nanoparticles are higher than those found for liposomes in this study, but further investigations into other encapsulants may render liposomes competitive also in this aspect. Furthermore, the SPR technique is limited in the ability of multiplexing [13]. Here, liposomes with varying

refractive index can function as labels for simultaneous multiple analyte detection in combination with a SPR imaging system with spatial resolution.

The knowledge gained by the research described in this thesis can be used for the development of high-performing SPR (bio)sensors with liposome amplification. One desirable possibility is the capability of online measurements in real samples. Ultralow fouling surfaces have been developed for SPR sensing [14,15]. Here, secondary binding of liposomes will enable significantly improved signal-to-noise ratios and increase overall specificity of the assay. Additionally, assays requiring distinction between closely related structures will benefit from secondary tag binding such as the differentiation of glycosilated and non-glycosilated proteins. This is very elaborate for label-free SPR, as the difference in their refractive indices is negligible. Therefore, specific binding of liposomes to the glycan structure would be an elegant solution for this task.

The results from the non-specific binding studies provided important insight into adsorption/desorption processes of liposomes to solid surfaces and forms the underlying basis for the development of competitive assays based on desorption. Receptor-modified liposomes that are loosely yet effectively enough bound to the SPR surface *via* electrostatic interactions will bind to an analyte molecule. They will then be washed away if the attractive interactions between receptor and analyte plus the applied flow forces outweigh the non-specific binding to the sensor surface. This consequently will result in a concentration-dependent drop of the SPR signal. Experimental conditions such as flow rate and ionic strength of the buffer as well as the molecular weight and surface charge of the analyte will certainly affect the assay performance and need to be studied.

Finally, society as well as government regulations continue to demand decreasing limits of detection especially for health hazards and thus “classical” amplification strategies are often no longer sufficient. This explains the unceasing quest of researchers for better signal enhancement systems such as provided by nanoparticles, biomolecular reactions and chemical polymerization. In case of SPR spectroscopy, this means that the signal enhancement *via* an amplification tag such as liposomes for which non-specific binding to surfaces can be well-controlled as demonstrated in this thesis, can be combined with modifications of the sensor substrate such as bimetallic films [16] or the very promising nanohole arrays [17]. Thus, a dual or in combination with the previously mentioned

nanoparticle-containing liposomes even a triple amplification approach is obtained that makes the SPR technique very applicable and an attractive solution for future challenges.

References

[1] Y.K. Jung, T.W. Kim, J. Kim, J.-M. Kim, H.G. Park, Universal Colorimetric Detection of Nucleic Acids Based on Polydiacetylene (PDA) Liposomes, Adv. Funct. Mater. 18 (2008) 701–708. doi:10.1002/adfm.200700929.

[2] K.A. Edwards, A.J. Baeumner, Enhancement of Heterogeneous Assays Using Fluorescent Magnetic Liposomes, Anal. Chem. 86 (2014) 6610–6616. doi:10.1021/ac501219u.

[3] J. Zhou, Q. Wang, C. Zhang, Liposome–Quantum Dot Complexes Enable Multiplexed Detection of Attomolar DNAs without Target Amplification, J. Am. Chem. Soc. 135 (2013) 2056–2059. doi:10.1021/ja3110329.

[4] D. Tang, B. Zhang, J. Tang, L. Hou, G. Chen, Displacement-type Quartz Crystal Microbalance Immunosensing Platform for Ultrasensitive Monitoring of Small Molecular Toxins, Anal. Chem. 85 (2013) 6958–6966. doi:10.1021/ac401599t.

[5] A.K. Krieg, G. Gauglitz, Ultrasensitive label-free immunoassay for optical determination of amitriptyline and related tricyclic antidepressants in human serum, Anal. Chem. (2015). doi:10.1021/acs.analchem.5b01895.

[6] R. Bruck, E. Melnik, P. Muellner, R. Hainberger, M. Lämmerhofer, Integrated polymer-based Mach-Zehnder interferometer label-free streptavidin biosensor compatible with injection molding, Biosens. Bioelectron. 26 (2011) 3832–3837. doi:10.1016/j.bios.2011.02.042.

[7] M. Iqbal, M.A. Gleeson, B. Spaugh, F. Tybor, W.G. Gunn, M. Hochberg, et al., Label-Free Biosensor Arrays Based on Silicon Ring Resonators and High-Speed Optical Scanning Instrumentation, IEEE J. Sel. Top. Quantum Electron. 16 (2010) 654–661. doi:10.1109/JSTQE.2009.2032510.

[8] E. Valera, W.W. Shia, R.C. Bailey, Development and validation of an immunosensor for monocyte chemotactic protein 1 using a silicon photonic microring resonator biosensing platform, Clin. Biochem. (2015). doi:10.1016/j.clinbiochem.2015.09.001.

[9] S. Zeng, D. Baillargeat, H.-P. Ho, K.-T. Yong, Nanomaterials enhanced surface plasmon resonance for biological and chemical sensing applications, Chem. Soc. Rev. (2014) 3426–3452. doi:10.1039/c3cs60479a.

[10] S.H. Baek, A.W. Wark, H.J. Lee, Dual Nanoparticle Amplified Surface Plasmon Resonance Detection of Thrombin at Subattomolar Concentrations, Anal. Chem. 86 (2014) 9824–9829. doi:10.1021/ac5024183.

[11] H. Yockell-Lelièvre, N. Bukar, K.S. McKeating, M. Arnaud, P. Cosin, Y. Guo, et al., Plasmonic sensors for the competitive detection of testosterone, Analyst. 140 (2015) 5105–5111. doi:10.1039/C5AN00694E.

[12] J. Wang, Z. Zhu, A. Munir, H.S. Zhou, Fe_3O_4 nanoparticles-enhanced SPR sensing for ultrasensitive sandwich bio-assay, Talanta. 84 (2011) 783–788. doi:10.1016/j.talanta.2011.02.020.

[13] M.-C. Estevez, M.A. Otte, B. Sepulveda, L.M. Lechuga, Trends and challenges of refractometric nanoplasmonic biosensors: A review, Anal. Chim. Acta. 806 (2014) 55–73. doi:10.1016/j.aca.2013.10.048.

[14] H. Vaisocherová, W. Yang, Z. Zhang, Z. Cao, G. Cheng, M. Piliarik, et al., Ultralow Fouling and Functionalizable Surface Chemistry Based on a Zwitterionic Polymer Enabling Sensitive and Specific Protein Detection in Undiluted Blood Plasma, Anal. Chem. 80 (2008) 7894–7901. doi:10.1021/ac8015888.

[15] O.R. Bolduc, J.N. Pelletier, J.-F. Masson, SPR Biosensing in Crude Serum Using Ultralow Fouling Binary Patterned Peptide SAM, Anal. Chem. 82 (2010) 3699–3706. doi:10.1021/ac100035s.

[16] K.-S. Lee, J.M. Son, D.-Y. Jeong, T.S. Lee, W.M. Kim, Resolution Enhancement in Surface Plasmon Resonance Sensor Based on Waveguide Coupled Mode by Combining a Bimetallic Approach, Sensors. 10 (2010) 11390–11399. doi:10.3390/s101211390.

[17] K. Yokoyama, M. Oishi, M. Oshima, Development of an enhanced surface plasmon resonance sensor substrate by investigating a periodic nanohole array configuration, J. Appl. Phys. 118 (2015) 023101. doi:10.1063/1.4926502.

Curriculum Vitae

Persönliche Daten

Christoph Fenzl | Abteistr. 2 | 94136 Thyrnau | christoph.fenzl@ur.de

Geburtsdatum: 20.08.1986 | Geburtsort: Hutthurm, Landkreis Passau

Staatsangehörigkeit: Deutsch | Familienstand: ledig, keine Kinder

Ausbildung

10/2012 - 12/2015 **Promotionsstudium, Chemie – Universität Regensburg**

Dissertation: "Liposomes as Versatile Tools for Signal Enhancement in Surface Plasmon Resonance Spectroscopy"

Institut für Analytische Chemie, Chemo- und Biosensorik (Prof. A. J. Bäumner)

10/2010 - 09/2012 **Master of Science, Chemie – Universität Regensburg**

Masterarbeit: "Colloidal photonic crystals for chemical sensor applications"

Institut für Analytische Chemie, Chemo- und Biosensorik (Prof. O. S. Wolfbeis)

10/2007 - 09/2010 **Bachelor of Science, Chemie – Universität Regensburg**

Bachelorarbeit: "Oberflächenplasmonenresonanz – Untersuchungen der Wechselwirkung verschiedener Antikörper mit auf Gold immobilisierten Staphylokokken – Enterotoxinen"

Institut für Analytische Chemie, Chemo- und Biosensorik (Prof. O. S. Wolfbeis)

10/2006 - 07/2007 **Ausbildung zum Rettungssanitäter – Bayerisches Rotes Kreuz, Passau**

07/2006 - 03/2007 **Grundwehrdienst – Kaserne am Goldenen Steig, Freyung**

09/1997 - 06/2006 **Allgemeine Hochschulreife – Gymnasium Untergriesbach**

Bestandene Prüfung zur Studienförderung nach Art. 5 des Bayerischen Eliteförderungsgesetzes beim Ministerialbeauftragten in Landshut

09/1993 - 07/1997 **Grundschule Thyrnau**

Forschungstätigkeit

2012 - 2015 **Wissenschaftlicher Mitarbeiter – Doktorand, Universität Regensburg**

Herstellung und Charakterisierung (Größe, Struktur, Oberflächenladung, Konzentrationsbestimmung) hochstabiler anionischer Liposomen für (bio)analytische Anwendungen. Oberflächenplasmonenresonanz (SPR) – Untersuchung der nicht-spezifischen Wechselwirkungen mit Oberflächen unterschiedlicher Hydrophilie und Ladung. Entwicklung einer Methode zur SPR-Signalverstärkung durch den Einsatz von Liposomen.

2013 **Forschungsaufenthalt – Department for Biological and Environmental Engineering, Cornell University, Ithaca, NY, USA (Prof. A. J. Bäumner)**

Pathogendetektion mit Signalverstärkung in Lateral Flow Assays mit Liposomen, Gold-Nanopartikeln und Latex-Nanopartikeln. Fabrikation von mikrofluiden Sensorchips mit Techniken der Photolithographie, der Elektronenstrahlverdampfung, des Heißprägeverfahrens und der Elektroabscheidung im Reinraum. Dauer: 4 Monate

2012 **Wissenschaftlicher Mitarbeiter – Masterand, Universität Regensburg**

Synthese und Charakterisierung (Größe, Struktur, Oberflächenladung, Konzentrationsbestimmung) nanoskopischer Polystyrolpartikel. Herstellung kolloidaler photonischer Kristalle als Sensorplattform für organische Lösungsmittel sowie für die Ionenstärke wässriger Lösungen.

Auszeichnungen

2013 Preis der Fachgruppe Analytische Chemie der Gesellschaft Deutscher Chemiker für den besten Studierenden des Jahres 2012 im Fach Analytischer Chemie nach bestandener Masterprüfung

2013 Preis der Universitätsstiftung Dr. Alfons Paulus für den besten Masterabschluss in der Fakultät Chemie/Pharmazie

2011 Preis der Fachgruppe Analytische Chemie der Gesellschaft Deutscher Chemiker für den besten Studierenden des Jahres 2010 im Fach Analytischer Chemie nach bestandener Bachelorprüfung

2011 Preis der Universitätsstiftung Dr. Alfons Paulus für den besten Bachelorabschluss in der Fakultät Chemie/Pharmazie

Stipendien

2015 Kongressstipendium des Deutschen Akademischen Austauschdienstes

2015 Tagungsstipendium der Gesellschaft deutscher Chemiker

2014 Tagungsstipendium der Gesellschaft deutscher Chemiker

2012 Tagungsstipendium der Gesellschaft deutscher Chemiker

2009 - 2012 Studienstiftung des deutschen Volkes

2007 - 2012 Max-Weber-Programm Bayern

Publications

9. **C. Fenzl**, C. Genslein, C. Domonkos, K. A. Edwards, T. Hirsch, A. J. Baeumner
Investigating non-specific binding to chemically engineered sensor surfaces using liposomes as models. **2015**, submitted.

8. **C. Fenzl**, T. Hirsch, A. J. Baeumner
Nanomaterials as versatile tools for signal amplification in (bio)analytical applications. *Trends in Analytical Chemistry* **2015**, accepted for publication, doi: 10.1016/j.trac.2015.10.018.

7. **C. Fenzl**, T. Hirsch, A. J. Baeumner
Liposomes with High Refractive Index Encapsulants as Tunable Signal Amplification Tools in Surface Plasmon Resonance Spectroscopy. *Analytical Chemistry* **2015**, 87(21), 11157-11163, doi: 10.1021/acs.analchem.5b03405.

6. **C. Fenzl**, C. Genslein, A. Zöpfl, A. J. Baeumner, T. Hirsch
A photonic crystal based sensing scheme for acetylcholine and acetylcholinesterase inhibitors. *Journal of Materials Chemistry B* **2015**, 3, 2089-2095, doi: 10.1039/C4TB01970A.

5. **C. Fenzl**, T. Hirsch, O. S. Wolfbeis
Photonic Crystals for Chemical Sensing and Biosensing. *Angewandte Chemie International Edition* **2014**, 53(13), 3318-3335, doi:10.1002/anie.201307828.

4. **C. Fenzl**, M. Kirchinger, T. Hirsch, O. S. Wolfbeis
Photonic Crystal-Based Sensing and Imaging of Potassium Ions. *Chemosensors* **2014**, 2(3), 207-218, doi:10.3390/chemosensors2030207.

3. **C. Fenzl**, S. Wilhelm, T. Hirsch, O.S. Wolfbeis

Optical Sensing of the Ionic Strength Using Photonic Crystals in a Hydrogel Matrix. *ACS Applied Materials & Interfaces* **2013**, 5(1), 173-178, doi:10.1021/am302355g.

2. **C. Fenzl**, T. Hirsch, O.S. Wolfbeis

Photonic Crystal Based Sensor for Organic Solvents and for Solvent-Water Mixtures. *Sensors (Basel)* **2012**, 12(12), 16954-16963, doi:10.3390/s121216954.

1. T. Lang, T. Hirsch, **C. Fenzl**, F. Brandl, O. S. Wolfbeis

Surface Plasmon Resonance Sensor for Dissolved and Gaseous Carbon Dioxide. *Analytical Chemistry* **2012**, 84(21), 9085 – 9088, doi:10.1021/ac301673n.

Presentations

Oral Presentations

2015 **ANAKON**, Graz, Austria

2015 **9th Interdisciplinary PhD Student Seminar**, Berlin, Germany

2014 **Gordon Research Seminar**, Newport, RI, USA

2013 **9th International Students Conference "Modern Analytical Chemistry"**, Prague, Czech Republic

Poster Presentations

2015 **BBMEC 11**, Regensburg, Germany

2015 **2nd International Conference on Label-Free Technologies**, Boston, MA, USA

2014 **Gordon Research Seminar & Conference**, Newport, RI, USA

2014 **EUROPT(R)ODE XII**, Athens, Greece

2014 **Analytica Conference**, Munich, Germany

2013 **8th German BioSensor Symposium**, Wildau, Germany

2012 **EUROPT(R)ODE XI**, Barcelona, Spain

Eidesstattliche Erklärung

Ich erkläre hiermit an Eides statt, dass ich die vorliegende Arbeit ohne unzulässige Hilfe Dritter und ohne Benutzung anderer als der angegebenen Hilfsmittel angefertigt habe; die aus anderen Quellen direkt oder indirekt übernommenen Daten und Konzepte sind unter Angabe des Literaturzitats gekennzeichnet.

Weitere Personen waren an der inhaltlich-materiellen Herstellung der vorliegenden Arbeit nicht beteiligt. Insbesondere habe ich hierfür nicht die entgeltliche Hilfe eines Promotionsberaters oder anderer Personen in Anspruch genommen. Niemand hat von mir weder unmittelbar noch mittelbar geldwerte Leistungen für Arbeiten erhalten, die im Zusammenhang mit dem Inhalt der vorgelegten Dissertation stehen.

Die Arbeit wurde bisher weder im In- noch im Ausland in gleicher oder ähnlicher Form einer anderen Prüfungsbehörde vorgelegt.

Ort, Datum Unterschrift